貫通式ツール摩擦攪拌インクリメンタルフォーミングに関する研究

A Dissertation Submitted to the

University of Fukui for the Degree of

Doctor of Engineering

Research on Penetrating Tool Friction Stir Incremental Forming

貫通式ツール摩擦攪拌インクリメンタルフォーミングに関する研究

March 2020

JIANG WEI

RESEARCH ON PENETRATING TOOL FRICTION STIR INCREMENTAL FORMING

Wei JIANG

Advanced Interdisciplinary Science and Technology
Graduate School of Engineering (Doctor Program)
University of Fukui
Japan

ACKNOWLEDGEMENTS

The author sincerely acknowledges his indebtedness to Dr. Masaaki Otsu, Professor of the Faculty of Engineering, University of Fukui, for his continuous guidance and encouragement throughout this study. The author learned a lot from him about how to study and think.

The author's special thanks go to Dr. Takuya Miura, Assistant professor of the Faculty of Engineering, University of Fukui and Dr. Masato Okada, Associate professor of the Faculty of Engineering, University of Fukui for their valuable suggestions and help during this study.

Great acknowledgements are also made to Dr. Ryo Matsumoto, Associate professor of the Graduate School of Engineering, Osaka University, Dr. Takayuki Muranaka, Professor of the Department of Mechanical Engineering, National Institute of Technology, Fukui College, and Dr. Hidenori Yoshimura, Associate professor of the Faculty of Engineering, Kagawa University for their dedicate revision of the papers containing in this dissertation.

The author wishes to express his gratitude to Dr. Takahiro Ohashi, Professor of School of Science and Engineering, Kokushikan University, for his valuable discussions during this study.

The author wishes to express his sincere gratitude to Dr. Masanori Tao, former staff of Center for Innovative Research and Creative Leading Education, University of Fukui, and other staffs of Center for Innovative Research and Creative Leading Education, University of Fukui, for their help in manufacturing of tools and dies that used in this study.

The author also wishes to express his thank to members of Otsu Lab. for their friendship and warm help. The author spends a full and enjoyable research life there.

The author wishes to express his thanks to the Emori Asian Foreign Student Scholarship Foundation and Rotary Yoneyama Memorial Foundation, for their financial support during author's doctoral period.

Special acknowledgements are made to my wife and parents for their long-time support.

CONTENTS

CHAPTER 1

INTRODUCTION

1.1 Background

In recent years, market requirements for sheet metal products have shifted from mass production of a few varieties to producing small batches of larger varieties. This change made the conventional sheet metal forming methods hard to satisfy those requirements as the cost and time required for preparing dies and punches are too high. Incremental forming is a dieless sheet metal forming method which characters by the simple tooling and high formability. In incremental forming, sheets are formed into the objective shape incrementally by moving the forming tool along the contour lines of the objective shape. Single point incremental forming is the most common type of incremental forming. In single point incremental, because the tool deforms the sheets from one side, only bulgy shapes (concave or convex) can be formed. It is difficult to manufacture concave-convex mixed shapes by single point incremental forming.

For forming of concave-convex mixed shapes by incremental forming, two main variants of incremental forming have been proposed. One is two point incremental forming using a support or half die, and the other is double-sided incremental forming that employs two tools to form sheets from both sides of the sheet simultaneously. Both forming methods can form sheets into concave-convex mixed shapes, however, a half die is required for two point incremental forming and a special forming machine with two tools on both sides of the sheet is required for double-sided incremental forming. If concave-convex mixed shapes could be formed with a general 3-axis NC milling machine without dies or supports, incremental forming could be used for various applications.

Penetrating tool friction stir incremental forming (PTFSIF) is another variant of incremental forming to form concave-convex mixed shapes which developed by the authors. PTFSIF is a combination of single point incremental forming and bobbin tool friction stir welding. In PTFSIF, a penetrating tool can travel freely in the sheet metal

without leaving any defects in the sheet. Thus, concave-convex mixed shapes can be formed using the top and bottom tools, respectively. No special machines or dies are required in PTFSIF. However, the forming limit in height in PTFSIF is relatively small, less than 10 mm. The sheets fracture due to formation of groove-like defect at the advancing side, that the tool rotation and feeding direction are the same. It has been clarified that material flow from the advancing side to the retreating side causes the poor forming limit in height. For improving the forming limit in height, it is necessary to develop a method to avoid the formation of groove-like defect. The formation of groove-like defect and direction of material flow between advancing side and retreating side in PTFSIF were treated as two research directions in this dissertation.

1.2 Plastic Working

Plastic working is one of the oldest manufacturing processes in the world, which has more than 4000 years of history. In plastic working, the materials were formed into the objective shapes or dimensions by plastic deformation, which refers to the permanent deformation. The materials used in plastic working include metals, non-metal materials, several composite materials, etc. In those materials, since metals have excellent plasticity, metals become the main target for forming materials of plastic working. Plastic working was also be called metal forming. The production process of almost all metal products involves plastic working. The traditional products are kitchenware, hardware, hand tools, edged weapons, cymbals, jewelry and so on. Since the industrial revolution, they include automobiles, ships, airplanes, railroads, reactor vessels, etc.

The plastic working methods can be classified by the purpose. For example, rolling, extrusion, drawing and roll forming are a group for the manufacturing of the sheets, bars, wires, tube and so on. Forging is another group for the forming of the bulk metals. Forging involves free forging, rotary forging and die forging. Deep drawing, bulging, bending and spinning are methods for forming the sheets and tubes. Besides these, some methods which can be classified into other categories, like shearing and bonding, are also dealt with in plastic working as in those processes machineries of plastic working are used.

Plastic working has the following characteristics. First, the material loss in plastic working is small. For example, the yield in the cutting is about 50%, but in the cold forging, it is 90−95%. Second, the production rate is high. It is normal that the cycle time of plastic working of several accessories is less than 1/10 seconds. It is also normal that rolling speed is high to 100−150 km/h. Third, material properties can be improved. Grain size is changed throughout the plastic working process. Material properties changes such as refinement of inclusions and crushing of voids can be caused. In contrast with the advantages above, the disadvantages are as follows. First, forming accuracy is not so high. Since a huge forming force is employed, a deflection of machine or tool occurs. Second, the cost of the equipment is very high. Since the machines used in plastic working is usually in a big size and the cost for a die preparing is also high, plastic working is not suitable for the small lot production. It is thought when number of the product is less than 1000, cutting is profitable than plastic working.

Plastic working provides people with a wide variety of metal products that greatly improve people's life. Especially after entering the industrial age, the mass production characteristics of plastic working have made the material prosperity of the whole society. Modern society has put forward more and higher demands for plastic working. First, a higher production rate is required. The rapid growth of human demand has made plastic working with machine unable to meet people's needs. On this basis, more automated, continuous, and systematic plastic working which can improve the production rate is required. Second, it is more environmentally friendly and more energy efficient. Huge noise is generated during plastic working process, and the wastewater is also produced during the production. In most plastic working, materials require to be heated into a high temperature, which requires enormous energy. Third, it should adapt the small and medium-scale production. In modern society, market needs are shift to mass production to medium-scale production or small lot production. Fourth, it can manufacture the products with a higher added value. Fifth, it can manufacture the products with a higher accuracy, etc.

1.3 Incremental Sheet Forming

To form the sheet metals quickly and economically in manufacturing, dieless forming methods, in which no delicate dies are required, are demanded and incremental forming (or incremental sheet forming) is one method of dieless forming. In incremental forming, sheets are clamped by the blank holder and deformed locally by the forming tool, whose shape is a hemispherical end in general. By moving the tool along contour lines of the objective shape, sheets are formed incrementally into the objective shape [1-4]. Incremental forming has the following advantages [2, 5].

(1) Hardware requirement, including the forming machinery, apparatus and the tool, are simple. A common three-axis CNC machine, a robot arm or similar, both can be used as the incremental forming machine.

(2) Because no dies are required, sheets are formed into product quickly and economically. For this reason, incremental forming is very suitable for a small batch production of larger varieties.

(3) Formability of metal materials under localized deformation imposed by incremental forming is better than in the conventional sheet metal forming methods, such as deep drawing, stamping, etc.

(4) Forming load in incremental forming is much smaller than that of conventional press forming; this indicates that it is an energy-saving forming method.

Actually, the concept of forming without die is very old. In ancient times, blacksmiths made the sheet metal products by hand-working without die. In the later, with the invention of the press machine, human society enters the age of mass production. The press forms the sheet metal products with delicate dies at an extremely high speed. Although time and cost for preparing the dies used in the press forming are large, due to the large number of products, the manufacturing time and cost for a final single product are not large. In modern times, market needs are shifting from mass production of a few varieties to small-volume production in great varieties. Not only have these demands varied, but a shorter lead time is also required. The cost and time required for preparing dies and punches are too high for conventional press forming to satisfy those requirements. Various dieless forming methods using machine, such as spinning,

incremental forming, laser forming, peen forming, etc., have been developed in an effort to solve these problems [6-8].

In the early 1970's, Leszak [9] and Berghahn *et al*. [10] filed a patent for dieless forming, respectively. These are thought to be the origin of modern incremental forming, which forms the sheets incrementally into objective shape using machine. Although patents had been issued in that period, those did not lead to the present developments of incremental forming. Modern incremental forming rises from 1990's in Japan. Iseki and Matsubara *et al.* proposed several incremental forming methods and built the forming machine [11-15]. In 1992, Iseki *et al.* [11] developed a flexible and incremental sheet metal bulging machine using a path-controlled spherical roller. In 1993, Matsubara [12] studied a numerical control forming system and developed backward bulge incremental forming method, which was named two point incremental forming in the later [16-17]. In two point incremental forming, the sheets are fixed peripherally and a partial or a full support was employed during the forming [16]. The sheet is contemporarily deformed in two points: the contact points between the tool and the sheet and between the sheet and the support. Incremental forming conducted with in only one forming tool without any dies or supports was named single point incremental forming [1, 18-28] and forming conducted with two forming tools from both side of the sheets was named double-sided incremental forming [29-35]. Single point incremental forming, two point incremental forming and double-sided incremental forming are the most common sheet metal incremental forming methods classified with tooling. Figure 1.1 shows schematic illustration of single point incremental forming, two point incremental forming and double-sided incremental forming.

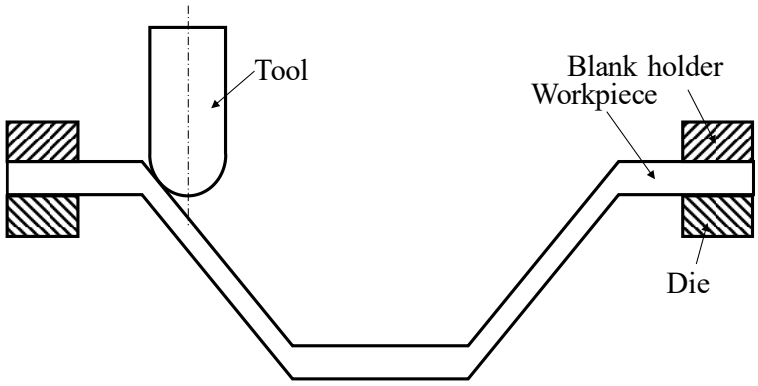

(a) Single point incremental forming

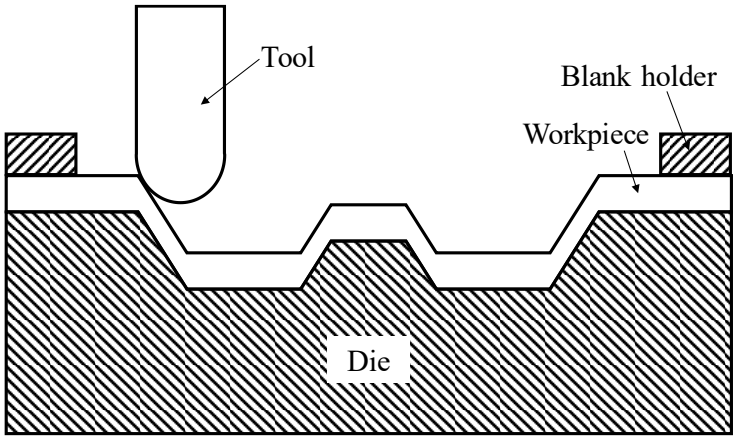

(b) Two point incremental forming

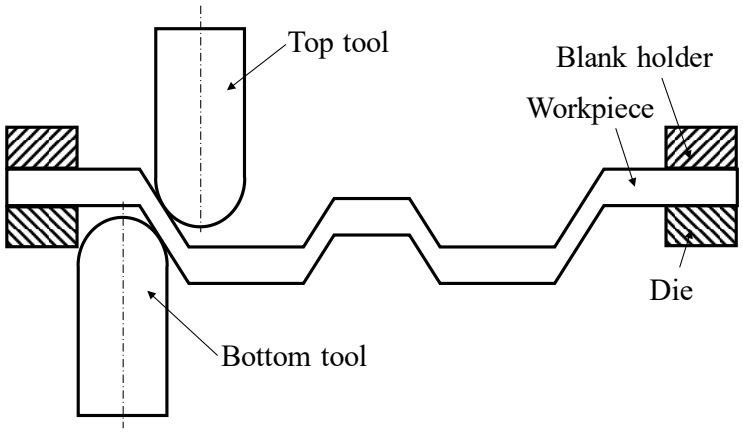

(c) Double-sided incremental forming

Fig. 1.1 Schematic illustration of single point incremental forming, two point incremental forming and double-sided incremental forming.

1.4 Study on Incremental Forming

In the former time, studies on incremental forming were concentrated on the forming possibility. Pure aluminum which owns good formability were used as workpieces and formed into cones and pyramids. The minimum formable wall angle of the objective shapes was treated as a benchmark of formability [20, 36-37] because incremental forming with pure shearing obey the sine law [13] as shown in Fig. 1.2. Kim *et al.* [38] and Park *et al.* [5, 38] investigated the formability of AA1050 in incremental forming by experiment and simulation and found that the forming limit curve of incremental forming is quite different from conventional sheet forming method. The formability of sheet metals in incremental forming appears better in incremental forming than that in conventional forming.

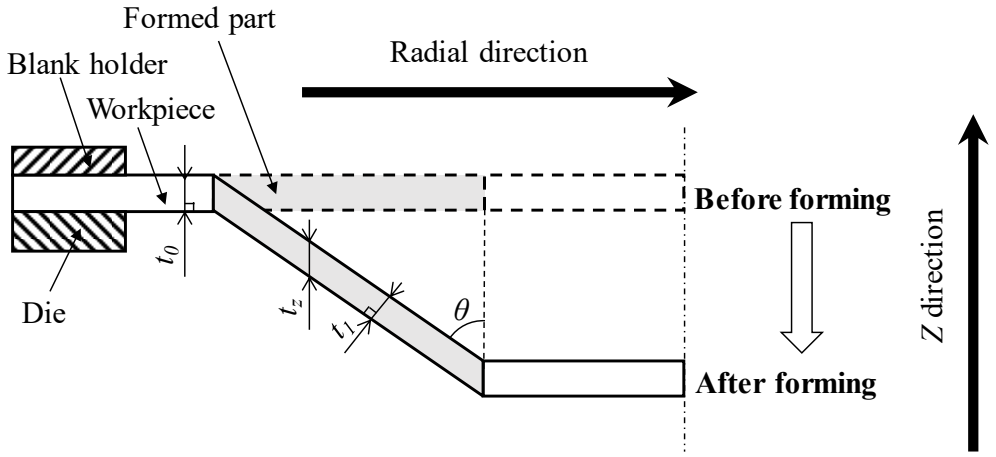

Fig. 1.2 Schematic illustration of the sine law in ideal incremental forming. (θ : wall angle, t_0 : initial sheet thickness, t_1 : thickness of formed sheet, t_z : thickness in Z direction of formed sheet, $t_1 = t_0 \sin(\theta)$, $t_z = t_0$)

Although formability of sheet metals in incremental forming was improved, it is still hard to form the high strength materials such as aluminum alloys, magnesium alloys and titanium alloys directly. For forming those hard to form materials by incremental forming, many variants of incremental forming were developed [39-42]. Duflou *et al*. [43] and Hino *et al*. [44] used a laser beam to heat the sheets locally in incremental forming. Fan *et al.* [45] and Shi *et al.* [46] used an electric current for generating heat in incremental forming, and Otsu *et al.* [41, 47-52] combined friction stir welding and single point incremental forming together, proposed a friction stir incremental forming. Comparing with heating the sheets by a laser beam or an electric current, which needs high cost and improved the complexity of forming, friction stir incremental forming has the advantages of simple tooling. In incremental forming with a laser or an electric current and friction stir incremental forming, both the formability of sheet metal and accuracy of formed sheet were improved.

The poor forming accuracy is also a problem in incremental forming. The elastic spring back and the free deformations are the reasons of poor forming accuracy in incremental forming [22, 53-54]. Therefore, improving the forming accuracy is focused on reduction of springback and free deformations. As mentioned above, incremental forming with a laser or an electric current and friction stir incremental forming can reduce springback of sheet metal by elevating forming temperature of sheet metal. On the other hands, supports which could be a backing plate [16, 55] or another tool on the other side of the sheet metal were used to reducing free deformation for improving forming accuracy [30-31, 34]. Meier *et al.* [29] firstly employed two industrial robots with two forming tools from both sides of the sheet for incremental forming, and this method was called double-sided incremental forming in the later. Maidagan *et al.* [30] and Cao *et al.* [33-34] developed a specific CNC machine for double-sided incremental forming. As the cost for specific machinery used in double-sided incremental forming, such as robots or CNC machine with two spindles on two sides of the sheets is high, research on other types of double-sided incremental forming, like using a C-frame [56] or a flexible die system [57] were used.

In single point incremental forming, because the tool plunges the sheets from one side, only bulge shapes (concave or convex) can be formed. Thus, forming of

concave-convex mixed shapes is a problem in incremental forming field. Until now, there are two main variants of incremental forming for solving this problem.

One is two point incremental forming as shown in Fig. 1.1 (b). In two point incremental forming, a half die or support with delicate shape is used for forming. Two point incremental forming cannot be treated as a truly dieless forming method since a shape dependent die is used. As the forming force in incremental forming is much smaller than that of conventional press forming, the dies or supports can be made of hard resin, woods or steel rather than alloy tool steels, which are expansive and hard to cutting. Amino Corporation formed the Mount Fuji model which has many folds on it successfully by two point incremental forming [65].

The other is double-sided incremental forming as shown in Fig. 1.1 (c). Actually, double-sided incremental forming was developed for forming concave-convex mixed shapes. Maidagan *et al.* [30] called this method as a truly "dieless" incremental forming process. As the specific machine is needed for double-sided incremental forming, a number of researches on double-sided incremental forming is less than single point incremental forming and two point incremental forming.

In the past three decades, researches on incremental forming were concentrated on improving formability and forming accuracy of incremental forming, but not only limit on that. Researches on incremental forming were very active. Those include researches on tool path generating, FEM in incremental forming, mechanical properties of incremental formed sheet, effects of the forming parameters on formability, micro incremental forming [38, 58-64], etc.

1.5 Friction Stir Welding

Friction stir welding is a solid-state welding method invented in 1991 at The Welding Institute in United Kingdom [66]. In friction stir welding, a non-consumable welding tool consist of a flat shoulder and a probe plunge into the workpieces at a high rotation rate and the tool moves along the welding line as shown as Fig. 1.3. Welding can be made because the materials under the shoulder of tool are heated into a soft status and flowed around the probe during the welding. Heats in friction stir welding are composed

of the frictional heat and the plastic deformation of workpieces [67]. Frictional heats are generated by the contact between the shoulder and the workpiece materials, and between the probe and the workpiece materials. Because the welding metal is not melted, in which about 80% of melting temperature of the metals is achieved, i.e. in friction stir welding of aluminum temperature of aluminum was 508°C, it is a solid-state welding method [68-72]. Due to this characteristic, friction stir welding owns lots of advantages comparing with conventional fusion welding. The advantages of friction stir welding can be listed as following [73-76].

(1) Compared with TIG and MIG, the welds strength with friction stir welding is higher.
(2) The distortion is significantly lower in comparison to MIG.
(3) It can weld hard to weld materials such as 2000 and 7000 series aluminum alloys, casting materials and composite materials.
(4) It can weld dissimilar metals.
(5) There are no solidification defects such as crack and porosity.
(6) As welding is conducted by machine, no skilled artisans are needed.
(7) It is a green and economic process.

As friction stir welding owns so many advantages, it has been widely used in railway systems [77-78], shipbuilding industry, aviation industry, constructional engineering [79], automotive industry, etc.

Bobbin tool friction stir welding [80-89] is a variant of friction stir welding developed for welding the thick plates as shown as Fig. 1.4. Since most frictional heat is generated from the friction between the shoulder and the workpieces [67], materials which far away from the top surface of workpieces cannot be heated enough and welded well in the conventional friction stir welding. Compared with the tool used in the conventional friction stir welding, the bobbin tool has two shoulders connected by the probe. During the welding, the workpieces are clamped by the top and bottom shoulders, and tool rotates to generate the frictional heat in top and bottom surfaces of the workpieces. As both sides of the workpieces are heated by frictional heat, it can be used in welding the thick plate [89]. Besides welding of thick plates, bobbin tool friction stir welding also has other advantages. First, with bobbin tool it is possible to weld closed profiles, which extends the range of applications. Second, as the bobbin tool penetrates

the workpieces during the welding, root defects which appear in conventional friction stir welding can be avoided. Third, the force in the direction of tool axis is much lower than that found in with conventional tools because the tool is suffered two forces in the direction of tool axis with opposite direction [89]. Fourth, low distortion is appeared due to uniform heat input.

Friction stir welding by a tool without probe (also called pinless tool) [90] is another variant of friction stir welding which has been used in spot joining and common joining. Without the probes, the end shape of the shoulder can be a flat or dome. Contrary to bobbin tool friction stir welding, friction stir welding by tool without probe was developed for welding thin plate, referring to sheet thickness less than 1 mm. In conventional friction stir welding of thin plate, since it is difficult to manufacture a probe with a smaller size and the thin plate is easy to fracture, the welding tool without probe is better than that with probe. In conventional friction stir welding, the tool fractures at the probe when tool feed rate is high. Because no probe in the tool, the tool welds at a high tool feed rate which improves the welding efficiency.

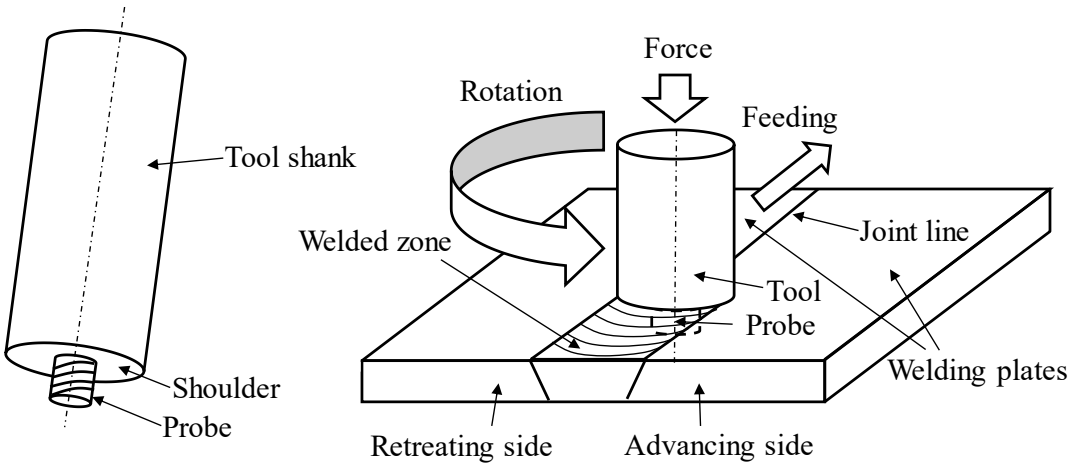

(a) Friction stir welding tool (b) Schematic illustration of friction stir welding

Fig. 1.3 Tool for friction stir welding and schematic illustration of friction stir welding.

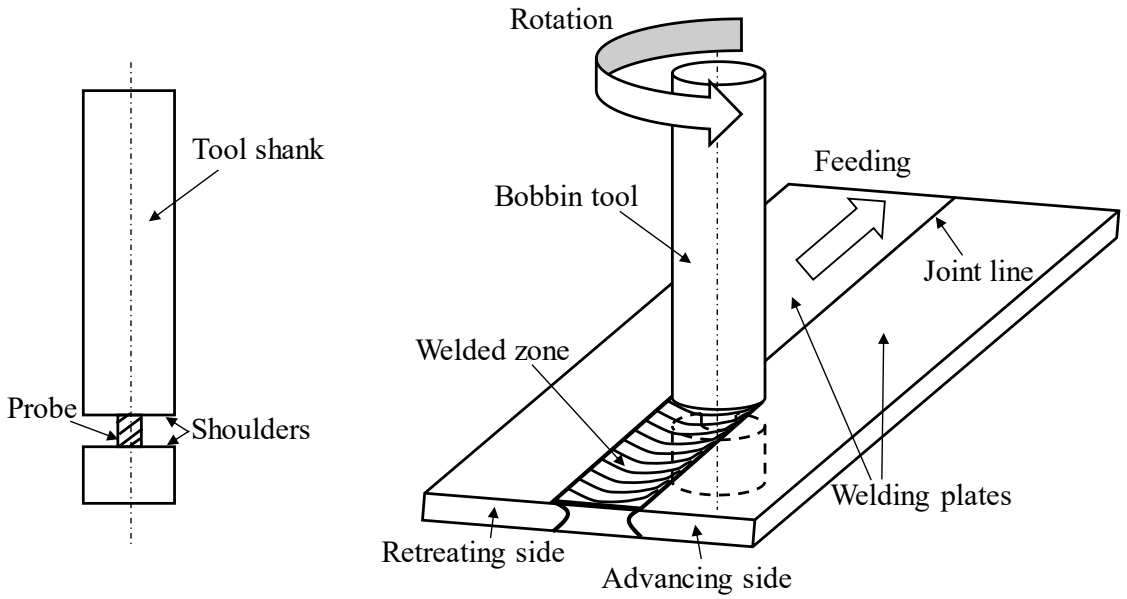

(a) Bobbin tool (b) Schematic illustration of bobbin tool friction stir welding

Fig. 1.4 Bobbin tool and schematic illustration of bobbin tool friction stir welding.

1.6 Friction Stir Incremental Forming

Friction stir incremental forming is a variant of incremental forming where friction stirring is applied to incremental forming for forming hard to form materials. In friction stir incremental forming, the sheet is formed like the ordinary incremental forming except rotation rate of the forming tool is very fast at a range of 1000 to 10000 rpm. Figure 1.5 shows schematic illustration of friction stir incremental forming. As forming tools rotates at a high rotation rate, friction between the forming tool and workpiece is intense, which causes friction stirring as well as friction stir welding (friction stir welding by tool without probe). In friction stir incremental forming, the workpiece is heated by the frictional heat and grain refinement due to dynamic recrystallization during forming is observed at the formed area. Thus, materials that hard to form at room temperature such as hard aluminum alloys, magnesium alloys and titanium alloys can be formed by this process. Table 1.1 shows the differences between friction stir incremental forming and ordinary incremental forming.

Penetrating tool friction stir incremental forming is one kind of friction stir incremental forming, which is combined incremental forming with bobbin tool friction stir welding. Figure 1.6 shows schematic illustration of penetrating tool friction stir incremental forming. It was developed for solving the problem of concave-convex forming in incremental forming field. In penetrating tool friction stir incremental forming, a bobbin tool with a large radius was used. During the forming, the sheet is clamped by the top and bottom tools. The penetrating tool passes through the sheets without leaving any holes or defects. On the basis of this, concave shapes are formed by pushing with top tool and convex shapes are formed by pulling with the bottom tool.

Details of the development of penetrating tool friction stir incremental forming will be introduced in Chapter 2.

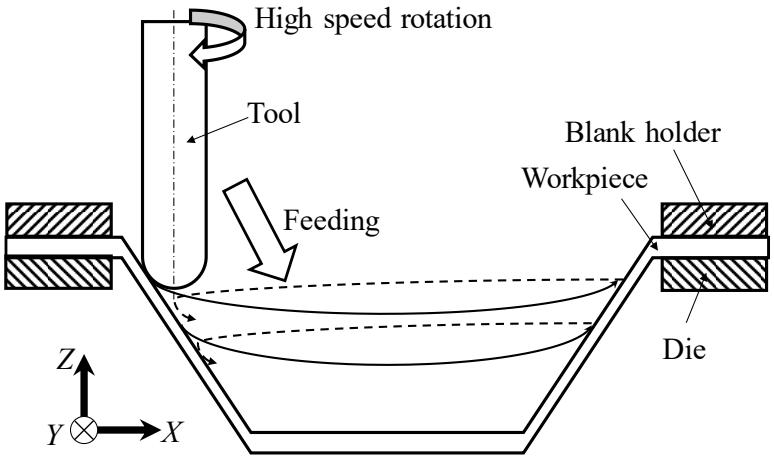

Fig. 1.5 Schematic illustration of friction stir incremental forming.

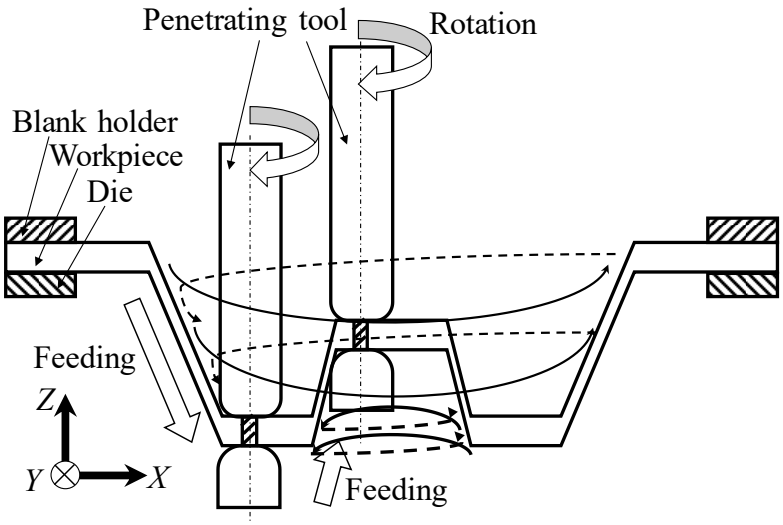

Fig. 1.6 Schematic illustration of penetrating tool friction stir incremental forming.

Table 1.1 Differences between friction stir incremental forming and ordinary incremental forming.

	Friction stir incremental forming	Ordinary incremental forming
Tool rotation rate	Several thousands	Nearly to 0
Lubricating oil	Not used	Used
Frictional heat and tool stirring action	Utilized	Reduced as much as possible

1.7 Research Objective

In single point incremental forming, sheets are deformed locally by a hemispherical ended tool, and then formed into an objective shape incrementally by moving the tool along the contour lines of the objective shape. Because the tool deforms the sheets from one side, only bulgy shapes (concave or convex) can be formed by single point incremental forming. The forming of concave–convex mixed shapes is difficult to manufacture by conventional incremental forming methods. For solving this problem, a novel forming method, named penetrating tool friction stir incremental forming, was developed. A penetrating tool, having the shape of the two tools, which are vertically symmetric and connected by a probe, was used. During the welding process, a sheet is clamped by the top and bottom shoulders. The probe penetrates the sheet, and a hole generated by passing the probe is filled again after passing of the tool. On the basis of this, concave shapes were formed by the pushing with the top tool and convex shapes by pulling the bottom tool. Although penetrating tool friction stir incremental forming has shown the formability by forming the sheets into concave, convex and concave-convex mixed shapes, the problem is that the forming limit in heights is too shallow to actual use. In penetrating tool friction stir incremental forming, groove-like defects occur with the forming proceeded and sheets are penetrated by the groove-like defects finally. The formation of the groove-like defects is caused by the metal flow from advancing side to retreating side.

The aim of this dissertation is to improve the forming limit in height without any defects. Two kinds of strategies were imposed to overcome the formation of groove-like defects. One is trial to control the extent of the metal flow. The other is to control the direction of metal flow. For controlling the extent of the metal flow, it is necessary to investigate the relationship between the defect formation and the experimental conditions, such as tool rotation and feed rates etc. For changing the metal flow direction, it has to change the tool rotating direction or direction of tool path.

1.8 Outline of Dissertation

It is difficult to form the sheets into concave-convex mixed shapes by single point incremental forming because the sheets were deformed from one side. In bobbin tool friction stir welding, the tool penetrated the sheets and both sides of the sheets are welded. Developing a new incremental forming method by utilizing the characteristic of bobbin tool friction stir welding for forming concave-convex mixed shapes and improving the forming limit in height was treated in this dissertation.

This dissertation consists of six chapters:

Chapter 1 presents the background of plastic working, introduction of manufacturing methods relevant to this dissertation and motivation of this thesis. The outline of this thesis is included in it.

Chapter 2 presents the development of penetrating tool friction stir incremental forming by combining incremental forming and bobbin tool friction stir welding. An original tool was designed for forming the sheets into concave-convex mixed shapes using only one tool without a die. Using the developed tool, commercial pure aluminum sheets with 2 mm thickness were formed into concave, convex and concave-convex mixed shapes. In addition, the distribution of thickness in direction vertical to the sheet plane (always said to the *Z* direction) of the sheets formed by this method were measured and material flow during the forming was discussed.

In Chapter 3, forming conditions, including pitch in radial direction, initial radius of forming cones and wall angle, were changed to investigate these effects on the defect formation behavior, which estimated by counting numbers of cycles when the groove-like defects occurred.

Chapter 4 presents the relationship among the defect formation, tool temperature and revolutionary pitch in penetrating tool friction stir incremental forming. To measure tool temperature during forming, a K type thermocouple was embedded in the forming tool and a data logger was kept in a self-made container, which installed in the spindle and it rotates with the spindle simultaneously. Tool rotation and feed rates were changed for varying the revolutionary pitch to investigate groove-like defect formation and the measured tool temperature was used to analyze the defect formation.

In Chapter 5, one-way tool path and alternating tool path direction strategies were used in penetrating tool friction stir incremental forming. Forming limits in height with one-way tool path and alternating tool path were compared, and distributions of volume change per unit length were used for explaining the results of forming limits in height. In addition, formable working conditions were investigated, and concave-convex mixed shapes were formed by penetrating tool friction stir incremental forming with the alternating tool path.

Finally, the concluding remarks for the present study are given in Chapter 6.

References

[1] J. Jeswiet, F. Micari, G. Hirt, A. Bramley, J. Duflou and J. Allwood, Asymmetric single point incremental forming of sheet metal , *CIRP Ann*., **54** (2005), 88-114.

[2] W.C. Emmens, G. Sebastiani and A.H. Boogaard, The technology of incremental sheet forming—A brief review of the history, *J. Mater. Process. Technol*., **210** (2010), 981-997.

[3] Y. Li, X.X. Chen, Z. Liu, J. Sun, F. Li, J. Li and G. Zhao, A review on the recent development of incremental sheet-forming process, *Int. J. Adv. Manuf. Technol*., **92** (2017), 2439-2462.

[4] J. Duflou, A. Habraken, J. Cao, R. Malhotra, M. Bambach, D. Adams, H. Vanhove, A. Mohammadi and J. Jeswiet, Single point incremental forming: state-of-the art and prospects, *Int. J. Mater. Form*., **11** (2018), 743-773.

[5] M. Shim and J.J. Park, The formability of aluminum sheet in incremental forming, *J. Mater. Process. Technol*., **113** (2001), 654-658.

[6] O. Music, J.M. Allwood and K. Kawai, A review of the mechanics of metal spinning, *J. Mater. Process. Technol*., **210** (2010), 3-23.

[7] F. Cook, D. Cwlentano and J.R. Grez, Experimental-numerical methodology for the manufacturing of cranial prosthesis via laser forming, *Int. J. Adv. Manuf. Technol*., **86** (2016), 2187-2196.

[8] H.Y. Miao, D. Demers, S. Larose, C. Perron and M. Levesque, Experimental study of shot peening and stress peen forming, *J. Mater. Process. Technol*., **210** (2010), 2089-2102.

[9] E. Leszak, Apparatus and process for incremental dieless forming, US 3342051, (1964)

[10] W.G. Berghahn et al., Method of dieless forming surface of revolution, US 3316745, (1965)

[11] H. Iseki, K. Kato and S. Sakamoto, Flexible and incremental sheet metal bulging using a path-controlled spherical roller, *Trans. Jpn. Soc. Mech. Eng. C*, **58** (1992), 3147-3155. (In Japanese)

[12] S. Matsubara,, Incremental nosing of a circular tube with a hemispherical head tool—A study of a numerical control forming system I—, *J. Jpn. Soc. Technol. Plast*., **35** (1994), 256-261. (In Japanese)

[13] S. Matsubara,, Incremental backward bulge forming of a sheet metal with a hemispherical head tool—A study of a numerical control forming system II—, *J. Jpn. Soc. Technol. Plast*., **35** (1994), 1311-1316. (In Japanese)

[14] H. Iseki and H. Kumon,, Forming limit of incremental sheet metal stretch forming using spherical rollers, *J. Jpn. Soc. Technol. Plast*., **35** (1994), 1336-1341. (In Japanese)

[15] K. Kitazawa and N. Kobayashi, Depression phenomena in shallow conical stretching of aluminum sheets by CNC incremental forming process with a single tool-path schedule, *J. Jpn. Inst. Light Met*., **49** (1999), 30-34. (In Japanese)

[16] A. Attanasio, E. Ceretti, C. Giardini and L. Mazzoni, Asymmetric two points incremental forming: Improving surface quality and geometric accuracy by tool path optimization, *J. Mater. Process. Technol*., **197** (2008), 59-67.

[17] J. Li, J. Shen and B. Wang, A multipass incremental sheet forming strategy of a car taillight bracket, *Int. J. Adv. Manuf. Technol*., **69** (2013), 2229-2236.

[18] G. Ambrogio, I. Costantino, L.D. Napoli, L. Filice, L. Fratini and M. Muzzupappa, Infulence of some relevant process parametes on the dimensional accuracy in incremental forming: a numerical and experimental investigation, *J. Mater. Process. Technol*., **153-154** (2004), 501-507.

[19] J. Duflou, Y. Tunckol, A. Szekeres and P. Vanherck, Experimental study on force measurements for single point incremental forming, *J. Mater. Process. Technol*., **189** (2007), 65-72.

[20] G. Hussain, G. Lin and N. Hayat, A new parameter and its effect on the formability

in single point incremental forming: A fundamental investigation, *J. Mech. Sci. Technol*., **24** (2010), 1617-1621.

[21] K. Hamilton and J. Jeswiet, Single point incremental forming at high feed rates and rotational speeds: Surface and structural consequences, *CIRP Ann*., **59** (2010), 311-314.

[22] K. Essa and P. Hartley, An assessment of various process strategies for improving procession in single point incremental forming, *Int. J. Mater. Form*., **4** (2011), 401-412.

[23] C. Radu, Effects of process parameters on the quality of parts processed by single point incremental forming, *Int. J. Mod. Manuf. Technol*., **III** (2011), 91-96.

[24] D. Xu, W. Wu, R. Malhotra, J. Chen, B. Lu and J. Cao, Mechanism investigation for the influence of tool rotation and laser surface texturing (LST) on formability in single point incremental forming, *Int. J. Mach. Tools Manuf. Des. Res. Appl*., **73** (2013), 37-46.

[25] B.B.L. Isidore, G. Hussain, S.P. Shamchi and W.A. Khan, Prediction and control of pillow defect in single point incremental forming using numerical simulations, *J. Mech. Sci. Technol*., **30** (2016), 2151-2161.

[26] H. Zhu, J. Ju and J. Bai, Research on the forming direction optimization for the uniformity of the sheet part thickness in the CNC incremental forming, *Int. J. Adv. Manuf. Technol*., **93** (2017), 2547-2559.

[27] M. Durante, A. Formisano and F. Lambiase, Incremental forming of polycarbonate sheets, *J. Mater. Process. Technol*., **253** (2018), 57-63.

[28] K. Jackson and J. Allwood, The mechanics of incremental sheet forming, *J. Mater. Process. Technol*., **209** (2009), 1158-1174.

[29] H. Meier, V. Smukala, O. Dewald and J. Zhang, Two point incremental forming with two moving forming tools, *Key Eng. Mater*., **344** (2007), 599-605.

[30] E. Maidagan, J. Zettler, M. Bambach, P.P. Rodriguez and G. Hirt, A new incremental forming sheet forming process based on a flexible supporting die system, *Key Eng. Mater*., **344** (2007), 607-614.

[31] R. Malhotra, J. Cao, F. Ren, V. Kiridena, Z.C. Xia and N.V. Reddy, Improvement of geometric accuracy in incremental forming by using a squeezing toolpath strategy with two forming tools, *J. Manuf. Sci. Eng*., **133** (2011), 10 pages.

doi:10.1115/MSEC2011-50262.

[32] R. Xu, X. Shi, D. Xu, R. Malhotra and J. Cao, A preliminary study on the fatigue behavior of sheet metal parts formed with accumulative-double-sided incremental forming, *Manuf. Lett*., (2014), 8-11.

[33] B. Lu, Y. Fang, D.K. Xu, J. Chen, S. Ai, H. Long, H. Ou and J. Cao, Investigation of material deformation mechanism in double side incremental sheet forming, *Int. J. Mach. Tools Manuf. Des. Res. Appl*., **93** (2015), 37-48.

[34] Z. Zhang, H. Ren, R. Xu, N. Moser, J. Smith, E.N. Agbor, R. Malhotra, K. Ehmann and J. Cao, A mixed double-sided incremental forming toolpath strategy for improved geometric accuracy, *J. Manuf. Sci. Eng*., **137** (2015), 7 pages. doi:10.1115/1.4031092.

[35] G. Buffa, D. Campanella and L. Fratini, On the improvement of material formability in SPIF operation through tool stirring action, *Int. J. Adv. Manuf. Technol*., **66** (2013), 1343-1351.

[36] K. Suresh and S.P. Regalla, Analysis of formability in single point incremental forming using finite element simulations, *Procedia Mater. Sci*., (2014), 430-435.

[37] Y.H. Kim and J.J. Park, Effect of process parameters on formability in incremental forming of sheet metal, *J. Mater. Process. Technol*., **130-131** (2002), 42-46.

[38] N. Suzuki and T. Sano, Development of incremental forming process with localized heating for titanium alloy sheet, *J. Jpn. Soc. Technol. Plast*., **52** (2011), 579-583. (In Japanese)

[39] G. Ambrogio, F. Gagliardi, S. Bruschi and L. Filice, On the high-speed single point incremental forming of titanium alloys, *CIRP Ann*., **32** (2013), 243-246.

[40] M. Otsu, M. Yasunaga, M. Matsuda and K. Takashima, Friction stir incremental forming of A2017 aluminum sheets, *Procedia Eng*., (2014), 2318-2323.

[41] H. Khazaali and F.F. Saniee, A comprehensive experimental investigation on the infulences of the process variables on warm incremental forming of Ti-6Al-4V titanium alloy using a simple technique, *Int. J. Adv. Manuf. Technol*., **87** (2016), 2911-2923.

[42] J. Duflou, J. D'houdt, Applyzing TRIZ for systematic manufacturing process innovation: the single point incremental forming case, *Procedia Eng*., **9** (2011), 528-537.

[43] R. Hino, F. Yoshida, Incremental sheet forming with local heating, *J. Jpn. Soc. Technol. Plast*., **51** (2010), 297-301.

[44] G.Q. Fan, F.T. Sun, X.G. Meng, L. Gao, G.Q. Tong, Electric hot incremental forming of Ti-6Al-4V titanium sheet, *Int. J. Adv. Manuf. Technol*., **49** (2010), 941-947.

[45] X.F. Shi, L. Gao, H. Khalatbari, Y. Xu, H. Wang, L.L. Jin, Elecric hot incremental forming of low carbon steel sheet: accuracy, *Int. J. Adv. Manuf. Technol*., **68** (2013), 241-247.

[46] M. Otsu, H. Matsuo, M. Matsuda and K. Takashima, Friction stir incremental forming of aluminum alloy sheets, *Steel Res. Int*., **81** (2010), 942-945.

[47] M. Otsu, T. Ichikawa, M. Matsuda and K. Takashima , Development of friction stir incremental forming , *J. Jpn. Soc. Technol. Plast*., **52** (2011), 490-494 (In Japanese)

[48] W. Peng, H. Ou and A. Becker, Double-sided incremental forming: A review, *J. Manuf. Sci. Eng*., **141** (2019), 12 pagers. doi:10.1115/1.4043173.

[49] M. Otsu, T. Ichikawa, M. Matsuda and K. Takashima , Formabilities of AZ31, AZ61 and AZ80 magnesium alloy sheets and mechanical properties of formed parts by friction stir incremental forming—Development of friction stir incremental forming 2nd report—, *J. Jpn. Soc. Technol. Plast*., **52** (2011), 705-709. (In Japanese)

[50] M. Otsu, H. Matsuo, M. Matsuda and K. Takashima, Forming of A5052 aluminum alloy sheets by friction stir incremental forming —Development of friction stir incremental forming 3rd report—, *J. Jpn. Soc. Technol. Plast*., **52** (2011), 710-714. (In Japanese)

[51] M. Otsu, T. Ichikawa, M. Matsuda and K. Takashima , Improvement of formability of magnesium alloy sheets by friction stir incremental forming, *Steel Res. Int. Special Eds*., (2011), 537-541.

[52] M. Otsu, H. Matsuo, M. Matsuda and K. Takashima, Friction stir incremental forming of titanium sheets, *Proc. 4th Int. Conf. Met. Form.*, (2012), 419-422.

[53] G. Ambrogio, V. Cozza, L. Filice and F. Micari, An analytical model for improving precision in single point incremental forming, *J. Mater. Process. Technol*., **191** (2007), 92-95.

[54] G. Ambrogio, L.D. Napoli and L. Filice, A novel approach based on multiple back-drawing incremental forming to reduce geometry deviation, *Int. J. Mater.*

Form., **2** (2009), 9-12.

[55] V. Franzen, L. Kwiatkowski, G. Sebastiani, R. Shankar, A.E. Tekkaya and M. Kleiner, Dyna-Die: Towards full kinematic incremental forming, *Int. J. Mater. Form*., **1** (2008), 1163-1166.

[56] Y.J. Wang, Y. Huang, J. Cao and N.V. Reddy, Experimental study on a new method of double side incremental forming, *ASME Int. Manuf. Sci. and Eng. Conf.*, **1** (2019), 601-607.

[57] D. Panjwani, S. Priyadarshi, P.K. Jain, M.K. Samal, J.J. Roy, D. Roy and P. Tandon, A novel approach based on flexible supports for forming non-axisymmetric parts in SPIF, *Int. J. Adv. Manuf. Technol*., **92** (2017), 2463-2477.

[58] Y.H. Kim and J.J. Park, Effect of process parameters on formability in incremental forming of sheet metal, *J. Mater. Process. Technol*., **130-131** (2002), 42-46.

[59] M. Rauch. J.Y. Hascoet, J.C. Hamann and Y. Plennel, A new approach for toolpath programming in incremental sheet forming, *Int. J. Mater. Form*., **1** (2008), 1191-1194.

[60] A. Blaga, O. Bologa, V. Oleksik and R. Breaz, Influence of tool path on main strains, thickness reduction and forces in single point incremental forming process, *Proc. Manuf. Sys*., 6 (2011), 191-196.

[61] H. Zhu and N. Li, A new STL model-based approach for tool path generation in CNC incremental forming, *Int. J. Adv. Manuf. Technol*., **69** (2013), 277-290.

[62] A. Blaga and V. Oleksik, A study on the influence of the forming strategy on the main strains, thickness reduction, and forces in a single point incremental forming process, *Adv. Mater. Sci. Eng*., **2013** (2013), 10 pages. doi: 10.1155/2013/382635.

[63] H.K. Nirala, P.K. Jain, J.J. Roy, M.K. Samal and P. Tandon, An approach to eliminate stepped features in multistage incremental sheet forming process: Experimental and FEA analysis, *J. Mech. Sci. Technol*., **31** (2017), 599-604.

[64] G. Hapsari, R.B. Hmida, F. Richard, S. Thibaud and P. Malecot, A procedure for ductile damage parameters indentification by micro incremental sheet forming, *Procedia Eng*., (2017), 125-130.

[65] "Incremental forming", Website of Amino Corp., https://amino-corp.com/web/development/dielessNCforming, Date: 2020-01-05 (In Japanese)

[66] W.M. Thomas et al. friction welding, US 5460317, (1995)

[67] Φ. Frigaard, Φ. Grong, and O.T. Midling, A process model for friction stir welding of age hardening aluminum alloys, Metall. *Mater. Trans. A*, **32A** (2001), 1189-1200.

[68] K. Colligan, Material flow behavior during friction stir welding of aluminum, *Weld J.*, (1999), 229-237.

[69] T.U. Seidel and A.P. Reynolds, Visualization of the material flow in AA2195 friction-stir welds using a marker insert technique, *Metall. Mater. Trans. A*, **32A** (2001), 2879-2884.

[70] J.A. Schneider and A.C. Nunes, Characterization of plastic flow and resulting microtextures in a friction stir weld, *Metall. Mater. Trans. B*, **35B** (2004), 777-783.

[71] L.M. Ke L. Xing and J.E. Indacochea, Material flow patterns and cavity model in friction-stir welding of aluminum alloys, *Metall. Mater. Trans. B*, **35B** (2004), 153-160.

[72] H. Fujii, Y.G. Kim, T. Tsumura, T. Komazaki and K. Nakata, Estimation of material flow in stir zone during friction stir welding by distribution measurement of Si particles, *Mater. Trans*., **47** (2006), 224-232.

[73] H. Okamura, K. Aota, H. Takai and M. Ezumi, Problems for application and situation of development in friction stir welding, *J. Jpn. Weld. Soc*., **72** (2003), 436-444. (In Japanese)

[74] N. Yamamoto, J. Liao and K. Nakata, Friction stir weldability of high strength Mg alloy, *J. high Temp. Soc*., **37** (2011), 197-202. (In Japanese)

[75] H. Fujii, FSW, *J. Jpn. Weld. Soc*., **78** (2009), 274-282. (In Japanese)

[76] H. Fujii, Friction stir welding of steels, *J. Jpn. Weld. Soc*., **77** (2008), 731-744. (In Japanese)

[77] H. Mori, M. Noda and T. Tominaga, Current state on application of friction stir welding for rolling stock, *J. Jpn. Inst. Light Met*., **57** (2007), 506-510. (In Japanese)

[78] T. Miyamichi, Application of friction stir welding to railroad carbody, *Electr. Furn. Steel*, **78** (2007), 141-147. (In Japanese)

[79] H. Okamura, K. Aota and M. Ezummi, Friction stir welding of aluminum alloy and application to structure, *J. Jpn. Inst. Light Met*., **50** (2000), 166-172. (In Japanese)

[80] J. Hilgert, H.N.B. Schmidt, J.F. dos Santos and N. Huber, Thermal models for bobbin tool friction stir welding, *J. Mater. Process. Technol*., **211** (2011), 197-204.

[81] S. Tanaka and M. Kumagai, Optimization of controlling method of FSW using self-reacting tool, *Q. J. Jpn. Weld. Soc*., **29** (2011), 353-357.

[82] W.Y. Li, T. Fu, L. Hutsch, J. Hilgert, F.F. Wang, J.F. dos Santos and N. Huber, Effects of tool rotational and welding speed on microstructure and mechanical properties of bobbin-tool friction stir welded Mg AZ31, *Mater. Des*., **64** (2014), 714-720.

[83] M.K. Sued, D. Pons, J. Lavroff and E.H. Wong, Design features for bobbin friction stir welding tools: Development of a conceptual model linking the underlying physics to the production process, *Mater. Des*., **54** (2014), 632-643.

[84] S. Chen, H. Li, S. Lu, R. Ni and J. Dong, Temperature measurement and control of bobbin tool friction stir welding, *Int. J. Adv. Manuf. Technol*., **86** (2016), 337-346.

[85] J.C. Hou, H.J. Liu and Y.Q. Zhan, Influences of rotation speed on microstructures and mechanical properties of 6061-T6 aluminum alloy joints fabricated by self-reacting friction stir welding tool, *Int. J. Adv. Manuf. Technol*., **73** (2014), 1073-1079.

[86] S.S. Chaudhary and K.H. Bhavsar, A review of bobbin tool friction stir welding (FSW) process, *Int. J. Sci. Technol. Eng*., **2** (2016), 630-633.

[87] W.M. Thomas, C.S. Wiesner, D.J. Marks and D.G. Staines, Conventional and bobbin friction stir welding of 12% chromium alloy steel using composite refractory tool materials, *Sci. Technol. Weld. Joining*, **14** (2009), 247-253.

[88] H. Zhang, M. Wang, X. Zhang and G. Yang, Microstructural characteristics and mechanical properties of bobbin tool friction stir welded 2A14-T6 aluminum alloy, *Mater. Des*., **65** (2015), 559-566.

[89] P.L. Threadgill, M.M.Z. Ahmed, J.P. Martin, J.G. Perrett and B.P. Wynne, The use of bobbin tools for friction stir welding of aluminium alloys, *Mater. Sci. Forum*, **638-642** (2010), 1179-1184.

[90] A. Kinya and I. Kenji, Friction stir welding of aluminum lap joint by tool without probe, *Q. J. Jpn. Weld. Soc*., **26** (2008), 284-291.

CHAPTER 2

DEVELOPMENT OF PENETRATING TOOL FRICTION STIR INCREMENTAL FORMING

2.1 Introduction

Single point incremental forming (SPIF) is a commonly studied variant of incremental forming (IF). In SPIF, the peripheral region of a sheet is fixed to a table and a forming tool locally indents the sheet to induce plastic deformation. Because the tool pushes the sheet from one side, only a bulged shape can be formed. Concave-convex mixed shapes cannot be formed by conventional SPIF, which limits its applications. To form sheets into concave-convex mixed shapes by incremental sheet metal forming, two main variants have been proposed. The first is two points incremental forming (TPIF), in which a support or a die is used under the sheets [1-2]. A support or a die can be a full or partial die. The other method is double-sided incremental forming (DSIF), which employs two tools to form the sheets from both sides simultaneously [3-4]. Although TPIF and DSIF can form sheets into concave-convex mixed shapes, the fabrication of a half die is required for TPIF and a special forming machine with two tools on both sides of the sheet is also needed. Die making in TPIF loses an important advantage of incremental sheet metal forming and using a special machine negatives the advantage of using a common 3-axis milling machine. If concave-convex mixed shapes could be formed with a common 3-axis NC milling machine without dies or supports, incremental sheet metal forming could be used for a greater variety of applications.

Friction stir welding (FSW), which is characterized by high welding efficiency and easy operation, has attracted significant attention [5]. Bobbin tool friction stir welding (BTFSW) is a type of FSW [6] where a bobbin tool, owing to the shape of the two shoulders, is vertically symmetric and connected by a probe to be used as the tool. During the welding process, a sheet is clamped by the top and bottom shoulders. The probe penetrates the sheet, and a hole is generated by passing the probe and is filled again after passing of the tool.

Utilizing the characteristics of BTFSW with a bobbin tool penetrating a sheet, a novel forming method for producing concave-convex mixed shapes with one tool and without dies or supports could be developed by combining BTFSW and IF. In this novel forming process, a “bobbin tool” with a larger radius corner was used and concave shapes were formed by pushing the sheet with the top tool. Convex shapes were formed by pulling the sheet with the bottom tool, and concave-convex mixed shape were formed by combining the use of the top and bottom tools. Otsu et al. combined FSW with IF and developed a novel incremental forming method called friction stir incremental forming (FSIF). This combined method achieved great success, allowing magnesium and aluminum alloys sheets to be formed successfully without using external heating [7-8]. Therefore, it is possible to combine BTFSW and IF. Because the tool penetrates the sheet during forming, the tool was called the penetrating tool. This novel forming method involves a combination of BTFSW and IF, and was called penetrating tool friction stir incremental forming (PTFSIF).

In this study, penetrating tool friction stir incremental forming is developed by combining BTFSW and IF. An original tool was designed for forming the sheets into concave-convex mixed shapes using only one tool without a die, of course, concave shape and convex shape only can also be formed by this proposed method. Using the developed tool, commercial pure aluminum sheets with 2 mm thickness were formed into concave, convex, and concave-convex mixed shapes. In addition, the distributions of thickness in Z direction of the sheets formed by this method were measured and material flow during the forming was discussed.

2.2 Penetrating Tool Friction Stir Incremental Forming

2.2.1 Penetrating Tool and Its Forming Principle

The hemispherical ended tool generally used in IF, typical tool shape used in BTFSW, and shape of the proposed penetrating tool are shown in Fig. 2.1. The bobbin tool contains two shoulders connected by a probe, generally composed of a screw thread. The hemispherical ended tool is typically used for incremental sheet metal forming. The penetrating tool has both characteristics of bobbin and an incremental sheet metal

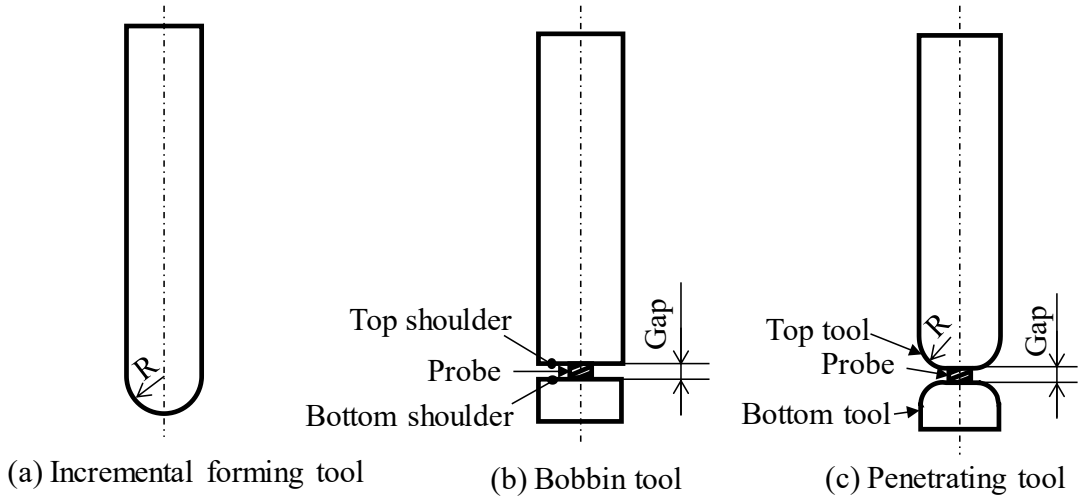

Fig. 2.1 Three kinds of tool shapes.

forming tools, but a larger corner radius of than a bobbin tool. Therefore, it is expected that the penetrating tool can perform both FSW and IF.

Figure 1.6 shows a schematic illustration of PTFSIF where a sheet is clamped in the gap between the top and bottom tools. The penetrating tool rotates at a high rate and travels along the desired tool path. During this process, the sheet is heated from the friction generated between the tool and sheet. Plastic flow occurs around the probe and under the shoulders due to the mechanical stirring by tool rotation. Thus, the tool can pass through the sheet freely without leaving a hole similar to general FSW. A concave or convex shape can be formed by pushing the sheet using the corner part of the tool and moving the tool upward or downward simultaneously similar to general IF. In addition, a concave-convex mixed shape can be formed by changing the vertical direction motion during forming.

2.2.2 Design of Penetrating Tool

Two general structures of a penetrating tool can be, similar to a bobbin tool: a monolithic structure or separable structure. A separable structure was used due to the disadvantages of monolithic structure listed below. The first and most important disadvantage is that it is impossible to remove a monolithic structured tool from the sheet after forming. Second, a whole part of the tool must be discarded upon probe

fracturing, which often occurs in BTFSW [9]. Third, it is impossible to adjust the gap, necessitating the manufacture of various penetrating tools of differential gap sizes. Fourth, it is difficult to manufacture a monolithic penetrating tools with a small gap.

A separable penetrating tool that can overcome the abovementioned disadvantages was designed, as shown in Fig. 2.2. The separable penetrating tool was composed of six parts: tool shank, top tool, middle screw (probe), bottom tool, screw locker, and joint screws. A commercial hexagonal bolt was used as a middle screw to join the top and bottom tools, which were also jointed with a screw locker, forming a column with a groove. The screw locker was jointed with the middle screw using the groove as a key. The screw locker, middle screw, and bottom tool were joined together by two joint screws. The top tool jointed the tool shank using the double-nut tightening method. A hole for tightening and removing the top tool was also drilled. Using a separable penetrating tool, the gap between the top and bottom tools can be adjusted, usability is improved, and cost and changing time were reduced when the middle screw must be changed because tool fracturing occurs. All parts were composed of a stainless steel (JIS: SUS304.). It should be noted that the combination of screw thread orientations and tool rotation directions can only be selected in the fixed combination, which means a right-thread bolt with clockwise (CW) tool rotation direction and a left-thread bolt with counterclockwise (CCW) tool rotation direction. The top tool and also the middle screw will be loosened from the tool shank because the top tool and also middle screw will be subjected a torque of the opposite direction to the tool rotation direction when the other combination was applied. In this work, combination of a right-thread screw and tool rotation direction of CW was used. Figure 2.3 shows the appearance of the prepared penetrating tool.

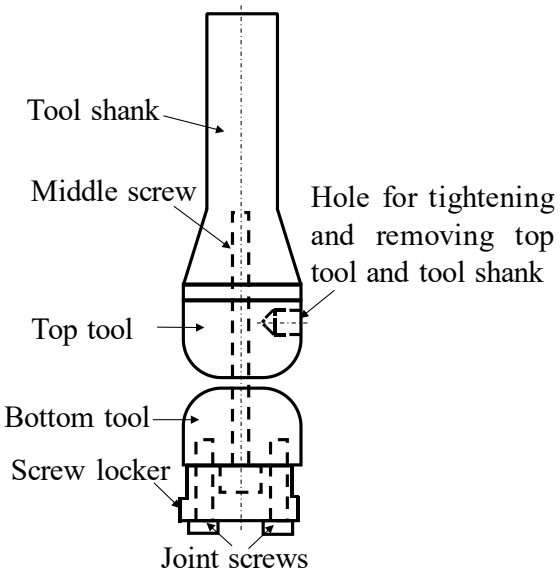

Fig. 2.2 Structure of separable penetrating tool.

Fig. 2.3 Photo of designed separable penetrating tool.

2.3 Experimental Methods

2.3.1 Friction Stir Welding Using Penetrating Tool

It is not advisable to conduct the PTFSIF experiment from the beginning because welding and forming will have to be optimized simultaneously in a 3-dimensional space. Thus, a friction stir welding experiment with stir-in-plate using the new developed penetrating tool was conducted as a preliminary experiment for finding the successful welding conditions, referred to the values of a gap between the top and bottom tools, tool rotation rate, and tool feed rate. Here the successful friction stir welding means tool travels freely without leaving any defects in the sheet.

A machining center (Okuma Corp., MILLAC44VII) was used for the friction stir welding experiment and Fig. 2.4 shows the experimental setup. A sheet was placed on a table with a square hole and fixed in place using a blank holder and bolts. Because the tool penetrates the sheet during forming, a tool hole was drilled in the left bottom corner of the square hole to adjust the location of the penetrating tool and sheet in the Z direction at the starting point. The developed separable penetrating tool was used as a welding tool and its dimensions are shown in Fig. 2.5. Commercial pure aluminum (JIS: A1050-O) sheets were used for the workpiece with dimensions of 200 mm × 200 mm × 2 mm. Pure aluminum was selected because the penetrating tool material was stainless steel (JIS: SUS304), which cannot be used in friction stir welding due to its insufficient hardness and heat resistance. The main parameters in friction stir welding were the gap between the top and bottom tools, G_p, tool rotation rate for welding, ω_w, and tool feed rate for welding, v_w. The values of these parameters used in the experiments are shown in Table 2.1. The rotational direction of the penetrating tool was CW.

Table 2.1 Experimental conditions of FSW.

Gap, G_p /mm	1.6, 1.8, 2.0
Tool rotation rate for welding, ω_w /rpm	1000, 2000, 3000
Tool feed rate for welding, v_w /mm·min^{-1}	200, 1000, 2000, 3000

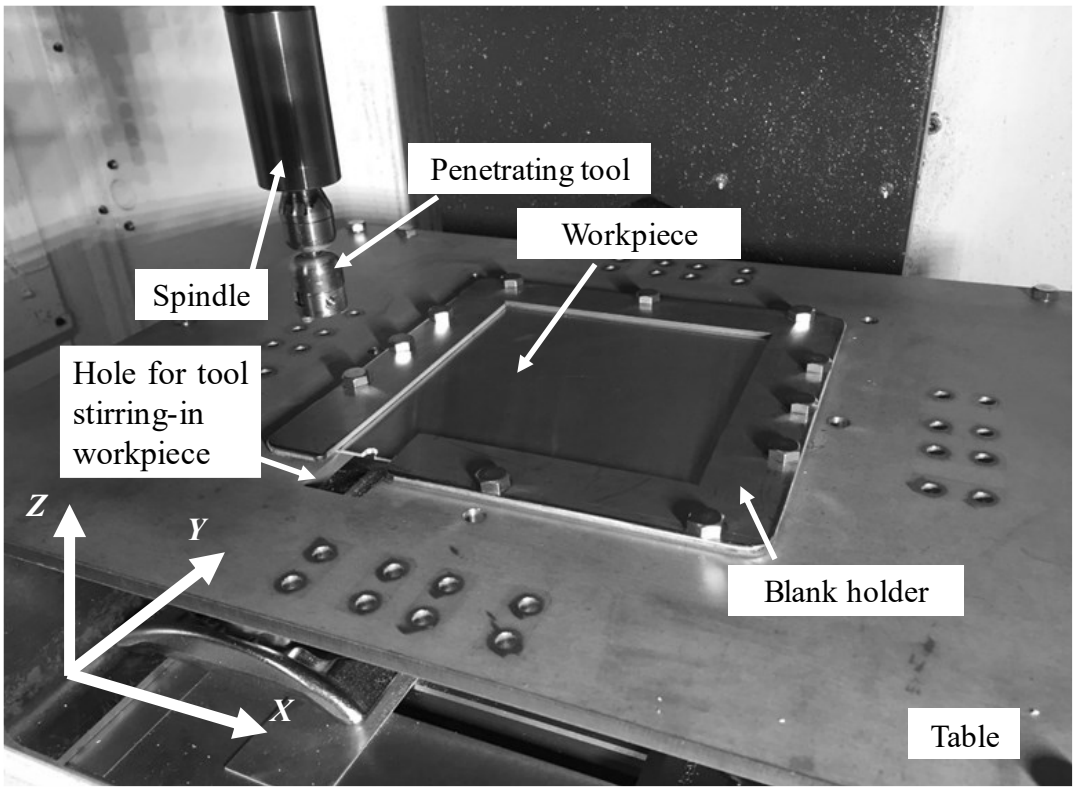

Fig. 2.4 Photo of experimental apparatus.

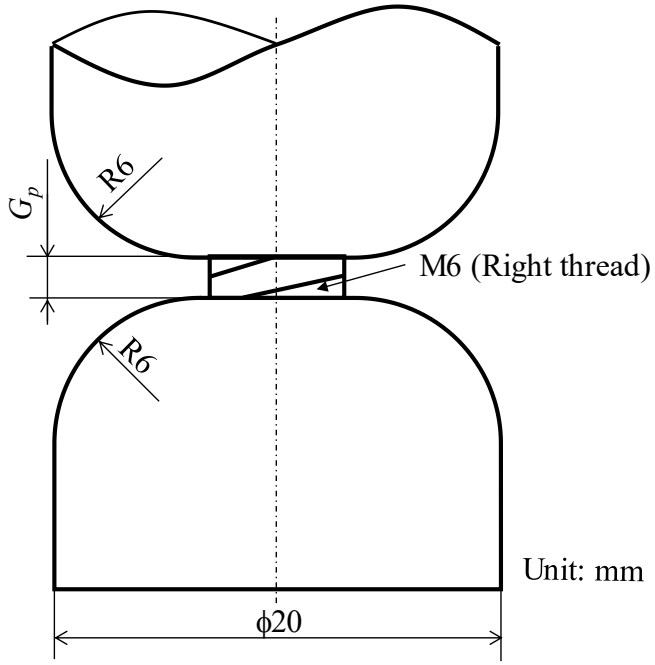

Fig. 2.5 Dimensions of penetrating tool.

When designing a tool path of friction stir welding experiment with stir-in-plate, following points should be considered. First, the welding length should be as long as possible because welding condition change with increase of welding length. Second, straight line, curve of CW direction and curve of CCW direction should be contained in the tool path. Third, the shape of the workpiece should be also taken into consideration. In this experiment, the used workpiece was a 200 mm × 200 mm square sheet. Considering above mentioned, a tool path as shown in Fig. 2.6 was designed for FSW, and corner radius of R = 20 mm was the results of those considerations.

In Fig. 2.6, the dotted line at the beginning of the tool path represents the FSW guide line. In BTFSW, setting a guide line is a common method for avoiding the tool fracture at the tool plunging stage. In the guide line, the tool was plunged into the sheet usually at a slower feed rate (comparing with tool feed rate for welding). In this work, tool was plunged into the sheet at a tool rotation rate for guide line of ω_g = 1000 rpm and tool feed rate for guide line of v_g = 200 mm/min. Subsequently, the tool rotation rate and feed rate were changed to tool rotation rate for welding, ω_w, and tool feed rate for welding, v_w. After welding, the tool was moved back to the starting point. Herein, since friction stir welding was used as a preliminary experiment for PTFSIF, the welding results were judged from appearance of the welded sheets and occurrence of tool fracture during FSW.

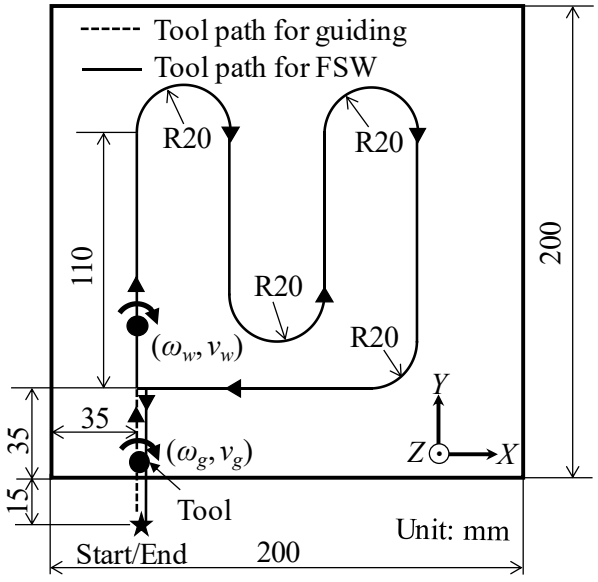

Fig. 2.6 Tool path of FSW. (ω_g = 1000 rpm, v_g = 200 mm/min)

2.3.2 Penetrating Tool Friction Stir Incremental Forming Experiment

The forming machine, penetrating tool, and workpieces used for the forming experiments were identical as those used in the friction stir welding experiments described in Section 2.3.1. The forming of three objective shapes, as well as concave, convex, and concave-convex mixed shapes were performed under tool path directions of CW and CCW. For the concave and convex shapes, the objective shape was a truncated cone, which is a classical forming objective shape in incremental forming field. The depth and height of the concave and convex cones were called d and h. The objective shape for the concave-convex mixed shape involved the overlap of a larger concave truncated cone with a smaller convex truncated cone at the concave cone center, where w was distance between the large concave and small convex cones. The bottom diameters of the objective concave, convex, and concave-convex mixed shapes were 114 mm with a wall angle θ of 45°. Figure 2.7 shows the tool path of PTFSIF of the three objective shapes. The guide line tool path for tool plunging into the sheet in PTFSIF was set to the same specifications described in Section 2.3.1, which the tool were plunged into the sheet at a tool rotation rate for guide line of ω_g = 1000 rpm and tool feed rate for guide line of v_g = 200 mm/min in the guide line. After leading the tool into the sheet, the tool rotation rate and feed rate were changed to the tool rotation rate for forming. ω_f, and tool feed rate for forming, v_f, using a contour line strategy. The gap, G_p, tool rotation rate for forming, ω_f, and tool feed rate for forming, v_f, were set based on the FSW experimental results reported in Section 2.4.1. Table 2.2 lists the experimental conditions of PTFSIF.

Forming was stopped when the NC program ended or sheet fracturing occurred. After forming, the sheet and tool were removed by disassembling the tool. After the penetrating tool was removed from the sheet, a key hole was left in the sheet as well as BTFSW. The top surface profile of the formed shape was measured using a laser displacement meter. The sheet thickness and thickness in Z direction of formed sheet were measured using the sectional profile photos via an image processing software.

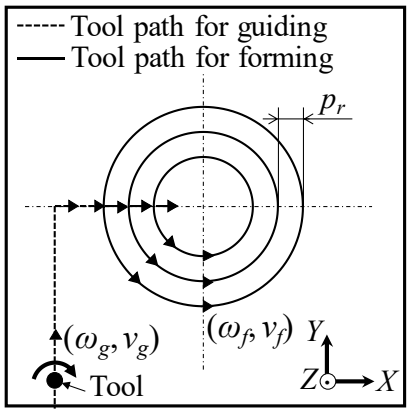

(a) Top view tool path of concave, convex and concave-convex forming

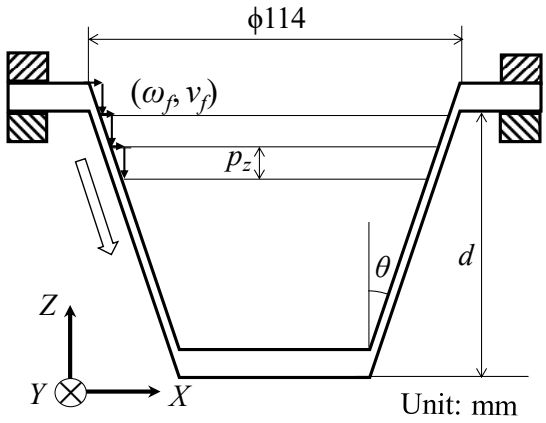

(b) Front view tool path of concave forming

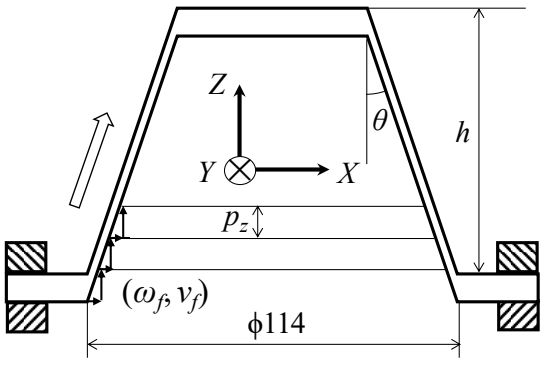

Unit: mm

(b) Front view tool path of concave forming

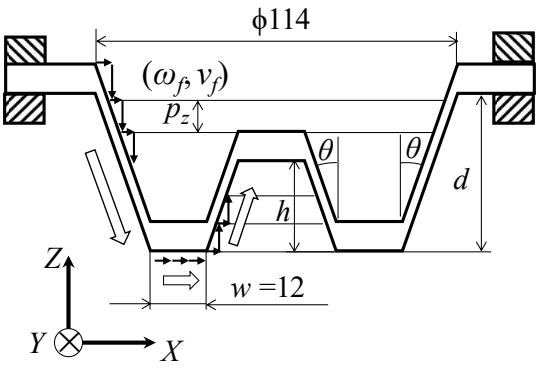

Unit: mm

(d) Front view tool path of concave-convex mixed forming

Fig. 2.7 Tool path of PTFSIF.

Table 2.2 Experimental conditions of PTFSIF.

Gap, G_p /mm	1.8
Tool rotation rate for forming, ω_f /rpm	1000, 2000, 3000
Tool feed rate for forming, v_f /mm·min^{-1}	200, 1000, 2000, 3000

2.4 Results and Discussions

2.4.1 Friction Stir Welding Using Penetrating Tool

Figure 2.8 shows the results of friction stir welding under different tool gaps, G_p, tool rotation for welding rates, ω_w, and tool feed rates for welding, v_w. Open circle marks indicate that FSW was successful. Cross marks indicate that sheet fractured. Triangle marks indicate that welded sheets with defects. Square marks indicate that tool fractured. It is clear that at G_p = 1.8 mm, the welding conditions was widest. Figure 2.9 shows the appearances of a successfully welded sheet, fractured sheet, and welded sheet with a defect in bottom surface. Thus, it was determined that the G_p should be set to a proper value smaller than the sheet thickness, but not excessively small. From these optimization results, G_p =1.8 mm was used in the subsequent PTFSIF.

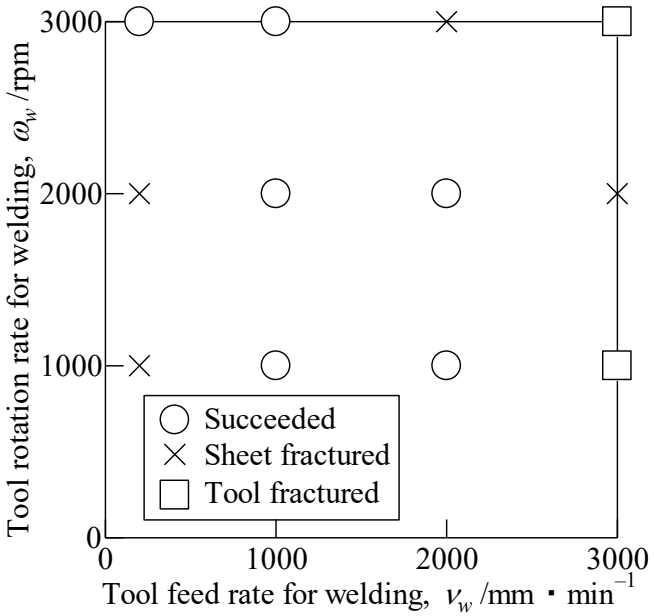

(a) G_p =1.6 mm

Fig. 2.8 Results of FSW with the penetrating tool under different gaps, tool rotation rates for welding, and tool feed rates for welding.

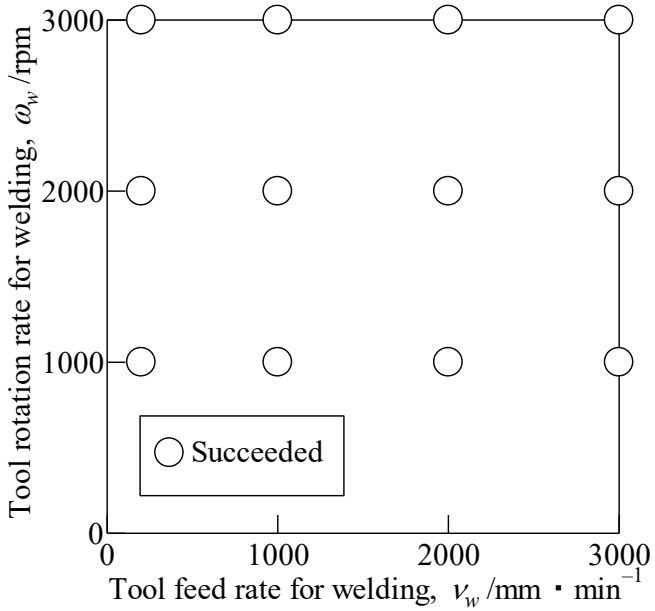

(b) G_p =1.8 mm

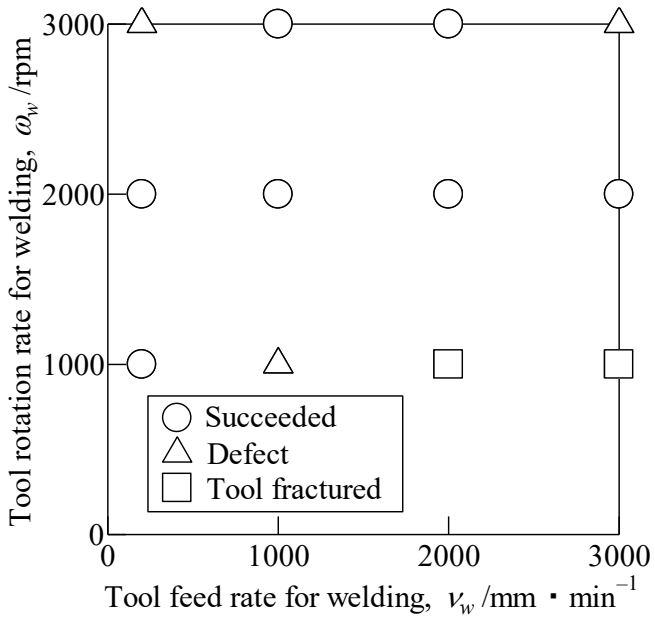

(c) G_p =2.0 mm

Fig. 2.8 Results of FSW with the penetrating tool under different gaps, tool rotation rates for welding, and tool feed rates for welding.

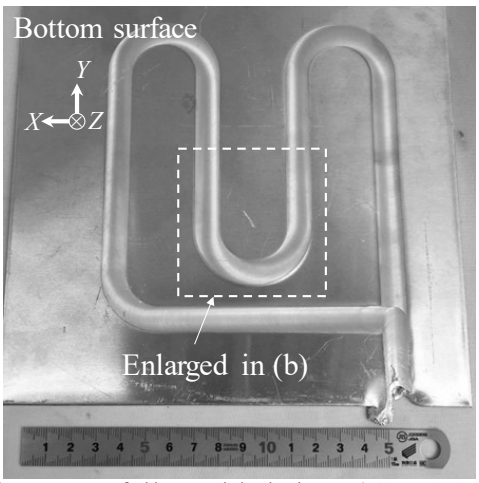

(a) Successfully welded sheet (G_p = 1.8 mm, ω_w = 1000 rpm, v_w = 200 mm/min)

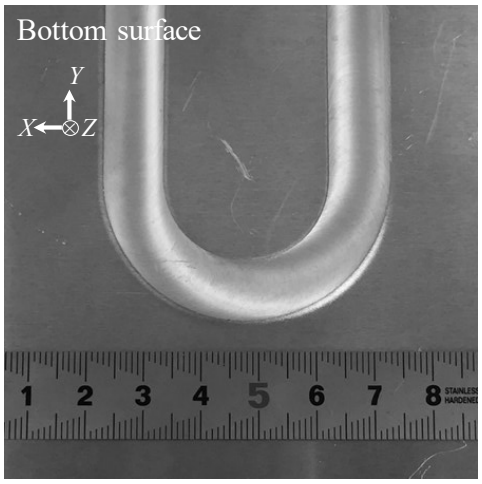

(b) Enlarged view of successfully welded sheet

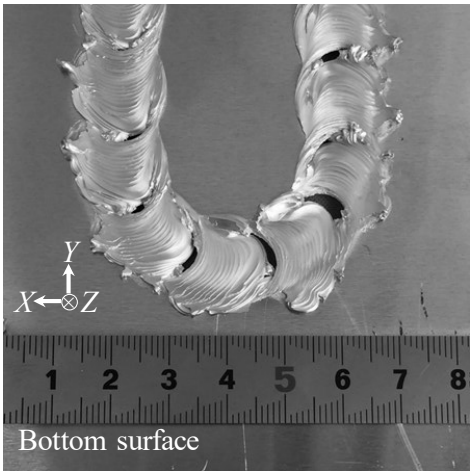

(c) Fractured sheet (G_p = 1.6 mm, ω_w = 3000 rpm, v_w = 2000 mm/min)

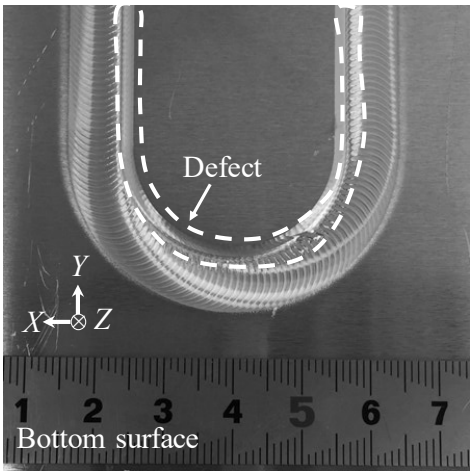

(d) Sheet with defect (G_p = 2.0 mm, ω_w = 1000 rpm, v_w = 1000 mm/min)

Fig. 2.9 Photo of FSWed sheet by penetrating tool.

2.4.2 Penetrating Tool Friction Stir Incremental Forming

Figure 2.10 shows the forming results of concave and convex shapes at different forming depths or heights under the tool path direction of CCW. The forming conditions involved a tool rotation rate for forming of ω_f = 1000 rpm and tool feed rate for forming of v_f = 200 mm/min. The open circle marks indicate that forming was successful, without defects or fractures after forming. Square marks indicate groove-like defects after forming. All of the groove-like defect was located in the bottom surface of the sheet. The cross marks indicate that the sheet fractured before forming completion. Figure 2.11 shows the appearances of a successfully formed sheet, groove-like defect in the sectional view, and the fractured sheet described in Fig. 2.10.

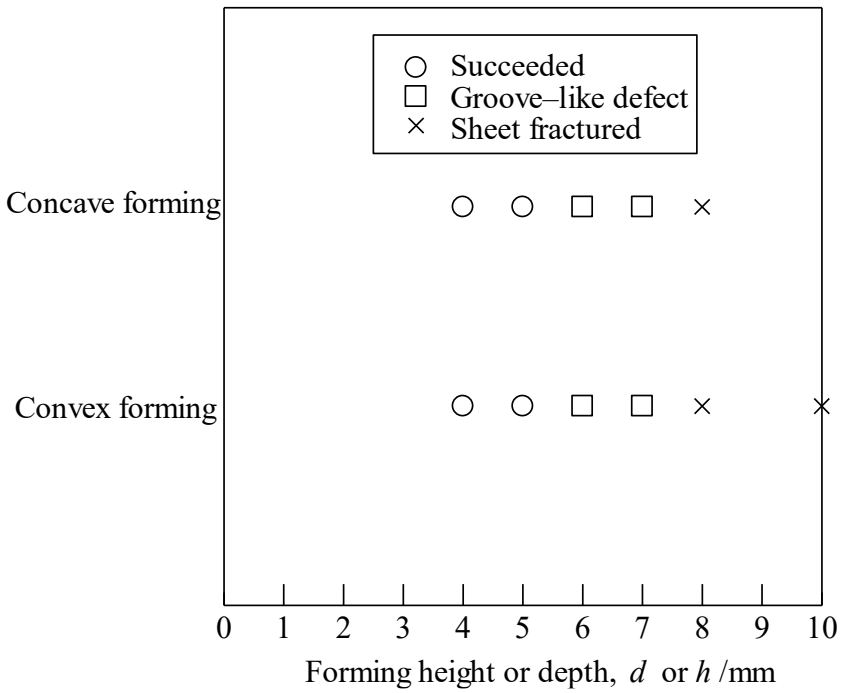

Fig. 2.10 Forming results of PTFSIF (tool rotation rate ω_f = 1000 rpm, v_f = 200 mm/min).

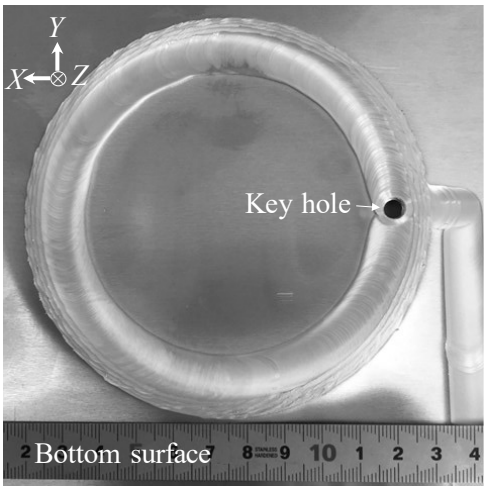

(a) Without defect

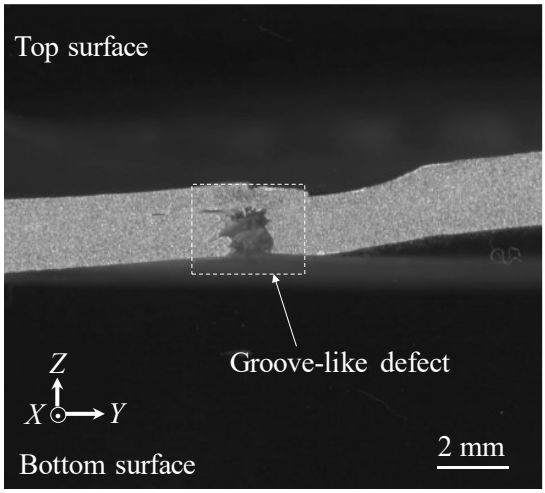

(b) With groove-like defect

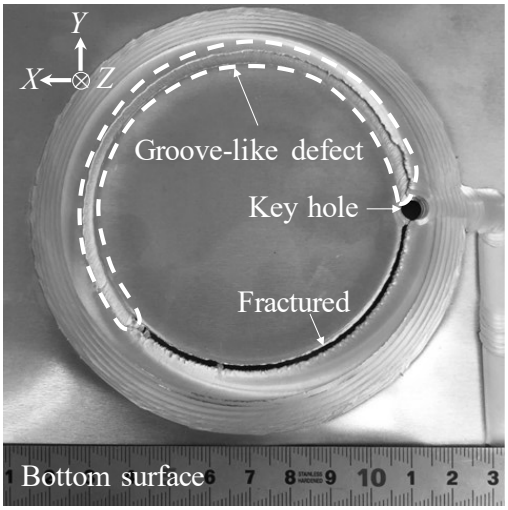

(c) Sheet fractured

Fig. 2.11 Appearance of forming results of PTFSIFed sheet of concave shape.

The forming results at varied tool rotation rates for forming, ω_f, tool feed rates for forming, v_f, and tool path direction of CW followed the same trend as shown in Fig. 2.10, which the sheet was formed successfully only at shallow depths or heights, and defects occurred when the forming continued. From those results, it was determined that concave and convex forming were possible by PTFSIF, but the formable depth or height was quite shallow.

The height or the depth of 7 mm, which are height or depth just before sheet fractured in the experiment as show in Fig.2.10, was used as samples of appearances and shapes of concave, convex and concave-convex mixed shape formed by PTFSIF. The appearances of concave, convex, and concave-convex mixed forming are shown in Fig. 2.12 and their measured surface profiles are plotted in Fig. 2.13. From Fig. 2.13, the surface conditions of the formed sheet were not optimal since the tool mark of each contour can be clearly observed. From Fig. 2.13, it is clear that an upheaval was formed because the materials in the center did not sink or rise to the same extent as the top or bottom tool pushing. All achieved depths or heights were shallower than the ideal shape.

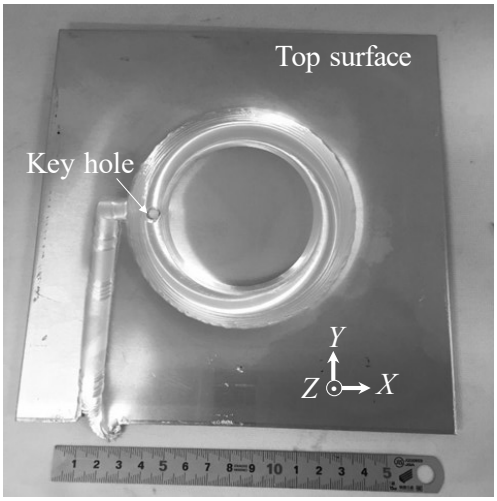

(a) Concave shape (d = 7 mm)

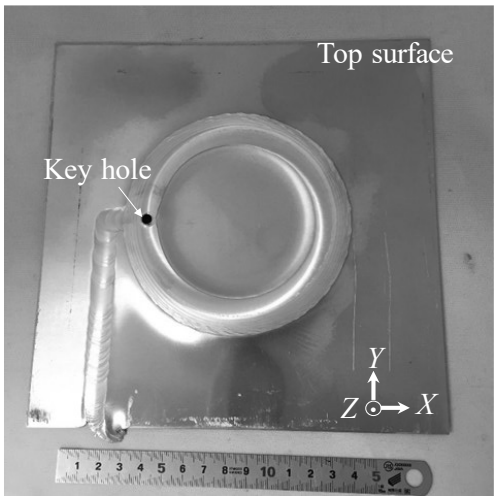

(b) Convex shape (h = 7 mm)

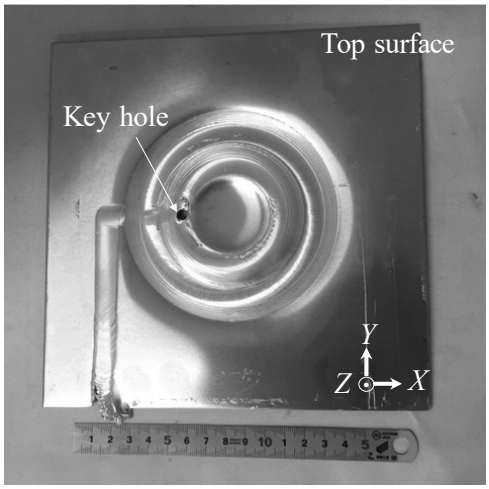

(c) Concave-convex mixed shape (d = 7 mm, h = 7 mm)

Fig. 2.12 Appearance of three kinds of shape formed by PTFSIF (ω_f = 1000 rpm, v_f = 200 mm/min).

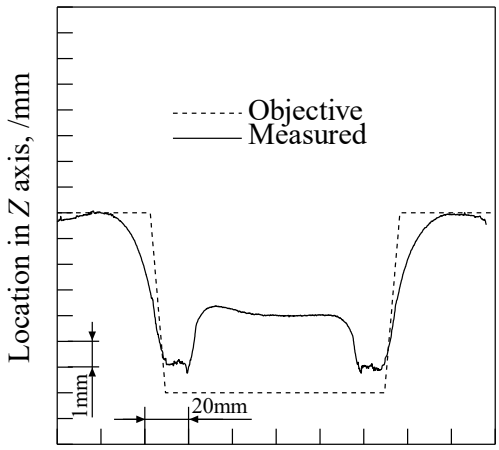

(a) Concave shape (d = 7 mm)

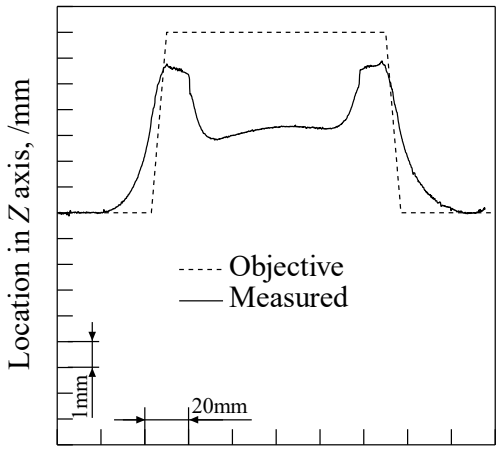

(b) Convex shape (h = 7 mm)

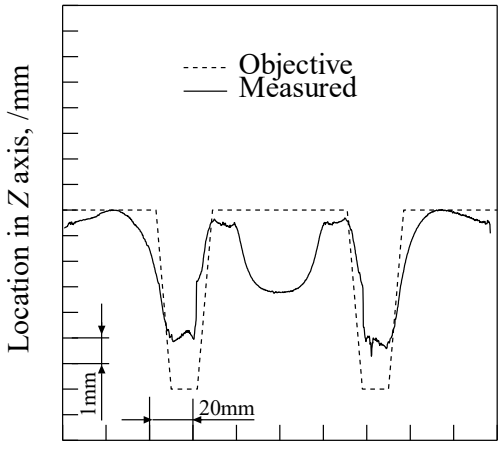

(c) Concave-convex mixed shape (d = 7 mm, h = 7 mm)

Fig. 2.13 Sectional profile of formed sheet by PTFSIF (ω_f = 1000 rpm, v_f = 200 mm/min).

2.4.3 Groove-like Defect and Material Flow

Figure 2.14 shows the appearance of a groove-like defect at forming depths of d = 6, 7, and 8 mm for concave forming. Groove-like defects occurred at d = 6 mm, but only occupied a small area, whereas the groove-like defects occurred over all the formed area at d = 7 mm. The width and depth of the groove-like defects at d = 8 mm were wider and deeper than that at d = 7 mm. The sheet fractured at d = 8 mm, indicating that the depth of a groove was equal to the original sheet thickness. These results indicate that groove-like defects become wider and deeper as the forming proceeds, finally resulting in sheet fracture as the groove penetrates into the sheet. Therefore, it is clear that the formation of groove-like defects during forming ensured that only shallow forming can be achieved.

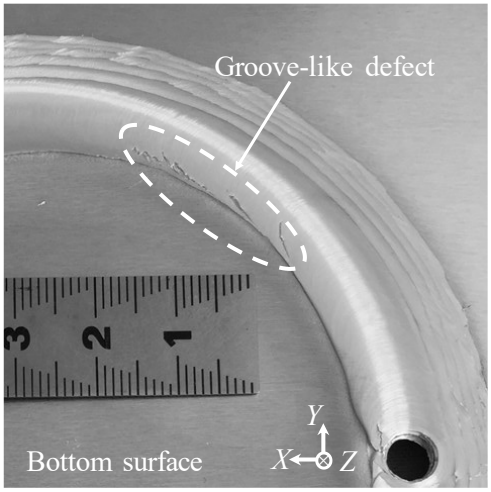

(a) d = 6 mm

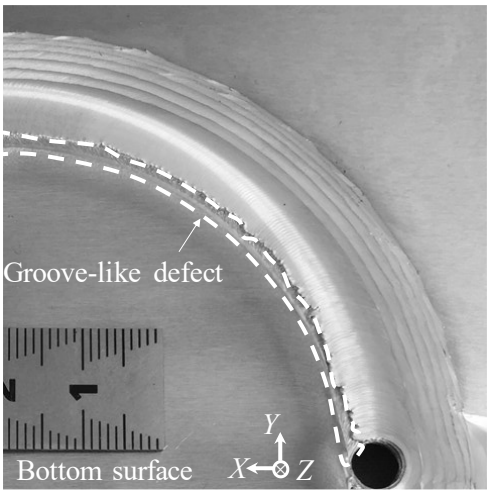

(b) d = 7 mm

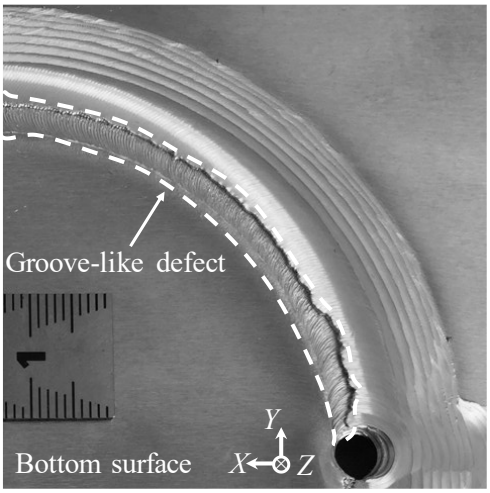

(c) d = 8 mm

Fig. 2.14 Appearance of groove-like defect in different forming depth.

In FSW, the advancing side (AS) is the side at which the tool rotation and traveling direction are the same, whereas the retreating side (RS) is the opposite [16]. In this experiment, the tool rotation direction was CW, so the location of AS and RS on the sheet depends on the tool path direction. The location of AS and RS on the sheet under tool path direction of CW and CCW were shown in Fig. 2.15. When tool path direction is CW, outer of the tool path is AS and the inner of the tool path is RS. From Fig.2.15, it should be noted that the area of AS increases with forming proceed. When the tool path direction is CCW, outer of the tool path is RS and the inner of the tool path is AS. So, the area of RS increases with proceeding of forming. In PTFSIF, whether for the tool path direction of CW or CCW, the groove-like defects formed at bottom surface because material was transferred from bottom surface to top surface due to the forming conditions where the right-thread screw and tool rotation were CW.

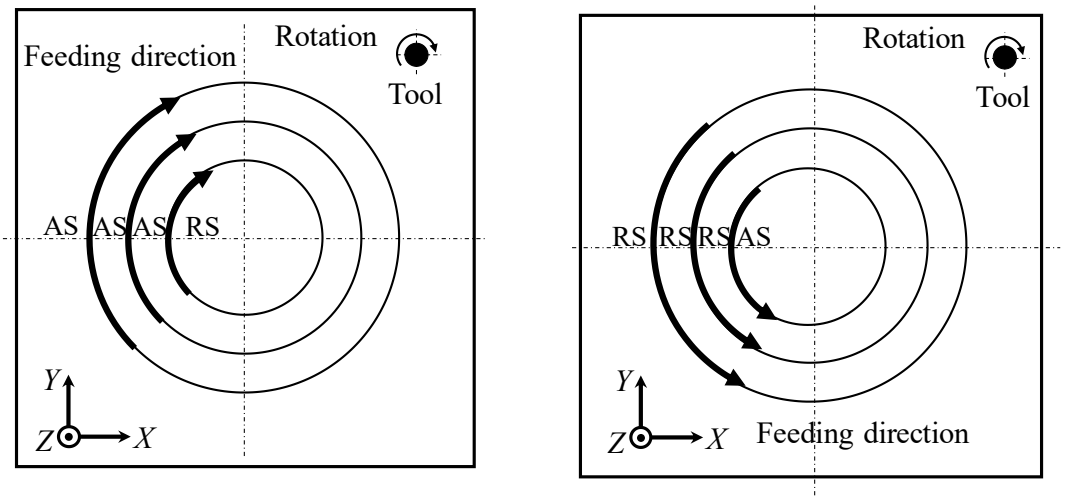

(a) Tool path direction of CW (b) Tool path direction of CCW

Fig. 2.15 Location of AS and RS on the sheet.

Figure 1.2 shows the ideal changing of sheet thickness during IF in cross-sectional plane perpendicular to Y-axis. θ is the wall angle, t_0 is the initial sheet thickness, t_1 is thickness of formed sheet, and t_z is thickness in Z direction of formed sheet. Thickness in Z direction, t_z was defined as the distance between upper and lower surface in the same location in X and Y direction. Because no material was consumed, the volume of sheet should not change, which means t_z equals t_0. Volume distribution was defined as material's volume along the radial direction. Because volume was effected by the thickness in Z direction of formed sheet, t_z, can be used as an indicator of material flow in and out in the AS and RS. Figure 2.16 shows sectional profiles of PTFSIFed concave shape under tool path direction of CW and CCW. For a better understanding of material flow, the sectional profile was divided into unformed, formed, tool place, and center parts. It can be seen that under the tool path direction of CW, burr was generated in the bottom of the sheet due to the material flow.

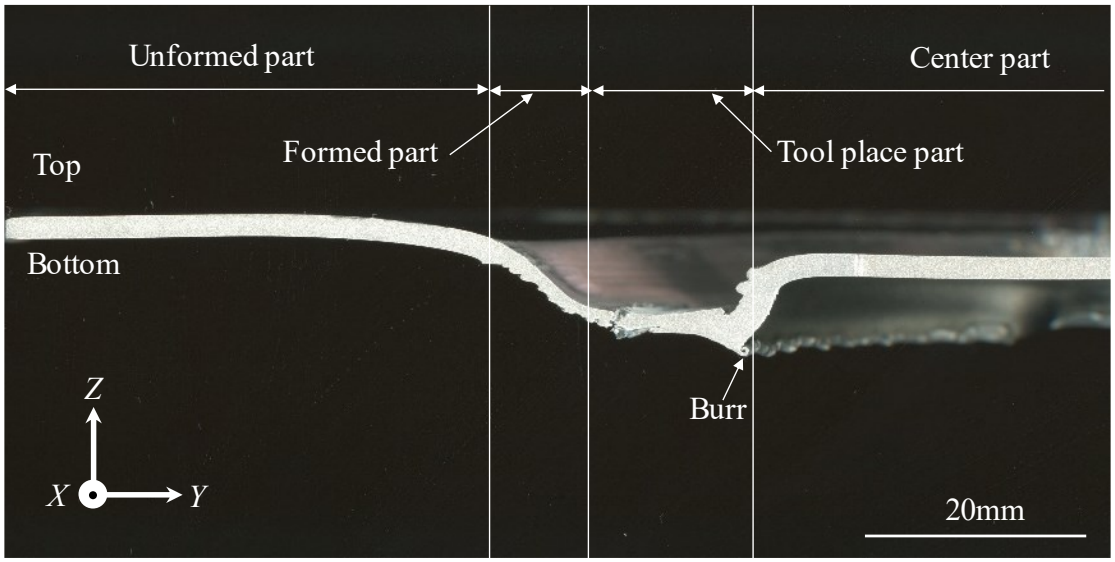

(a) CW

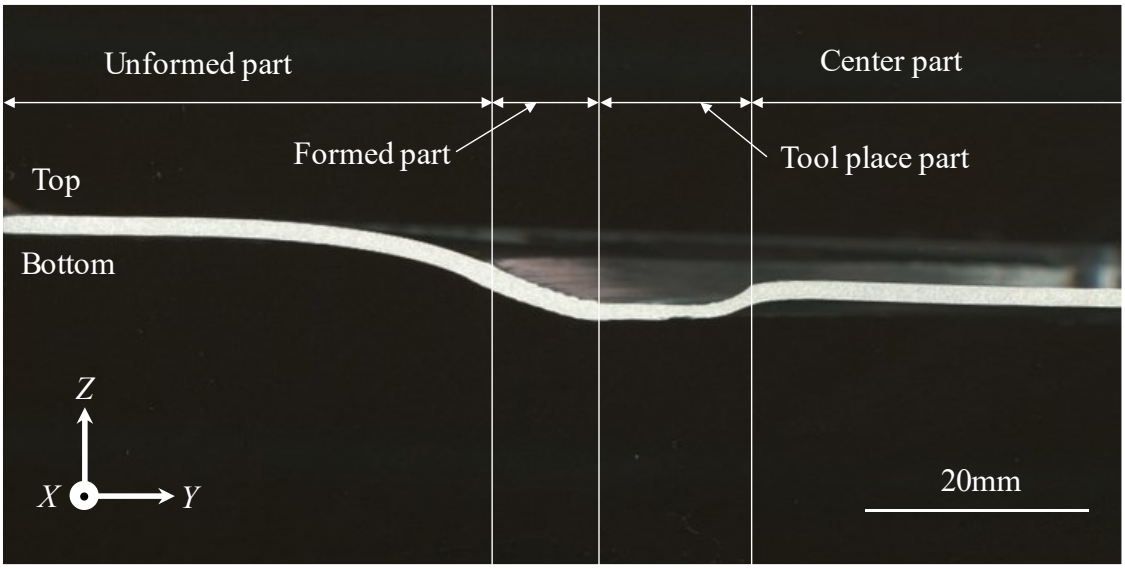

(b) CCW

Fig. 2.16 Appearance of cross section of formed sheet by PTFSIF (Concave shape).

The sheet thickness distributions of formed sheet, t_1 are shown in Fig. 2.17. From Fig. 2.17, it can be seen that the t_1 of formed part under tool path direction of CCW was thicker than t_0 and t_1 of formed part under tool path direction of CW was thinner than t_0. This is different from the thickness formed by general incremental forming where the thickness was assumed to observe the "sine law" [10].

As described above, t_z can be used as an indicator of material flow in incremental sheet forming. And as shown in Fig. 2.15, the tool path on the sheet was from periphery to center. Therefore, the area of center part was reduced as forming proceeded. From this point of view, the sheet can be divided into 5 areas, an unformed part, formed part, RS of tool place, AS of tool place and the center.

Figure 2.18 shows the distribution of t_z of AS and RS under tool path direction of CW and CCW. The thickness in the Z direction, t_z at the RS was larger than that at the AS whether the tool path direction was CW or CCW. This indicates that the material flows from the AS to RS during PTFSIF because the volume is constant. The formation of groove-like defects was caused by the material flow from the AS to RS, which is also the reason why groove-like defects only occurred in the AS.

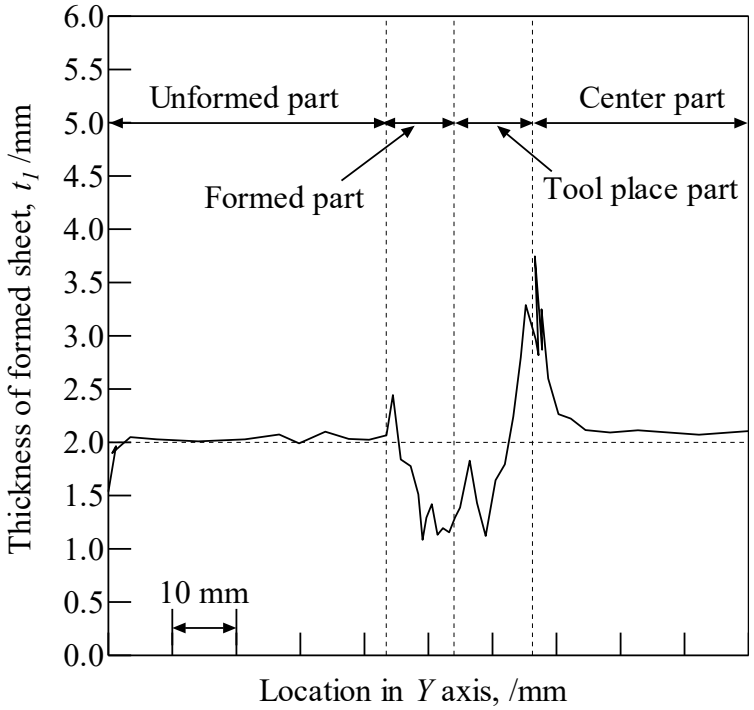

(a) Tool path direction of CW

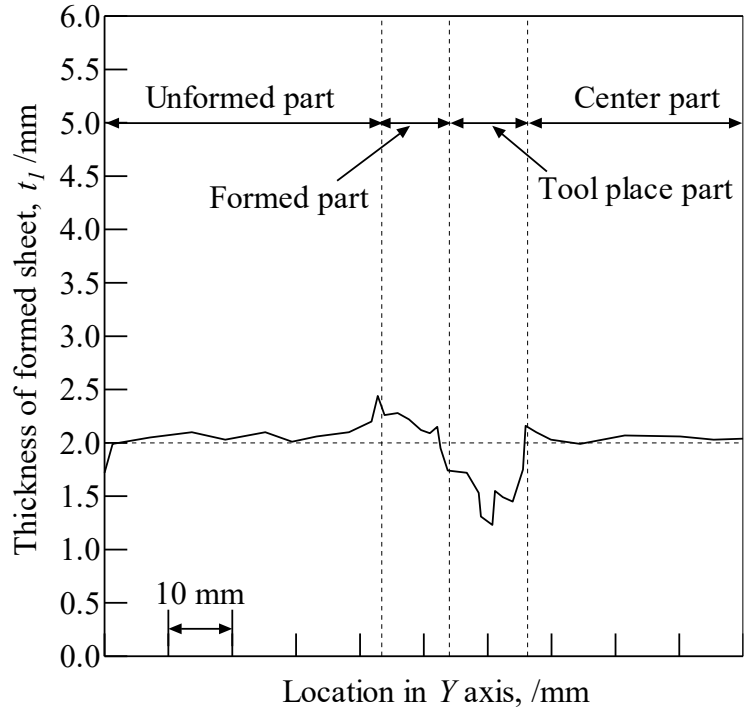

(b) Tool path direction of CCW

Fig. 2.17 Distribution of thickens of PTFSIFed sheet.

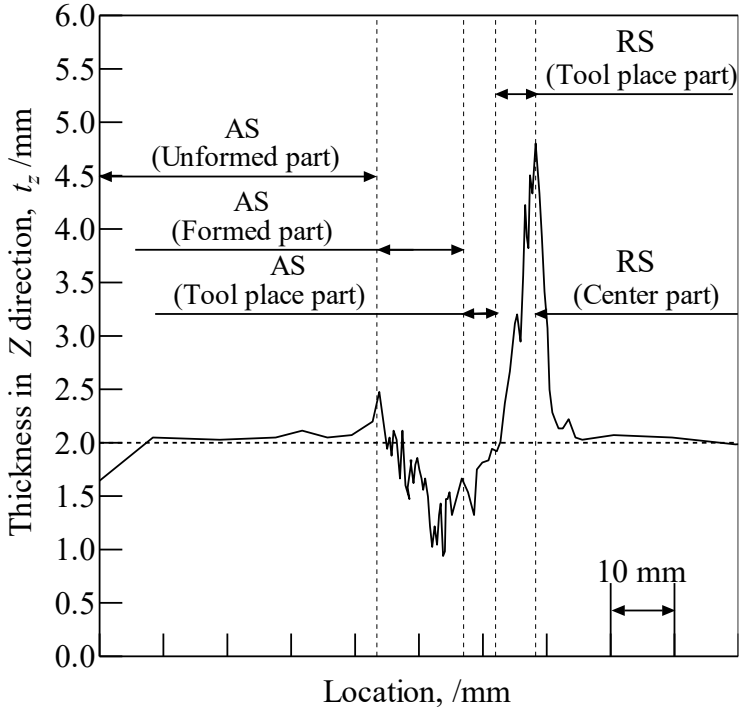

(a) Tool path direction of CW

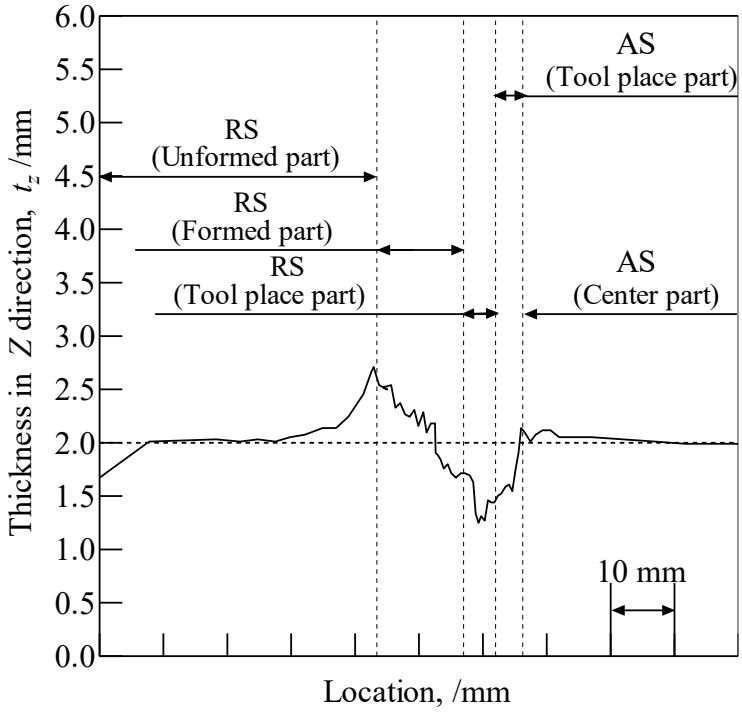

(b) Tool path direction of CCW

Fig. 2.18 Distribution of thickness in Z direction of PTFSIFed sheet in sectional direction (concave shape, ω_f = 1000 rpm, v_f = 200 mm/min, d = 10 mm).

2.5 Conclusions

Herein, friction stir incremental forming experiments were performed using a novel penetrating tool. The following results were obtained.

(1) Forming of concave, convex and concave-convex mixed shapes by the developed penetrating tool friction stir incremental forming was possible.

(2) The formable depth or height was shallow since groove-like defects occurred during the forming and penetrated the sheet.

(3) The material flows from the AS to the RS during penetrating tool friction stir incremental forming process. Excessive material flow caused the groove-like defects and sheet fractures.

(4) The thickness distribution of the formed sheet by penetrating tool friction stir incremental forming was different from general incremental forming.

References

[1] H. Amino, Development of dieless forming machine for metal plate, *J. Jpn. Soc. Technol. Plast*., **51** (2010), 1119–1123. (In Japanese)

[2] A. Attanasio, E. Ceretti, C. Giardini and L. Mazzoni, Asymmetric two points incremental forming: Improving surface quality and geometric accuracy by tool path optimization, *J. Mater. Process. Technol*., **197** (2008), 59-67.

[3] E. Maidagan, J. Zettler, M. Bambach, P. P. Rodríguez and G. Hirt, A new incremental sheet forming process based on a flexible supporting die system, *Key Eng. Mater*., **344** (2007), 607-614.

[4] H. Meier, V. Smukala, O. Dewald and J. Zhang, Two Point Incremental Forming with Two Moving Forming Tools, *Key Eng. Mater*., **344** (2007), 599-605.

[5] R. S. Mishra and Z. Y. Ma, Friction stir welding and processing, *Mater. Sci. Eng*., **R50** (2005), 1-78.

[6] W. M. Thomas, C. S. Wiesner, D. J. Marks and D. G. Staines, Conventional and bobbin friction stir welding of 12% chromium alloy steel using composite refractory tool materials, *Sci. Technol. weld. Joining*, **14** (2009), 247-253.

[7] M. Otsu, H. Matsuo, M. Matsuda and K. Takashima, Friction stir incremental forming of aluminum alloy sheets, *Steel Res. Int*., **81** (2010), 942–945.

[8] M. Otsu, T. Ichikawa, M. Matsuda and K. Takashima, Improvement of formability of magnesium alloy sheets by friction stir incremental forming, *Steel Res. Int. Special Eds*., (2011), 537–541.

[9] Japan welding society, Friction stir welding (SANPO publications, INC, 2006) 15.

[10] S. Matsubara, Incremental backward bulge forming of a sheet metal with a hemispherical head tool—A study of a numerical control forming system II—, *J. Jpn. Soc. Technol. Plast*., **35** (1994), 1311-1316. (In Japanese)

CHAPTER 3

GROOVE-LIKE DEFECT

3.1 Introduction

Even though PTFSIF can form concave-convex mixed shapes, its formability is still low as mentioned in chapter 2. The maximum forming depth is about 8 mm under the concave shapes forming. The reason why PTFSIF's maximum forming depth is shallow is that groove-like defects occurred in the advancing side [1]. The width and depth of the groove-like defects become larger as the process progresses. Finally, groove-like defects penetrate the workpiece and forming failed. As the pitch in Z direction p_z was constant in one forming process, forming depth was proportionate to the forming cycles. By comparing the numbers of forming cycles when groove-like defects occurred under different forming conditions, parameters which affect the groove-like defects formation behavior can be investigated.

In this chapter, numbers of forming cycles when the groove-like defects occurred were used as an evaluation item to investigate the formation of groove-like defects. Experimental conditions such as pitch in radial direction, initial radius of the objective cone and wall angle were varied to investigate groove-like defects.

3.2 Experimental Methods

Forming machine and workpieces were the same with chapter 2. Only concave shapes forming were conducted in this chapter and the forming objective shape is a frustum of cone. Figure 3.1 shows the forming tool path. In Fig.3.1 (b), the dotted line is a tool path for guiding in which the tool stir-in the workpiece. During the tool path for guiding, the tool did not move in the Z direction. The solid line is a tool path for forming. As a true spiral forming tool path was impossible to realize in the used machine, one cycle of 4 gradually decreasing quadrant arcs was used as the forming tool path.

The tool rotation rate for forming was ω_f = 600 rpm and tool feed rate for forming was v_f = 200 mm/min. Numbers of cycles before occurring groove-like defect N were used to research groove-like defects formation. Pitch in radial direction p_r, initial radius of the objective cone R_i and wall angle of the objective cone θ were varied to investigate groove-like defects formation behavior.

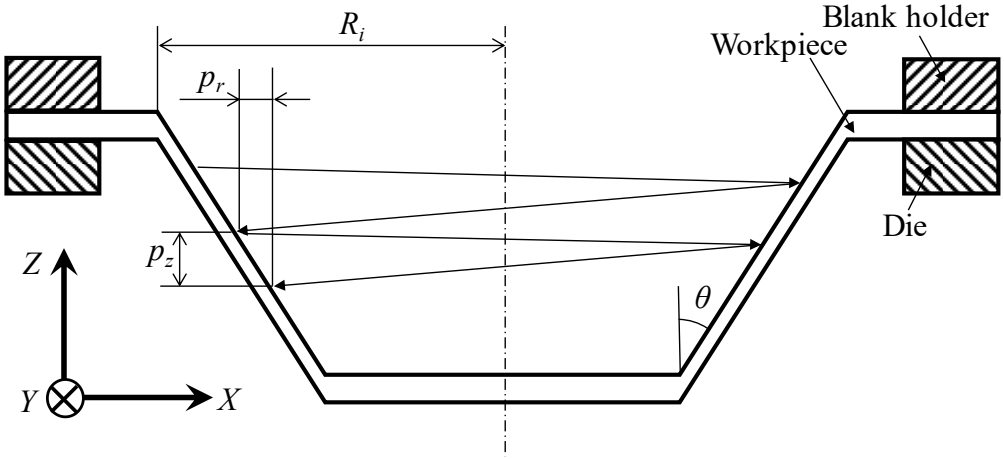

(a) Section view

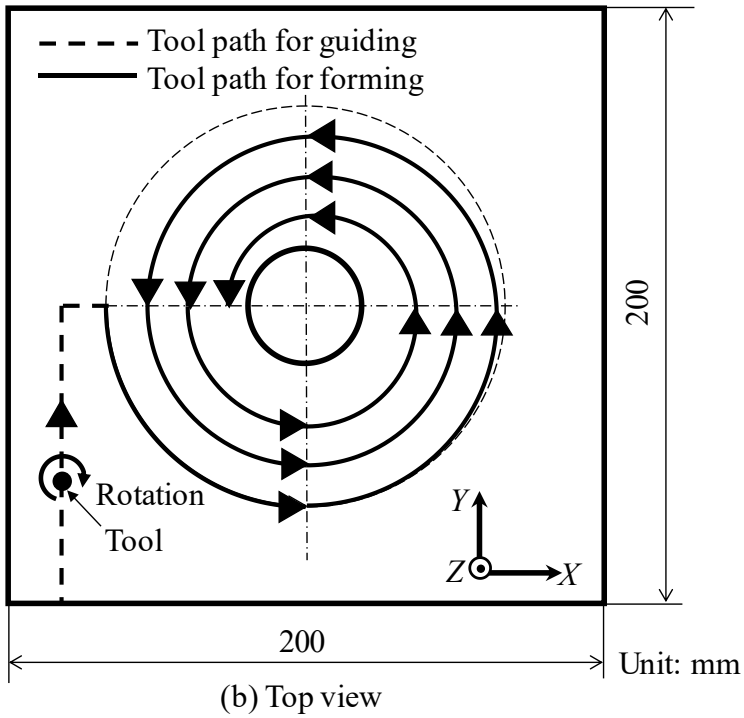

(b) Top view

Fig. 3.1 Tool path of PTFSIF.

3.3 Experimental Results and Discussions

3.3.1 Effect of Pitch in Radial Direction on Groove-like Defects Formation

Figure 3.2 shows the relation between number of cycle before occurring groove-like defects and pitch in radial direction. The initial radius of objective cone was R_i = 50 mm. Two wall angles which θ = 90° and θ = 45° were used. It should be note that when θ = 90°, penetrating tool did not form the sheet into a cone, but only friction stir in the sheet plane. The results showed groove-like defects occurred even in θ = 90°. And N decreased with the increasing of p_r. It was thought that this result was caused by the increasing p_z. Number of cycles before occurring groove-like defects under θ = 90° was larger than that of θ = 45° under the same pitch in radial direction.

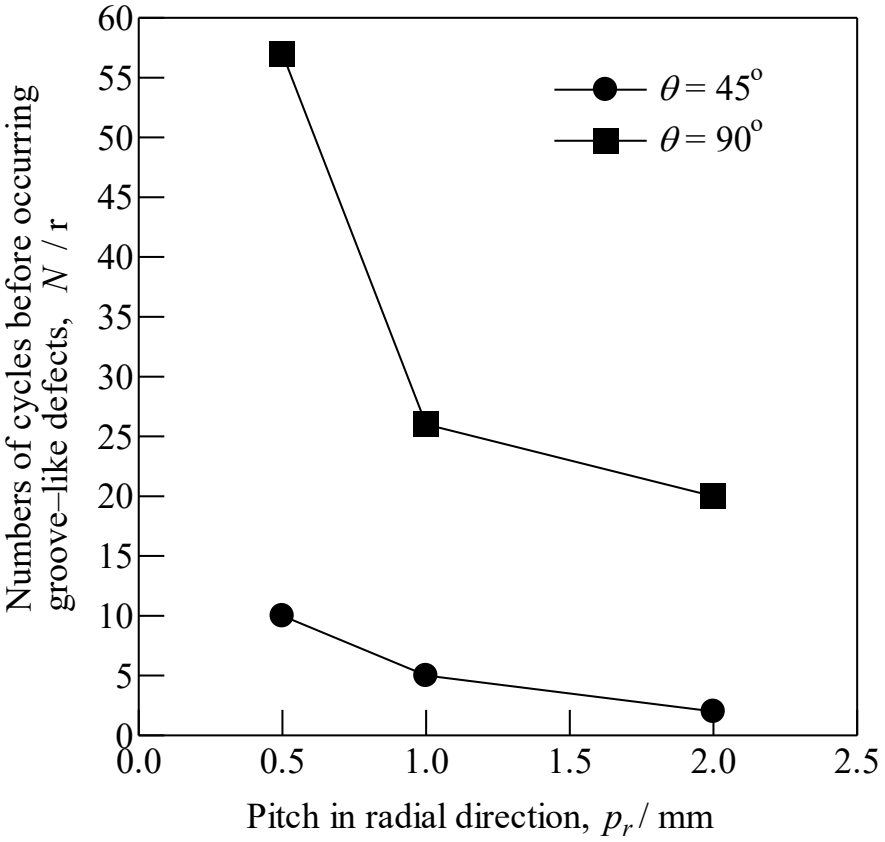

Fig. 3.2 Relation between number of cycles before occurring groove-like defects and pitch in radial direction. (θ = 45°, 90°, R_i = 50 mm)

3.3.2 Effect of Initial Radius on Groove-like Defects Formation

Figure 3.3 shows the relation between initial radius of objective cones and number of cycles before occurring groove-like defect. It is clear that number of cycles before occurring groove-like defect increased with the increasing of initial radius of objective cones. This result means that a groove-like defect was easy to form under a small initial radius. It can be explained by the backfill of material. When the initial radius of objective cone is small, the material is hard to backfill the hole drilled by the probe.

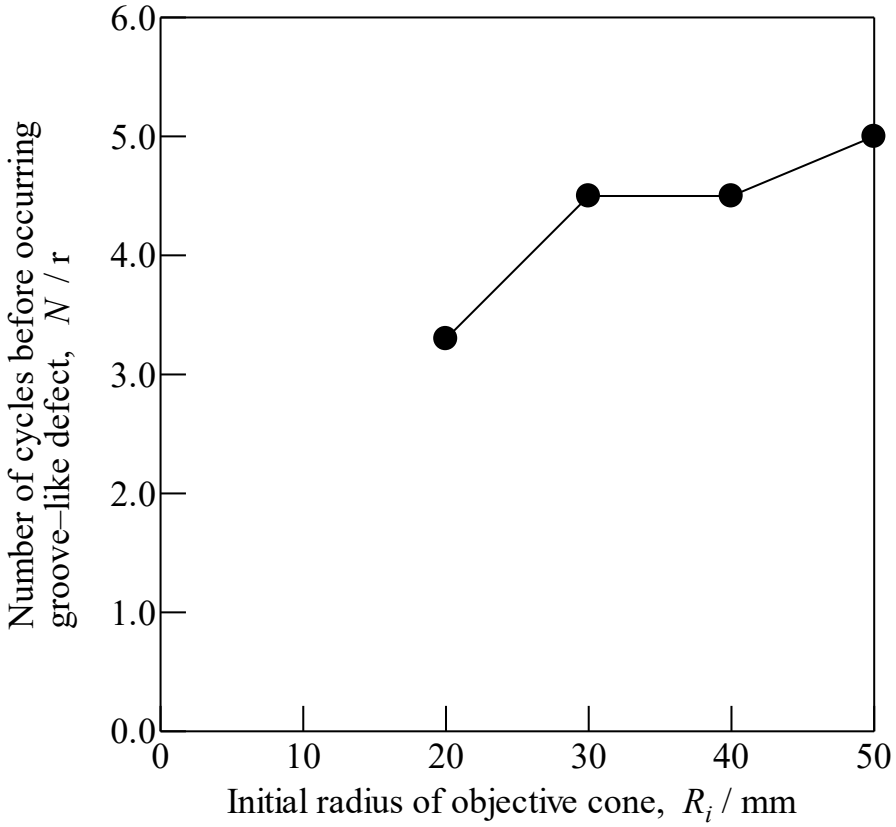

Fig. 3.3 Relation between number of cycles before occurring groove-like defects and initial radius of objective cone. (θ = 45° , p_r = 1 mm)

3.3.3 Effect of Wall Angle on Groove-like Defect Formation

Figure 3.4 shows the relation between wall angle and forming limit in height. The forming limit in height when wall angle $\theta = 90°$ was not connected with other wall angle, as penetrating tool travels in the sheet plane when wall angle $\theta = 90°$. It shows that forming limit in height slightly increased or decreased with the increasing wall angle. As the fluctuation was small, it can be seen that forming limit in height was stable at a value near to 5.2 mm. This means that wall angle has almost no effect on the forming limit in height.

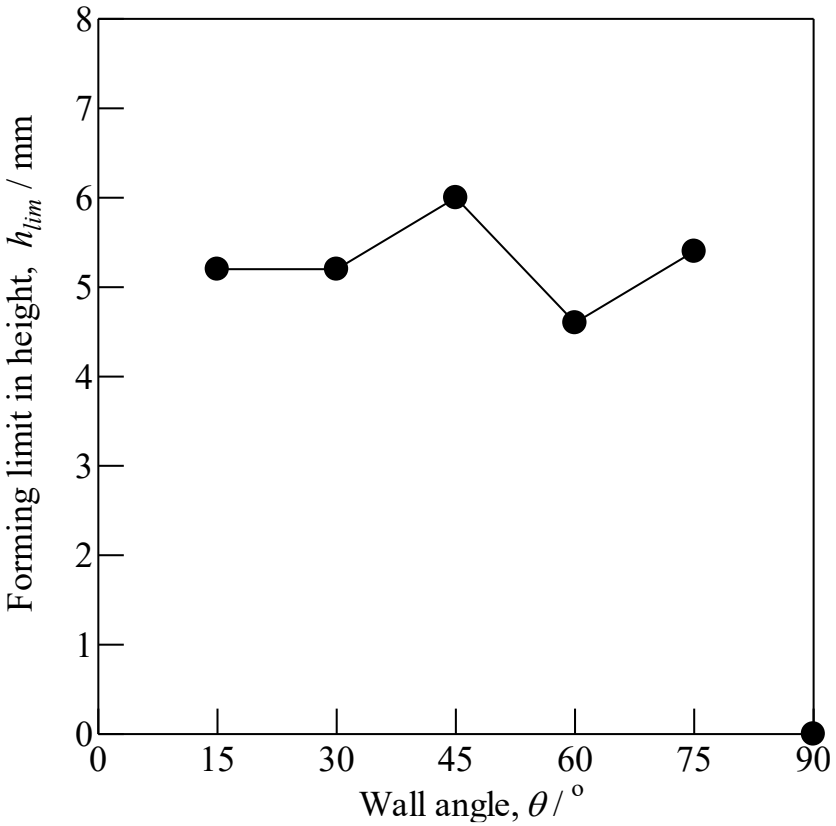

Fig. 3.4 Relation between numbers of cycles before occurring groove-like defects and wall angle θ . (p_r= 1 mm , R_i = 50 mm)

3.4 Conclusions

By comparing number of cycles before occurring groove-like defects, pitch in radius, initial radius of objective cone and wall angle on groove-like defects formation were investigated. Following results were obtained.

(1) Groove-like defects also exists in friction stir welding when an incremental forming tool path without motion in Z direction was used.
(2) Curvature radius in tool path has an effect on groove-like defects formation. Groove-like defects occur earlier when curvature radius is small.
(3) Number of cycles before occurring groove-like defects decreased with decreasing of wall angle θ, but the forming limit in height keeps same.

References

[1] W. Jiang, T. Miura, M. Otsu, M. Okada, R. Matsumoto, H. Yoshimura and T. Muranaka, Development of penetrating tool friction stir incremental forming, *Mater. Trans.* **60** (2019), 2416-2425.

CHAPTER 4

TOOL TEMPERATURE AND REVOLUTIONARY PITCH

4.1 Introduction

In PTFSIF, a penetrating tool of two shoulders connected by the probe is used. During the forming, the tool passes through the sheets without leaving a hole or any defects, because materials around the tool flow plastically. On the basic of that, the tool moves up and down, then concave, convex and concave-convex mixed shapes can be formed by PTFSIF. One of the problems of PTFSIF is the forming limit in height was too small to be used due to the formation of the defects during the forming [1]. In friction stir welding, the revolutionary pitch (the ratio of tool feed rate to tool rotation rate) is an important parameter. It is also known that in friction stir welding the defect formation has a strong relationship to forming temperature and revolutionary pitch [2-3]. Thus, it is expected that the defects that occurred in PTFSIF also have a relation to forming temperature and revolutionary pitch.

The objective of this chapter is to investigate the relationship between defect formation and forming temperature and revolutionary pitch. Tool feed and rotation rates were varied and tool temperature was measured by an embedded sheath thermocouple.

4.2 Experimental Methods

4.2.1 Forming Method

Forming machine used in experiment was same with chapter 2. Sheets were used for the workpiece with dimensions of 200 mm × 200 mm × 2 mm. The forming objective shape was a truncated pyramid with a side length of 100 mm. The wall angle of the pyramid was 45° and corner radius were 20 mm. Figure 4.1 shows the forming tool path. The dotted line in the tool path for guiding in which penetrating tool stir-into the sheet

through friction stir welding. In the tool path of guiding, tool feed rate was set to v_g = 200 mm/min. The solid line tool path was tool path for forming. In the tool path for forming, tool rotation rate remains the same, while tool feed rate changed to tool feed rate of forming, v_f. The pitch in Z direction p_z used in the experiment was 1 mm. p_r was pitch in radial direction. The forming depth of objective shape was 10 mm. In this study, tool rotation rate was set to 1000, 2000 and 3000 rpm. Tool feed rate was set to 200, 1000 and 2000 mm/min. The total number of experiments was 9.

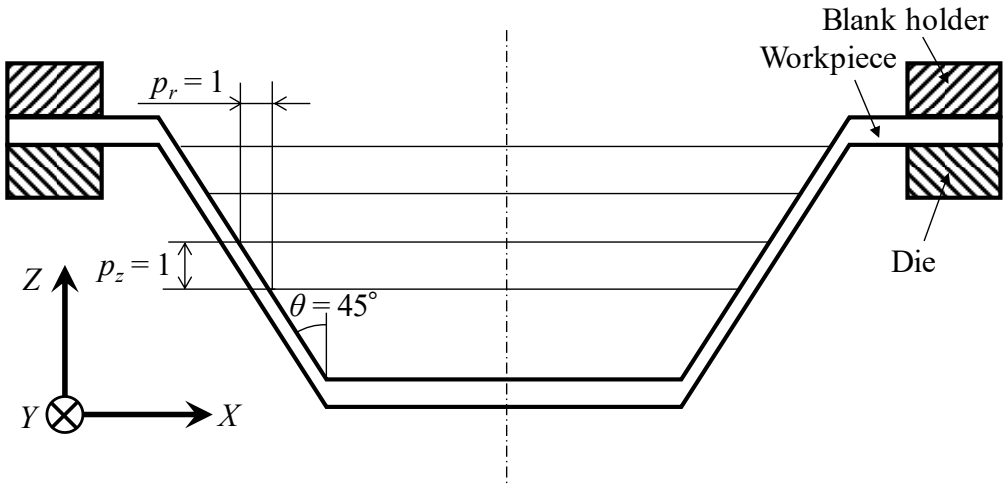

(a) Section view

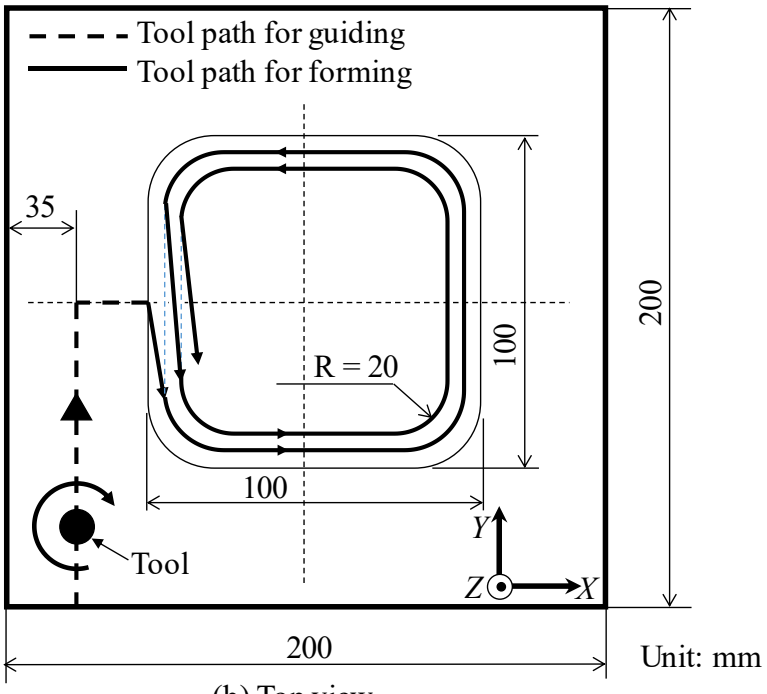

(b) Top view

Fig. 4.1 Tool path of PTFSIF.

4.2.2 Temperature Measuring Method

A K type sheath thermocouple was embedded in the top tool of penetrating tool for measuring the tool temperature during forming. Figure 4.2 shows the location of the embedded thermocouple. The diameter of the sheath thermocouple was 1.0 mm. The diameter of the hole for thermocouple was 1.02 mm and the distance from the top shoulder to a bottom of the hole was 0.1 mm. As the thermocouple rotates with the penetrating tool, the thermocouple must be fixed tightly. For fixing the thermocouple in the hole, inorganic heat-resistant bond (allowable temperature is less than 1400°C) was injected into the hole by an injection syringe to fix the thermocouple. A USB type data logger (Graphtec Corp., GL10-TK) was used for recording the measured temperature and was placed in a self-made holder which can be installed in the spindle and rotates with the spindle. The appearances of the data logger and the self-made holder were shown in Fig. 4.3 and 4.4, respectively. The sampling time of the used data logger was 5s. Figure 4.5 shows the illustration of temperature measuring system with embedded sheath thermocouple.

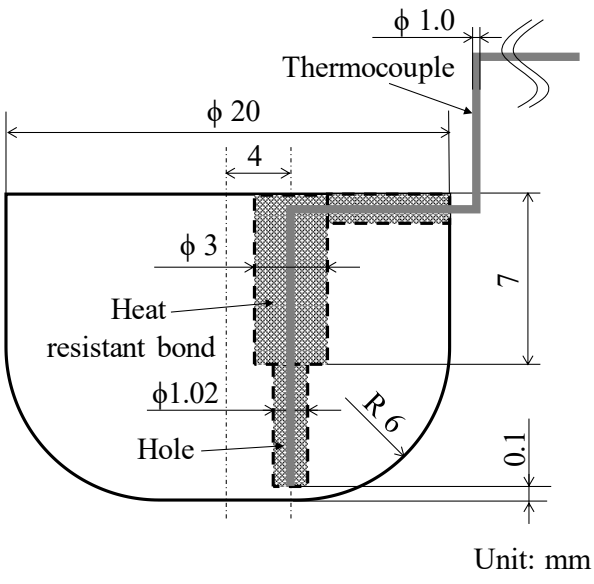

Fig. 4.2 Schematic illustration of location of embedded sheath thermocouple.

Fig. 4.3 Photo of the used USB type data logger.

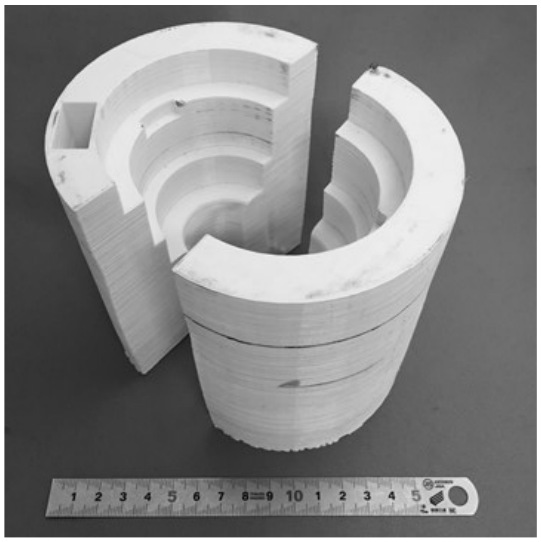

Fig. 4.4 Photo of the data logger holders.

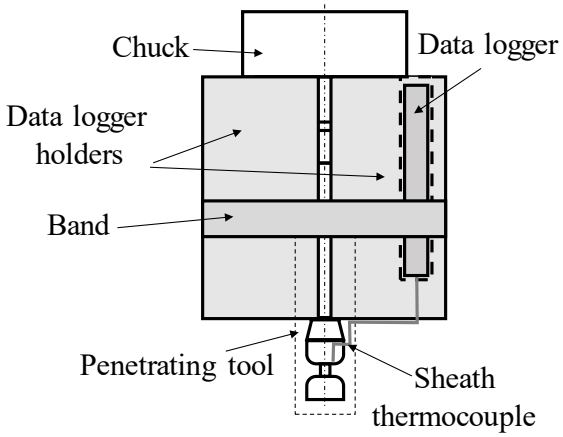

Fig. 4.5 Schematic illustration of temperature measuring system with embedded sheath thermocouple.

4.3 Experimental Results and Discussions

4.3.1 Validation of Measured Temperature

For validating the temperature measured by the embedded thermocouple, friction stir welding with stir-in plate experiment was carried out and tool temperature history of friction stir welding was measured by this temperature measuring system. The experimental machine and workpiece used in friction stir welding were the same to the penetrating tool friction stir incremental forming. The experimental conditions were tool rotation rate of ω_w = 3000 rpm, tool feed rate for guiding of v_g = 200 mm/min and tool feed rate for welding of v_w = 2000 mm/min. The measured temperature is shown in Fig. 4.6. The temperature rose quickly at the beginning of the welding, after that, the temperature increasing speed gradually decreased, and then temperature kept at a stable value. Because the characteristic of the measured temperature curve was similar to that in friction stir welding, in which temperature rose quickly and then stabilized at a temperature, the temperature measuring system is considerable to be valid.

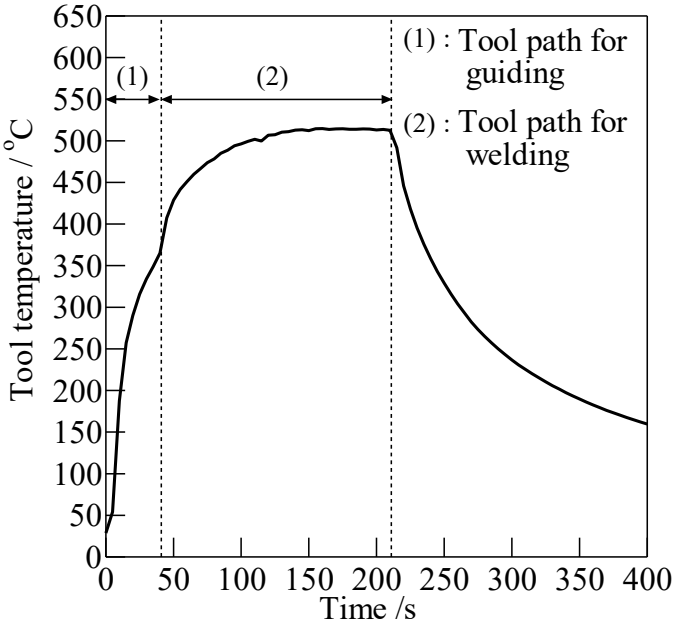

Fig. 4.6 Temperature history in FSW measured by embedded-sheath thermocouple temperature measuring system (ω_w = 3000 rpm, v_g = 200 mm/min, v_w = 2000 mm/min).

4.3.2 Defect Types

In all of the experimental results, the defects occurred in the sheets. Judging from the appearances of the defects, defects were divided into 3 types. The appearances of the defects were shown in Fig. 4.7. Defect I is not groove-like defect, which sheet fractured directly with a crack of irregular edge. Defect II is groove-like defect, and sheet fractured due to growth of the groove-like defect. Defect III is not groove-like defect, with a crack of regular and smooth edge.

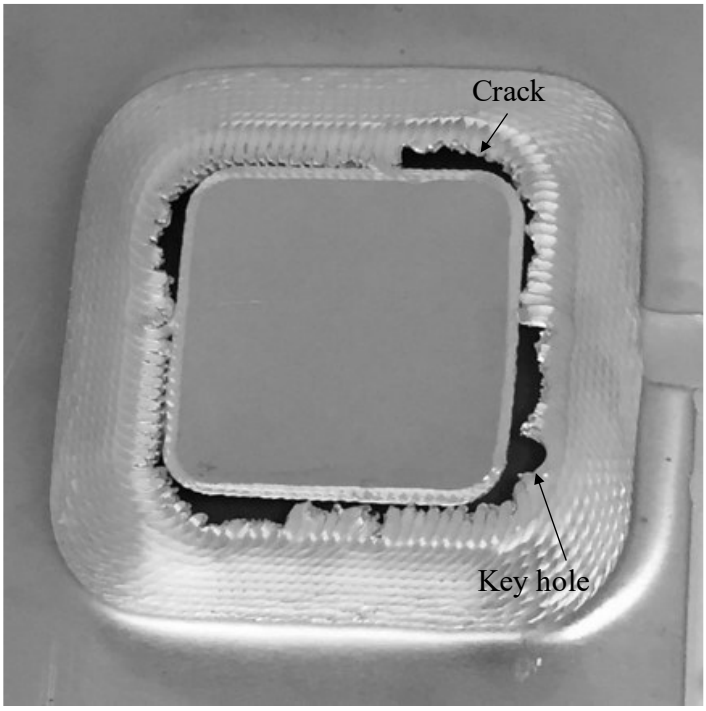

(a) Defect I

Fig. 4.7 Apperance of three defects.

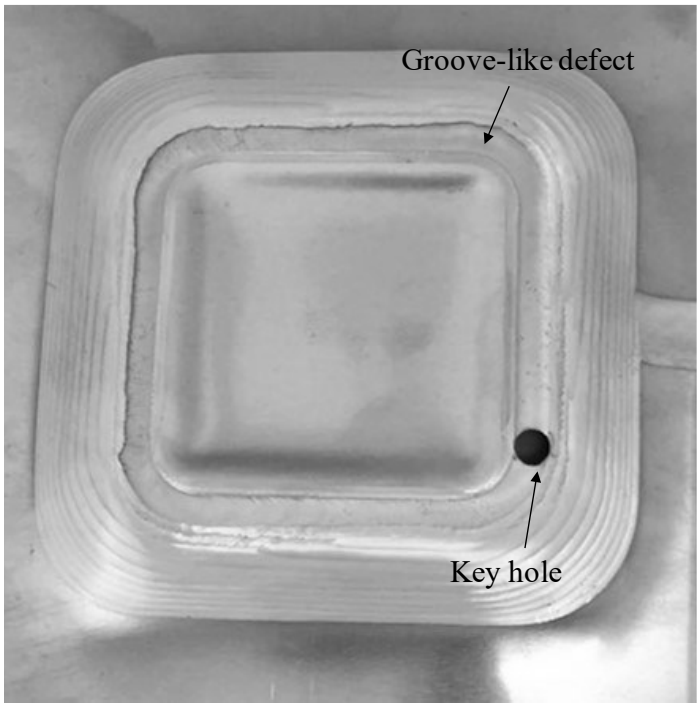

(b) Defect II

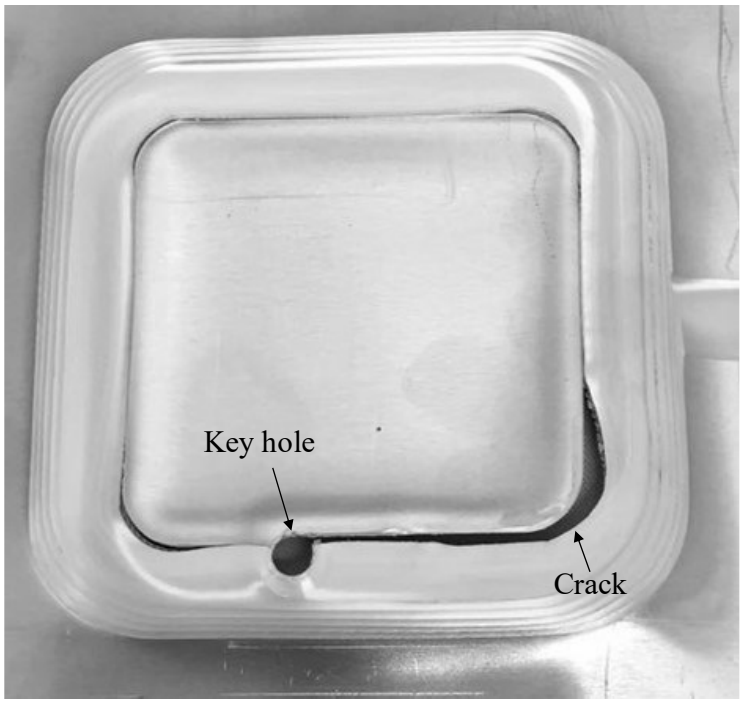

(c) Defect III

Fig. 4.7 Apperance of three defects.

4.3.3 Relation between Defect Formation and Revolutionary Pitch

To investigate the relation between the defect formation and the revolutionary pitch, mapping of the defect type was shown in Fig. 4.8. The horizontal axis respects to the tool feed rate for forming, and the vertical axis respects to the tool rotation rate for forming. Defect III was located in the top left, which refers to a small revolutionary pitch, and defect I was located in the bottom right corner which refers to a large revolutionary pitch. The defect II located between defects I and III. There are two cases of experiment that revolutionary pitch is 1.0 mm/rpm, but their defect types are different. One is defect I, another is defect II. So, defect formation cannot be judged only by the revolutionary pitch.

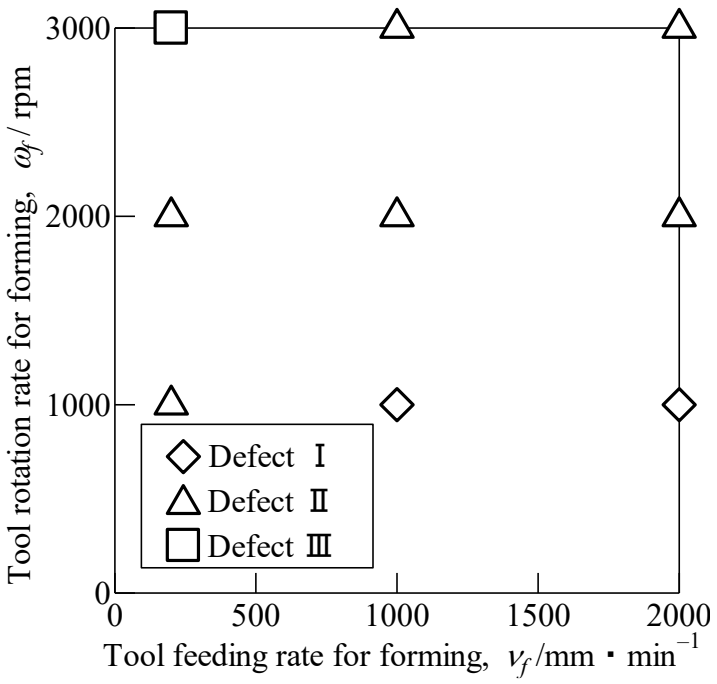

Fig. 4.8 Relation beetween tool rotation rate and tool feed rate.

4.3.4 Relation between Defect Formation and Tool Temperature

Figure 4.9 shows the relation between traveling length and tool temperature. The number of forming circle is shown in the figure. Open circle marks mean the groove-like defect occurred and cross marks mean the sheet fractured. The defect type was also marked in the figure for analyze. It can be seen that the tool temperature when defect III occurred was very high, and the tool temperature when defect I occurred was relatively low. The tool temperature when defect II occurred was between that of defects I and III.

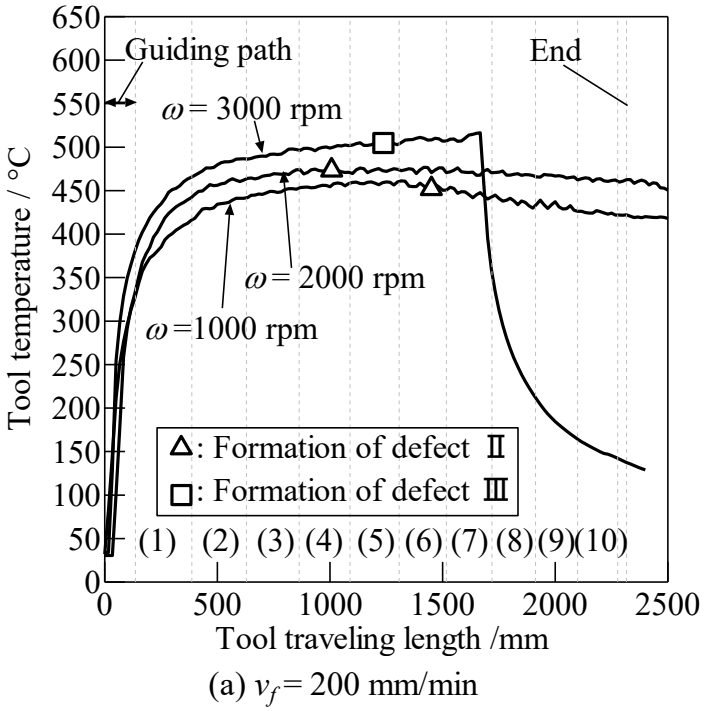

(a) v_f = 200 mm/min

Fig. 4.9 Relation between tool traveling length and tool temperature.

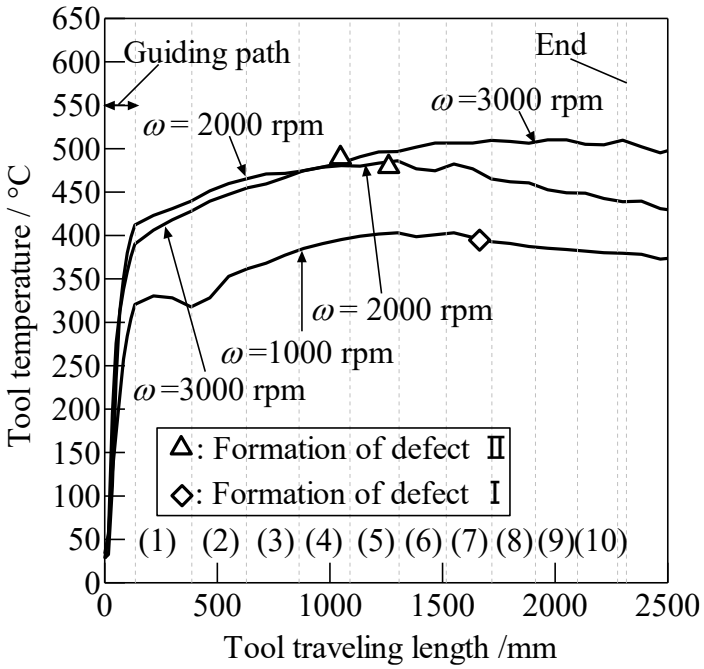

(b) v_f = 1000 mm/min

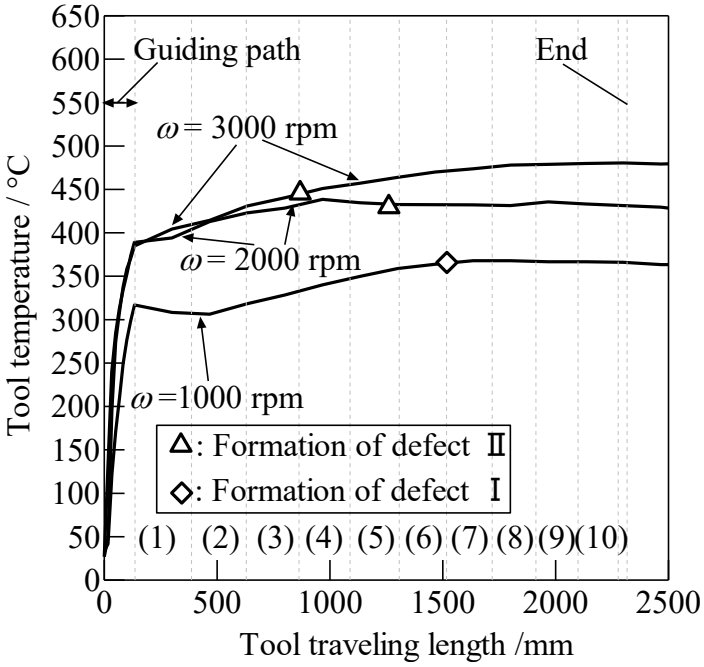

(c) v_f = 2000 mm/min

Fig. 4.9 Relation between tool traveling length and tool temperature.

4.4 Conclusions

For improving the forming limit in height of penetrating tool friction stir incremental forming, relationship between defect formation, revolutionary pitch and tool temperature were investigated. Tool rotation and feed rates were varied, and the tool temperature were measured by an embedded sheath thermocouple, which rotates with the spindle during the forming. The following conclusions were draw:

(1) Tool temperature during PTFSIF was measured successfully.

(2) It was found that tool temperature increased with the increasing of tool rotation rate and decrease with the increasing of tool feeding rate.

(3) Three kinds of defects were found in the forming results. Defect I is not groove-like defect, which sheet fractured directly with a crack of irregular edge. Defect Ⅱ is groove-like defect, and sheet fractured due to growth of the groove-like defect. Defect III is not groove-like defect, with a crack of regular and smooth edge. It was found the defect I caused by low temperature and defect III caused by high temperature.

(4) Defect formation cannot be determined by revolutionary pitch or tool temperature only.

References

[1] W. Jiang, T. Miura, M. Otsu, M. Okada, R. Matsumoto, H. Yoshimura and T. Muranaka, Development of penetrating tool friction stir incremental forming, *Mater. Trans.* 60 (2019), 2416-2425.

[2] H. Liu, M. Maeda, H. Fujii and K. Nogi, Tensile properties and fracture locations of friction-stir welded joints of 1050-H24 aluminum alloy, *J. Mater. Sci. Lett*, **22** (2003), 41-43.

[3] A. Fehrenbacher, N.A. Duffie, N.J. Ferrier, F.E. Pfefferkorn and M.R. Zinn, Effects of tool-workpiece interface temperature on weld quality and quality improvements through temperature control in friction stir welding, *Int. J. Adv. Manuf. Technol.,* **71** (2014), 165-179.

CHAPTER 5

IMPROVEMENT OF FORMING LIMIT IN HEIGHT WITH ALTERNATING TOOL PATH

5.1 Introduction

In Penetrating tool friction stir incremental forming (PTFSIF), a penetrating tool with a large radius corner, using a conventional bobbin tool, can travel freely in the sheet metal without leaving any defects in the sheet. Concave-convex shapes can be formed using the top and bottom tools, respectively. No specific machine or die are required in PTFSIF.

However, the forming limit in height in PTFSIF is relatively small, less than 10 mm [1]. The material flows from the advancing side (AS) to the retreating side (RS) causes a poor forming limit in height. The AS is the side at which the tool rotation and traveling direction are the same, and the RS is opposite [2]. In chapter 2, PTFSIF employed only a one-way tool path (OTPs), and the direction of the tool path did not change during forming, with a tool path direction of either clockwise (CW) or counterclockwise (CCW). In the forming with OTPs, positional relationship between AS and RS in the sheet does not vary during the forming, and direction of material flow is unidirectional, thus a groove-like defects is induced due to lack of material in AS. If the material flows bidirectionally in the sheet, a uniform volume distribution may be achieved, considerably improving forming limit in height. According to the definition of AS and RS, bidirectional material flow can be realizing using alternating tool paths (ATPs), in which the direction of the tool path was alternated in every forming circle path.

In this chapter, to improve the forming limit in height, PTFSIF with ATPs and OTPs, and the volume changes after forming were calculated to examine the results of forming limit in height. In addition, formable working conditions were investigated, and concave–convex mixed shapes were formed by PTFSIF with the ATP. Finally, forming of concave–convex mixed shapes which is the motivation of development PTFSIF were conducted by PTFSIF with the ATP.

5.2 Experimental Method

The forming machine and workpiece used in the chapter was same with chapter 2. Sheets were formed into convex shapes with a truncated cone having a bottom diameter of 140 mm, a wall angle of θ = 45° and a height of h = 50 mm. Two types of OTPs, with a tool path of CW and CCW, and two types of ATPs, with a tool path of CW+CCW and CCW+CW were used and forming limits in height with OTPs and ATPs were then compared. A tool path of CW+CCW means that direction of the tool path in the first forming circle was CW and the next was CCW. A tool path of CCW+CW means that the direction of the tool path in the first forming circle path was CCW and the next one was CW.

Figure 5.1 shows a tool path of CW+CCW. This tool path can be divided into two sections. One is the tool path for guiding, as shown as a dotted line in Fig. 5.1 (a), and the other one is the tool path for forming, as shown as a solid line in Fig. 5.1 (a). The tool rotation and feed rates in the tool path for guiding were set at a fixed value for tool stir-in the workpiece. After passing through the guiding path, tool rotation and feed rates were varied to tool rotation rate for forming of ω_f, and tool feed rate for forming of v_f for investigating formable working conditions. In this work, the following values were considered: tool stir-in the workpiece at a tool rotation rate for guiding of ω_g = 1000 rpm and tool feed rate for guiding of v_g = 200 mm/min. Further, contour-based tool path strategy was used. A sheet was formed with the tool path of CW in contour tool path, and then the tool was moved to the neighbor contour tool path and the sheet was formed with the tool path of CCW. The tool path between neighboring contours was named the connecting tool path in this study. In the connecting tool path, the tool was then moved to the inner contour in radial direction for pitch in radial direction p_r and then moved up for pitch in Z direction p_z as shown in Fig. 5.1 (b). From the preliminary experiments, the tool feed rate for connecting neighboring contours v_c was set to 200 mm/min to avoid the sheet fracturing at the connecting part. Pitch in Z direction p_z was 0.5 mm. Forming was terminated when sheet or tool fractured during the forming, and the height when sheet or tool fractured was defined as forming limit in height, h_{lim}.

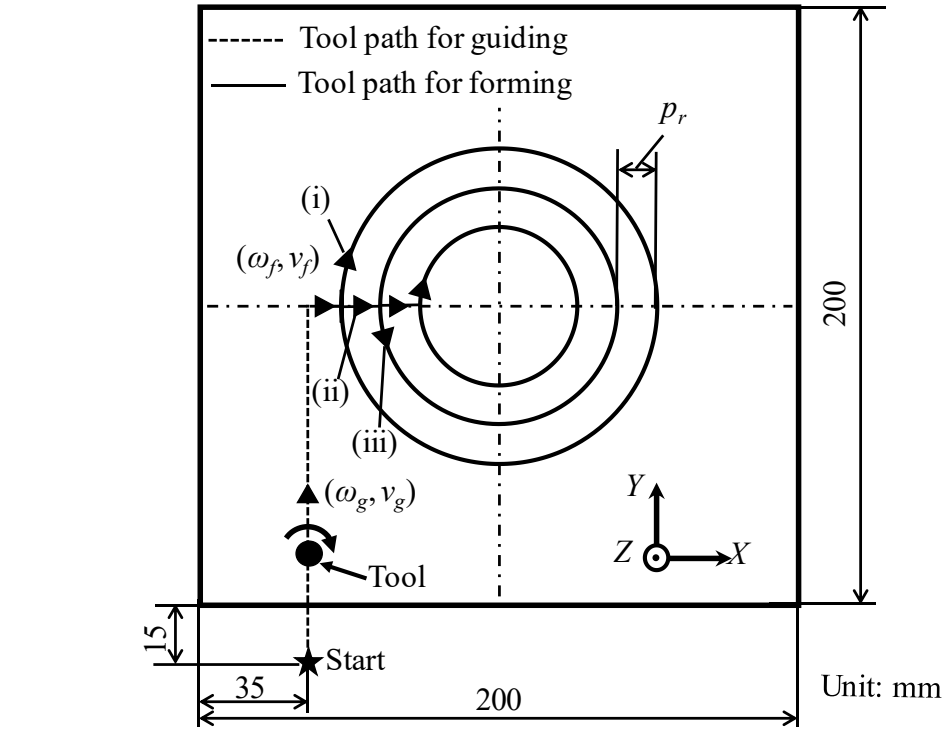

(a) Top view

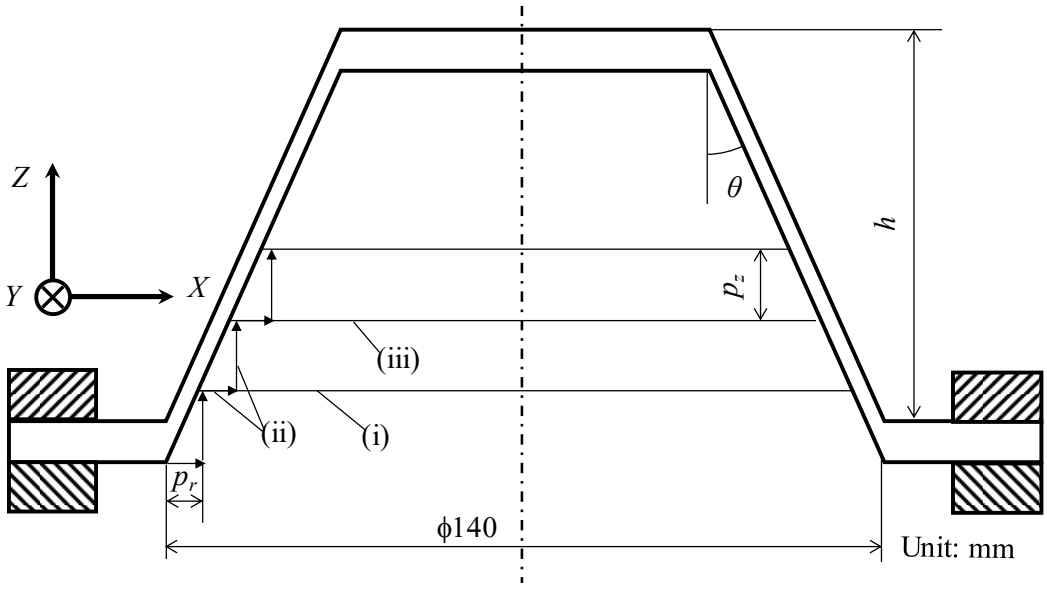

(b) Section view

Fig. 5.1 Tool path of CCW+CW in PTFSIF.

Figure 5.2 shows the variation in sheet thickness with ideal incremental forming. t_0 is initial sheet thickness; t_1 is sheet thickness of formed sheet; and t_z is thickness in Z direction of formed sheet, which was defined as a length between two points in top surface and bottom surface of formed sheet at the same x and y coordinates. Although t_z and t_0 are equal at any formed part because of only shearing conditions, t_z and t_0 are not equal due to the non-uniform volume distribution. The difference between t_z and t_0 can be used as an indicator for estimating the variation in volume with Z direction. Volume change per unit length considering volume change not only in Z direction but also in circumferential direction was introduced to estimate the volume change. $\delta_v(r)$ is volume change per unit length at position r and calculated by Eq. (1).

$$\delta_v(r)=\{t_z(r)-t_0\}\times 2\pi r \tag{1}$$

where r is distance from central axis of the truncated cone to measured point in radial direction. $t_z(r)$ means thickness in Z direction at position r.

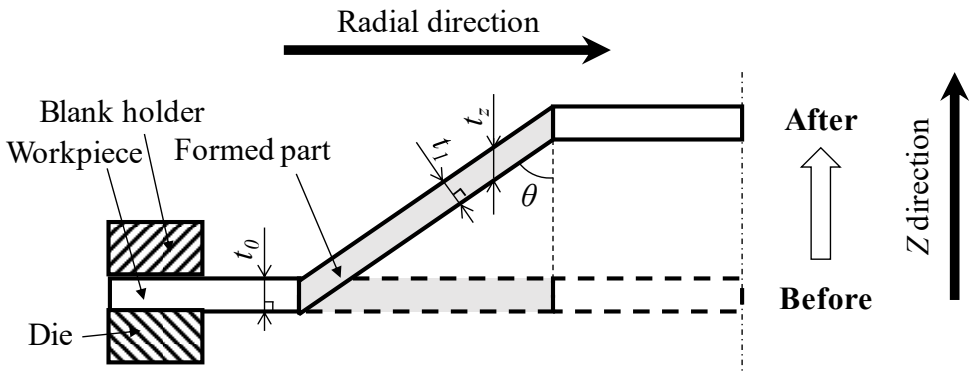

Fig. 5.2 Sheet thickness change in ideal incremental forming. (θ : wall angle, t_0 : initial sheet thickness, t_1 : thickness of formed sheet, t_z : thickness in Z direction of formed sheet, in ideal incremental forming, $t_z = t_0$)

In this study, the sheet was cut in half by wire electrical discharge machining and thickness in *Z* direction of formed sheet were measured using the sectional profile photos via image processing software. For comparing the amount of volume change with ATPs and OTPs, variance of distribution of volume change per unit length, σ^2 was calculated in Eq. (2).

$$\sigma^2 = \int_{r_1}^{r_2} \frac{\{\delta_v(r) - \overline{\delta_v}\}^2}{|r_2 - r_1|} dr \quad (2)$$

In Eq. (2), r_1 and r_2 are the lengths from the center of the cone to start and end measured points, respectively. $\overline{\delta_v}$ is average value of $\delta_v(r)$ from $r = r_1$ to r_2.

5.3 Results and Discussions

5.3.1 Experimental Reliability and Repeatability

In OTPs, only one type of fracture morphology caused by groove-like defects appeared under the same forming conditions. In ATPs, another fracture caused by larger upheaval in the center also appeared under the same forming conditions and both fractures occurred randomly. In a research on the probability of each defect, experiment under the same forming conditions was conducted 36 times, and number of fractures caused by groove-like defects and fractures caused by upheaval in center were 23 and 13, respectively. Thus, probability of fractures caused by groove-like defects and fractures caused by upheaval in center were 63.9% and 36.1%. Figure 5.3 shows sheets without fracture, fractures caused by groove-like defect, and those with large upheavals in the center.

For all fractures caused by groove-like defects, sheets fractured from the area of connecting tool path as shown in Fig. 5.3 (b); for those caused by larger upheaval in the center, the upheaval in the center became larger as forming proceeded, as shown in Fig. 5.3 (e), and then fractures progressed to the lower part in the sheet as shown in Fig. 5.3 (c).

The fact that the two fracture morphologies occurred randomly in the PTFSIF with ATPs in the same forming conditions indicated that experimental reliability of PTFSIF

with ATPs is not high, however, experimental repeatability of the same fracture morphology is high. For example, under forming conditions of tool path of CW+CCW, θ = 45°, ω_f = 1000 rpm, v_f = 1000 mm/min, results of forming limit in height h_{lim} for three times experiment were 30, 28.5 and 28 mm, respectively in fracture caused by groove-like defect. Under the same forming conditions, three results of forming limit in height in fracture caused by upheaval in center were 20, 18.5 and 19 mm, respectively. Because the difference among the three results under the same fracture morphology were not large, the experimental repeatability of this experiment is considered to be high.

Although the formation of fractures caused by groove-like defects can be explained by the material flow between AS and RS, which has been verified in the previous study [1], the reason for the formation of fractures caused by larger upheaval in the center is still unknown. In the following sections, only experimental results of fracture caused by groove-like defect were used.

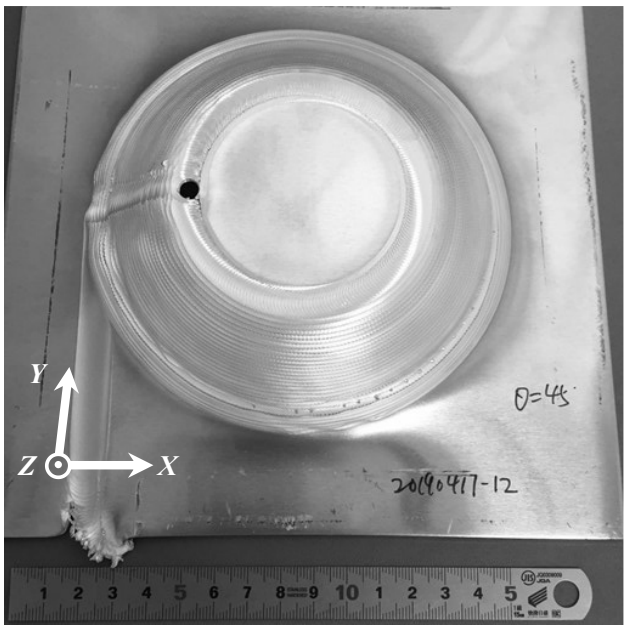

(a) Sheet without fracture

Fig. 5.3 Photos of sheet without fracture, fractures caused by groove-like defect (GF) and fractures caused by larger upheaval in center (UF). (CW+CCW, θ = 45°, ω_f =1000 rpm, v_f =1000 mm/min)

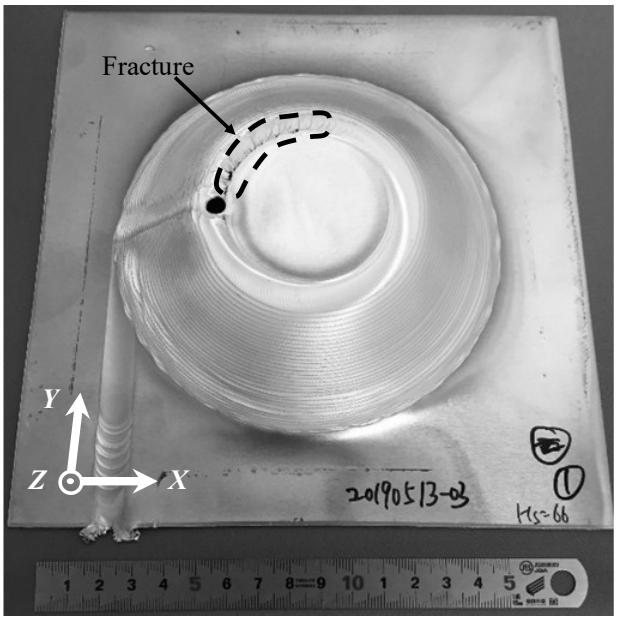

(b) Sheet fractured due to groove-like defect

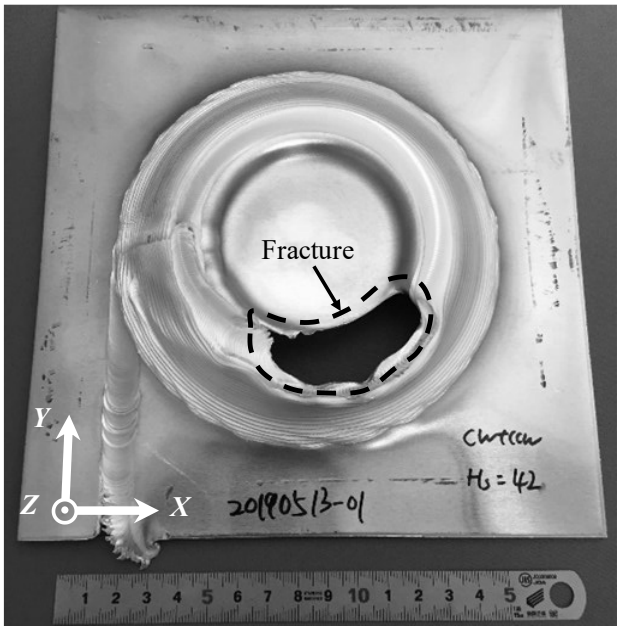

(c) Sheet fractured due to large upheaval in center

Fig. 5.3 Photos of sheet without fracture, fractures caused by groove-like defect (GF) and fractures caused by larger upheaval in center (UF). (CW+CCW, θ = 45°, ω_f =1000 rpm, v_f =1000 mm/min)

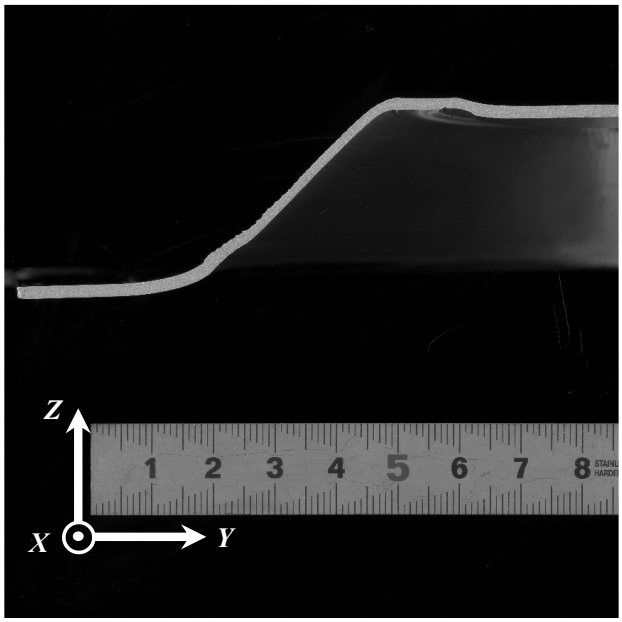

(d) Sectional image of groove-like defect

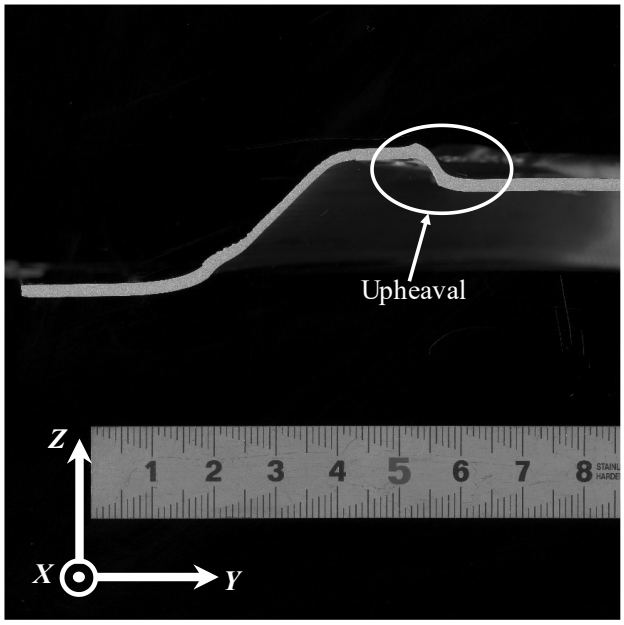

(e) Sectional image of large upheaval in center

Fig. 5.3 Photos of sheet without fracture, fractures caused by groove-like defect (GF) and fractures caused by larger upheaval in center (UF). (CW+CCW, θ = 45°, ω_f = 1000 rpm, v_f = 1000 mm/min)

5.3.2 Forming Limits in Height

Figure 5.4 compares the forming limits in height with ATPs and OTPs. Each experiment was conducted three times under the same conditions, and the average value of forming limits in height was plotted. The error bars express the maximum and minimum values. The forming limits in height with ATPs were approximately 30 mm and those with OTPs were lower than 10 mm. Compared with OTPs, forming limit in height with ATPs was drastically improved, with an almost 200% increase of forming limit in height. In ATPs, forming limit in height with tool path of CW+CCW was slightly larger than that with a tool path of CCW+CW. Forming limit in height with a tool path of CW was the lowest. This can be explained by the unidirectional material flow from the outer part of sheet (AS) to the inner part of sheet (RS). Excessive material in the inner part made the sheet difficult to deform because the tool forms sheets from outer to inner side.

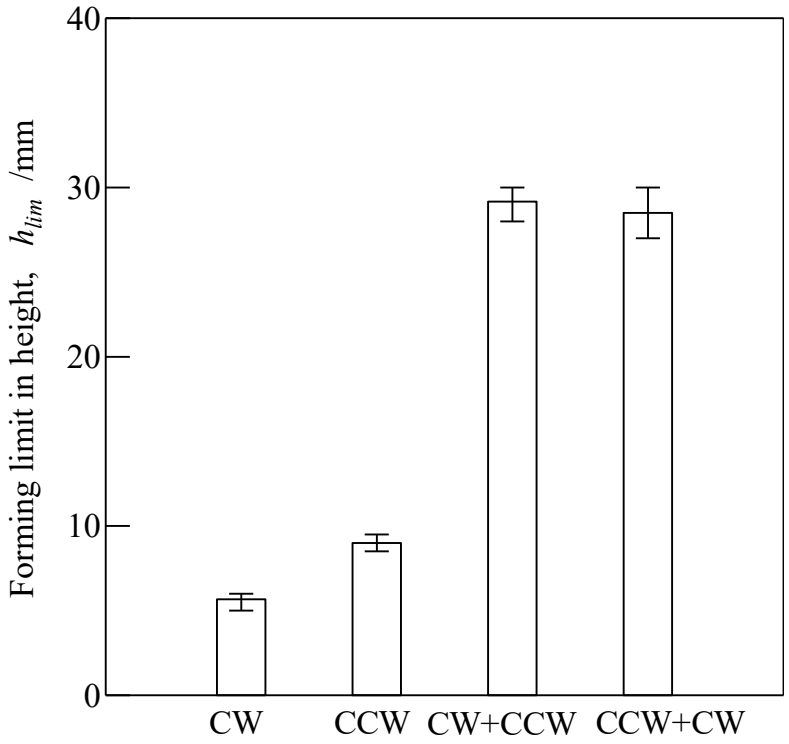

Fig. 5.4 Comparison of forming limit in height in PTFSIF with ATPs and OTPs. (θ = 45°, ω_f=1000 rpm, v_f=1000 mm/min, p_z = 0.5 mm, h = 50 mm, groove-like defects fracture morphology).

Figure 5.5 shows the schematic of definition of three areas in the formed sheet for investigating material flow. The formed sheet was divided into three parts: the formed, tool corner, and tool shoulder parts. The formed part is the area from the beginning of the forming point to the theoretical contacting point, the location of which can be determined by wall angle, θ. The tool corner part is the area from the forming theoretical contacting point to the edge of the tool shoulder. The tool shoulder part is defined as the area of the flat part of the penetrating tool.

Figure 5.6 shows the distributions of thickness in Z direction t_z and volume change per unit length in radial direction obtained with ATPs and OTPs. The forming conditions were θ = 45°, ω_f = 1000 rpm, v_f = 1000 mm/min and a height of h = 6 mm. The thick lines are results with OTPs and the thin lines are those with ATPs. The dotted line in Fig. 5.6 (b) is an ideal line of volume change per unit length, which is constant to zero because $t_z = t_0$ in ideal conditions. The formed part and tool center were also marked in the figure. Thickness in Z direction and volume change per unit length with ATPs were smaller in absolute value than those with OTPs at the formed part. The fluctuation of distribution with ATPs was smaller than those with OTPs.

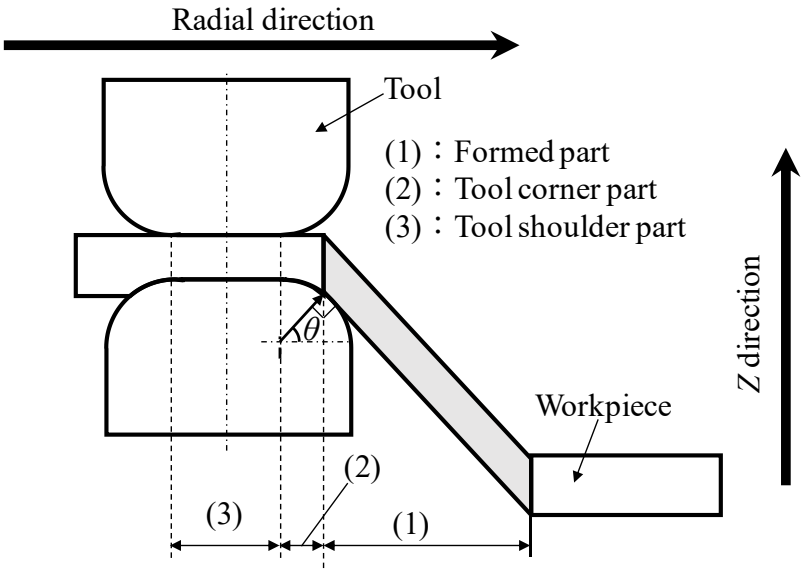

Fig. 5.5 Schematic illustration of different parts in the formed sheet with considering tool size.

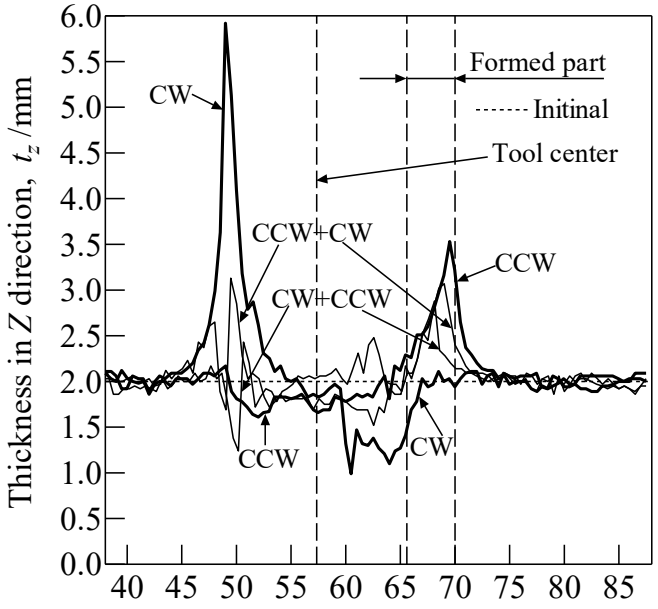

(a) Thickness in *Z* direction of formed sheet

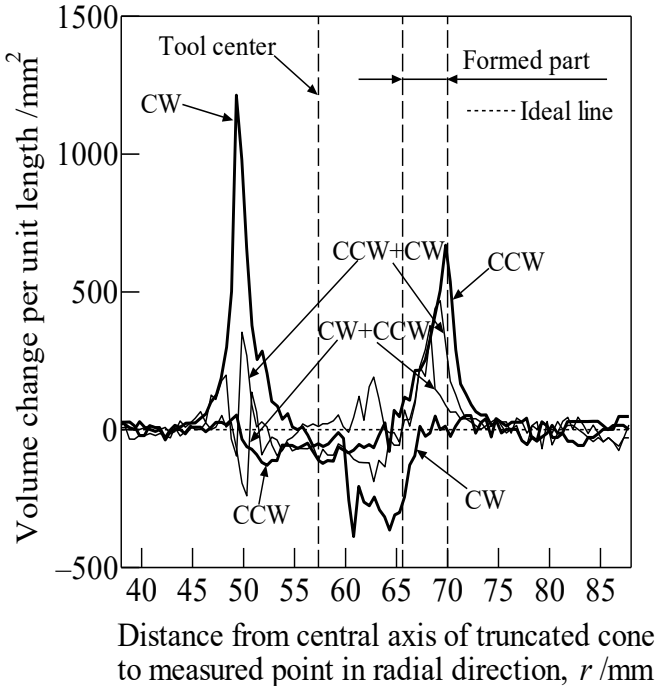

(b) Volume change per unit length

Fig. 5.6 Thickness in *Z* direction of formed sheet and volume change per unit length in radial direction. (θ = 45°, ω_f=1000 rpm, v_f=1000 mm/min, h = 6 mm)

Figure 5.7 compares the variances of volume change per unit length σ^2 with ATPs and OTPs. σ^2 with ATPs was smaller than that with OTPs. As σ^2 means the average of variation in volume following forming, a slight variation in uniform volume distribution leads to a considerable increase in the forming limit in height. Thus, the results of σ^2 with ATPs and OTPs correspond to those of forming limits in height in Fig. 5.4.

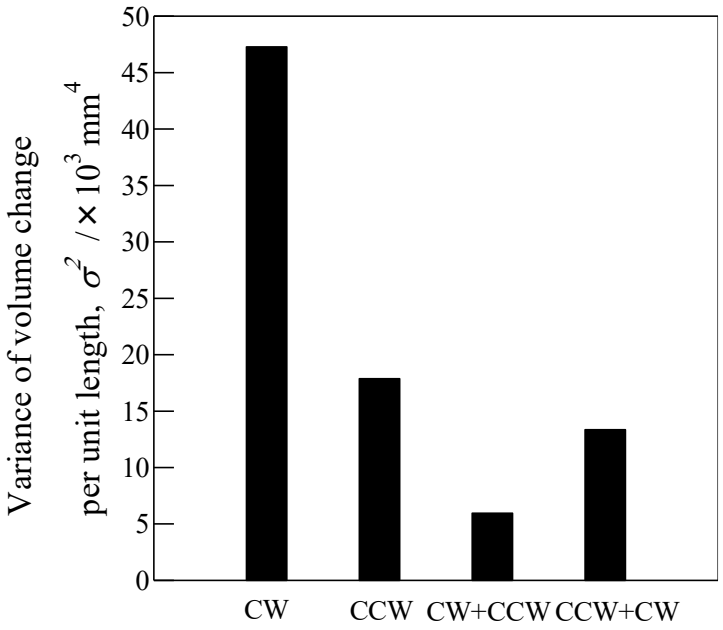

Fig. 5.7 Comparison of variance of volume change per unit length in PTFSIF with ATPs and OTPs. (ω_f = 1000 rpm, v_f = 1000 mm/min, θ = 45 °, h = 6 mm, groove-like defects fracture morphology)

Figure 5.8 shows the schematic illustration of material flow with ATPs and OTPs. As the positional relationship between AS and RS does not vary in two forming tool paths of neighboring contours in OTPs, the direction of material flow does not vary in OTPs. In contrast, as positional relationship of AS and RS alternates in two forming tool paths of neighbor contours, the direction of material flow alternates in ATPs. Therefore, the variance of volume change per unit length with ATPs was smaller than that with OTPs.

From those results, forming limits in height were improved with ATPs; this improvement can be attributed to material flow. As the variance σ^2 of CW+CCW is the smallest in the four types of tool paths used, the following experiments regarding formable working conditions and thickness of formed sheet were conducted using only the tool path of CW+CCW.

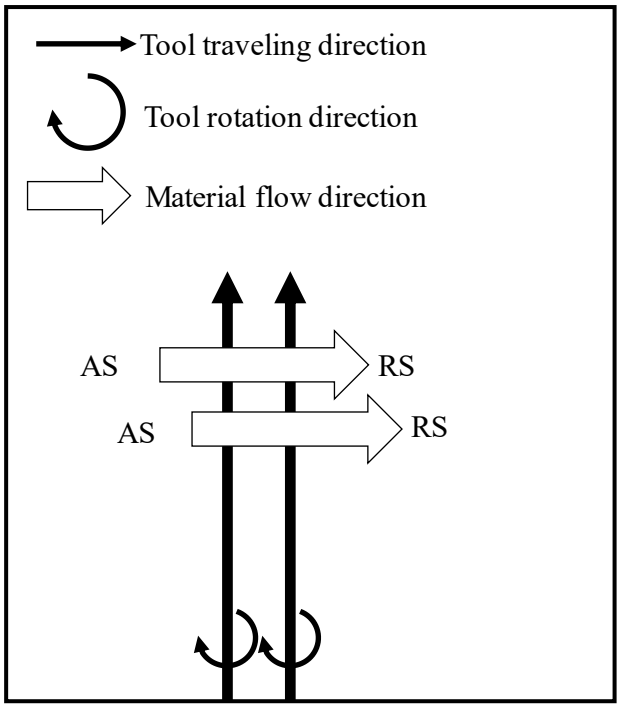

(a) OTP

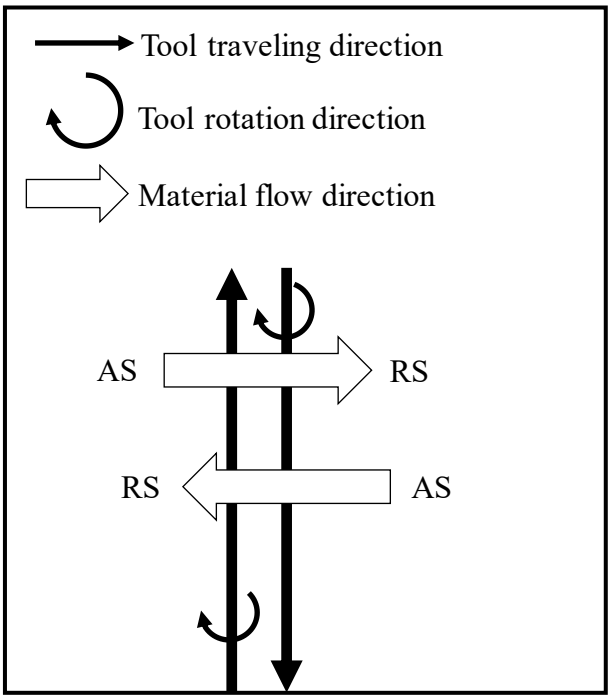

(b) ATP

Fig. 5.8 Schematic illustration of material flow in ATP and OTP. (a) OTP. (b) ATP.

5.3.3 Formable Working Conditions

Wall angle θ, tool rotation rate for forming ω_f, and tool feed rate for forming v_f, were varied for determining the formable working conditions using tool path of CW+CCW. Figure 5.9 shows formable tool feed and rotation rates for forming in PTFSIF at a wall angle of $\theta = 50°$. Open circle marks mean the forming was completed without sheet or tool fracture until forming height of $h = 30$ mm. Cross marks mean the sheet was fractured during the forming. Open triangle marks mean the tool fractured during the forming. Formable working conditions are surrounded by the failed ones, and this indicates that there are suitable combinations of tool rotation rate and tool feed rate in PTFSIF. This tendency is same for that of friction stir welding and friction stir incremental forming [3]. The absolute values of formable tool feed and rotation rates for forming in PTFSIF are smaller than those of conventional friction stir incremental forming. This is because two shoulders were used for generating frictional heat. In conventional friction stir incremental forming, friction stirring occurs from a relatively high value of tool rotation rate. The tool rotation rate is too small to generate sufficient frictional heat, and this is indicated by the open triangle marks located in the bottom of the formable region.

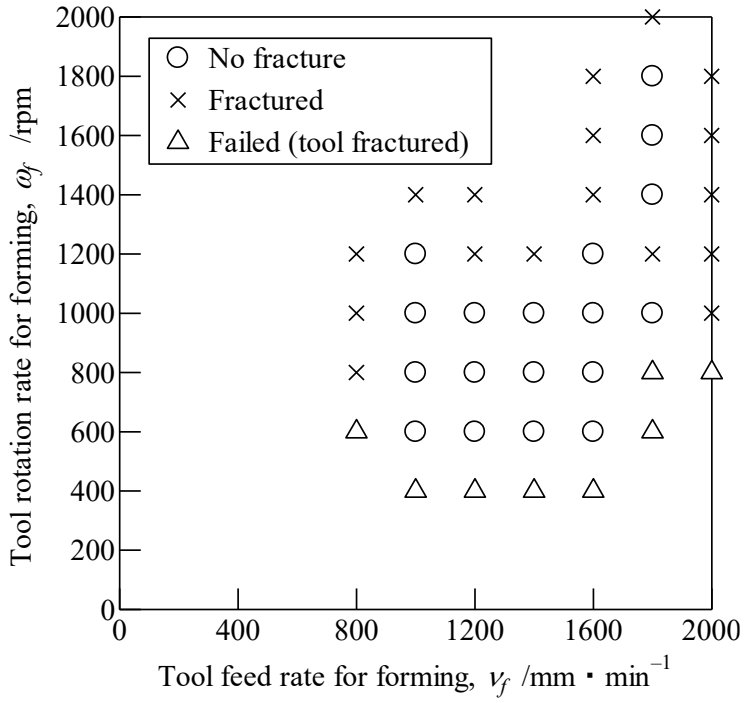

Fig. 5.9 Formable tool feed rate for forming and tool rotation rate for forming in PTFSIF with tool path of CW+CCW. (θ = 50°, h = 30 mm, groove-like defects fracture morphology)

Next, the tool rotation rate for forming was fixed to ω_f = 1000 rpm and the tool feed rate for forming was varies, and the formable wall angle was investigated. Figure 5.10 shows the formable wall angle in PTFSIF with a tool path of CW+CCW. Open circle marks mean that the forming was completed without fracture until a height of h = 30 mm. Cross marks mean the sheet was fractured during the forming. Comparing with conventional friction stir incremental forming, the range of the formable tool feed rate for forming from v_f = 800-1800 mm/min was narrow. In the formable working conditions, the relationship between the tool feed rate for forming and the minimum formable wall angle was similar to a V-shape. This result indicates that for a tool rotation rate for forming, there is a corresponding tool feed rate for forming.

Figure 5.11 shows the relation between the wall angle and forming limit in height with tool paths of CW+CCW and CCW. The closed circles depict the results with a tool path of CW+CCW and the open circles represent a tool path of CCW. The forming conditions were a tool rotation rate for forming of ω_f =1000 rpm and a tool feed rate for forming of v_f = 1000 mm/min. The objective height was h = 30 mm. Forming limits in heights with a tool path of CW+CCW were larger than those with a tool path of CCW. When the wall angle varies from 20° to 45°, the forming limit in height with a tool path of CW+CCW increased. The forming limit in height was 30 mm when the wall angle varies from 45° to 60°, which is the objective height. Although the forming limit in height also increased with increasing the wall angle from 20° to 45° with a tool path of CCW, it decreased when wall angle varied from 45° to 60°. The variation in forming limit in height with a tool path of CCW was very small. The increase of the forming limit in height with increase of the wall angle means forming was difficult in a small wall angle, which corresponds to the conventional incremental forming and friction stir incremental forming [4].

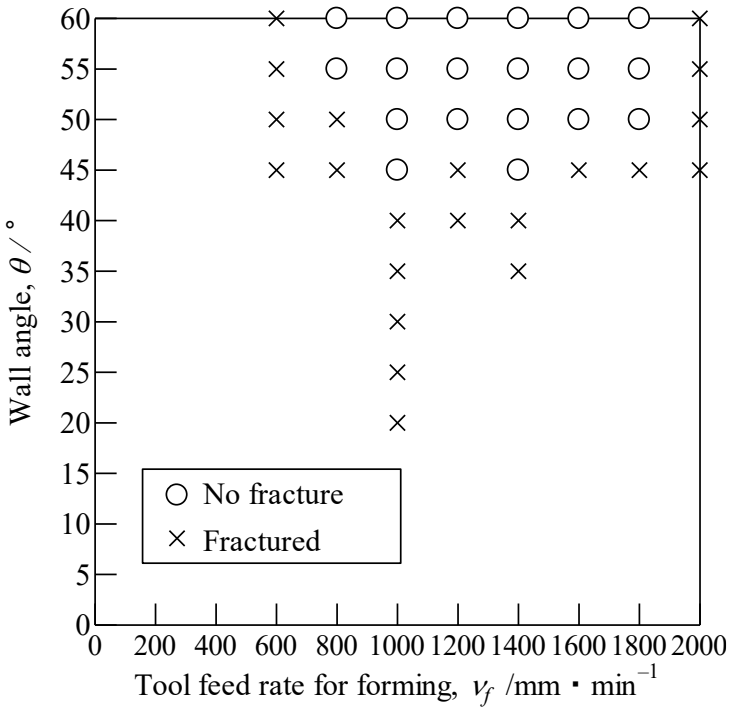

Fig. 5.10 Formable wall angle in PTFSIF with tool path of CW+CCW. (ω_f=1000 rpm, h = 30 mm, groove-like defects fracture morphology)

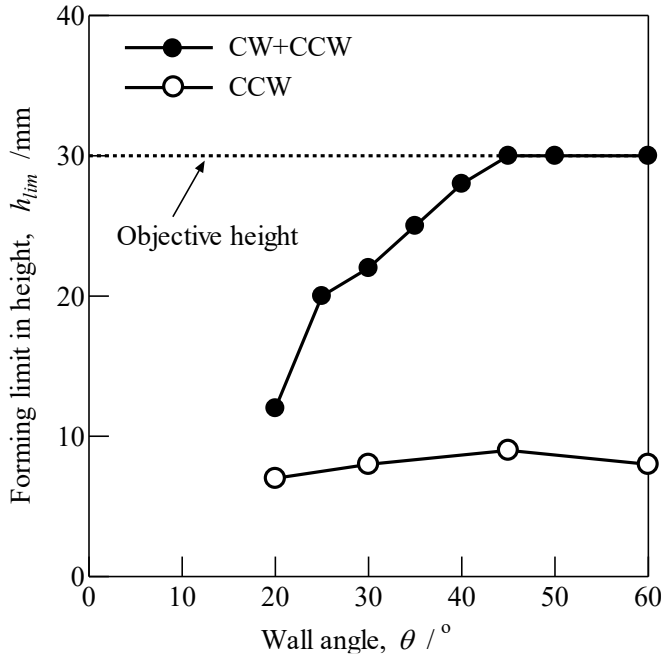

Fig. 5.11 Relation between forming limit in height and wall angle in PTFSIF with tool paths of CW+CCW and CCW. (ω_f = 1000 rpm, v_f = 1000 mm/min, h = 30 mm, groove-like defects fracture morphology)

5.3.4 Thickness of Formed Sheet in PTFSIF with ATP

Figure 5.12 shows the thickness distribution of a sheet formed in PTFSIF with a tool path of CW+CCW. Forming conditions were ω_f = 1000 rpm, v_f = 1000 mm/min, θ = 45° and h = 20 mm. The solid line indicates the measured thickness, and the dotted line indicates the ideal thickness, which were calculated by the sine law without considering the tool size. The curve of measured thickness was divided into three areas as well as shown in Fig. 5.5. From the results, thickness of formed part at the beginning of forming were larger than that of the initial sheet one. The thickness of the formed sheet decreased in the initial part and then stabilized at a value which is very near to the ideal thickness, and a uniform volume distribution was achieved.

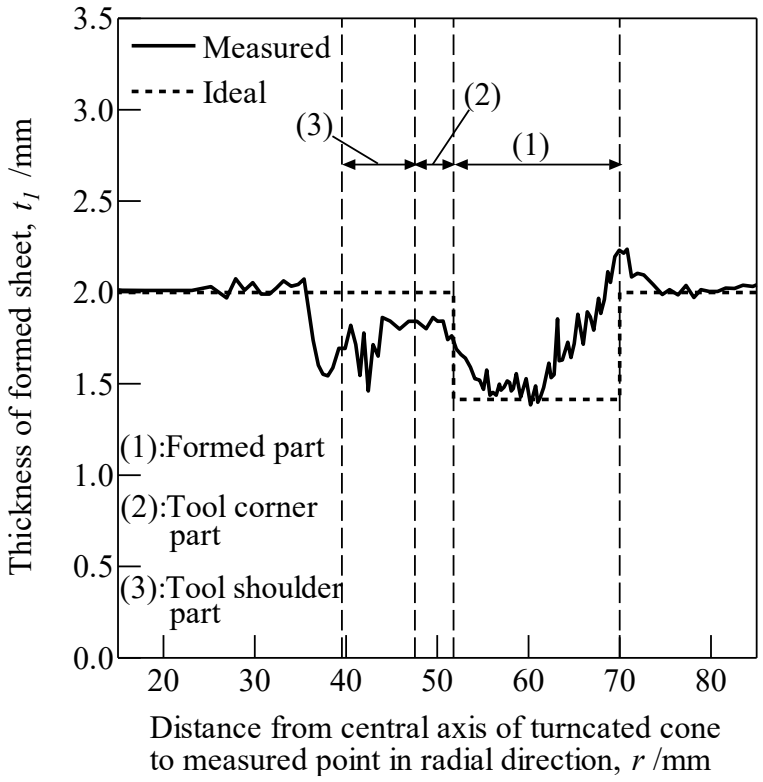

Fig. 5.12 Thickness of formed sheet in PTFSIF with tool path of CW+CCW. (ω_f = 1000 rpm, v_f = 1000 mm/min, θ = 45 °, h = 20 mm)

5.3.5 Forming of Concave–convex Mixed Shapes

Because forming limit in height was improved in PTFSIF with the tool path of CW+CCW, concave–convex mixed shapes could be formed. The objective shapes of concave–convex mixed comprises concentric concave and convex truncated cones. Figure 5.13 shows the successfully formed dimensions of the objective concave–convex mixed shapes. The forming tool path was CW+CCW. The forming conditions were ω_g = 1000 rpm, ω_f = 1000 rpm, v_g = 200 mm/min, v_c = 200 mm/min and v_f = 1000 mm/min. Pitch in Z direction was p_z =0.5 mm. In both forming of concave–convex mixed shapes and convex–concave mixed shapes, the sheets did not fracture until the forming had finished.

Figure 5.14 shows the profiles of formed concave–convex mixed shapes. Concave–convex mixed shapes were formed successfully. The ideal shapes and formed shapes were different at the center part and the connecting part which connected the concave shape to convex shape. The difference at the connecting part was caused by the alternated forming direction during the forming and difference at the center part was caused by the material flow direction.

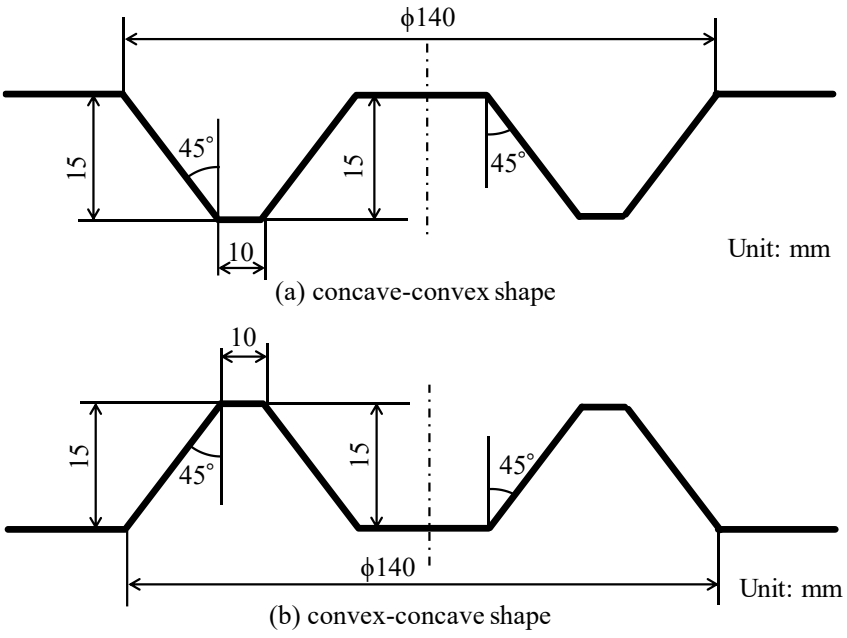

Fig. 5.13 Shapes and dimensions of objective concave-convex mixed shapes.

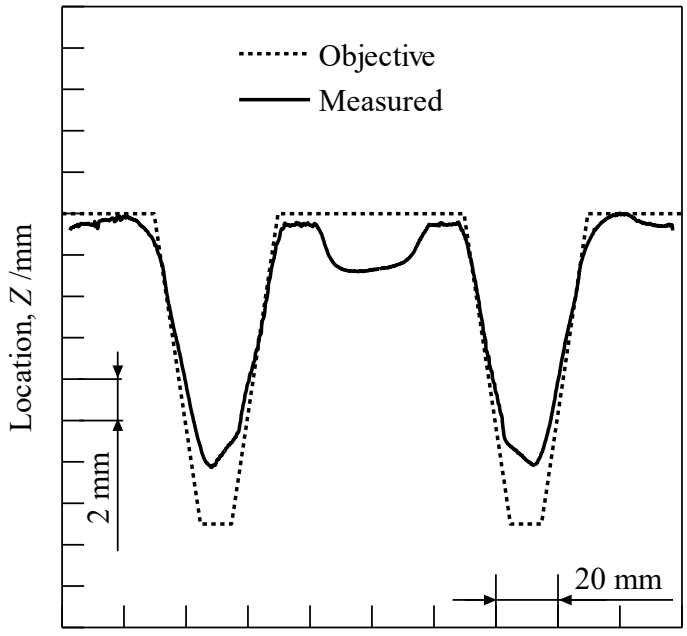

(a) concave-convex

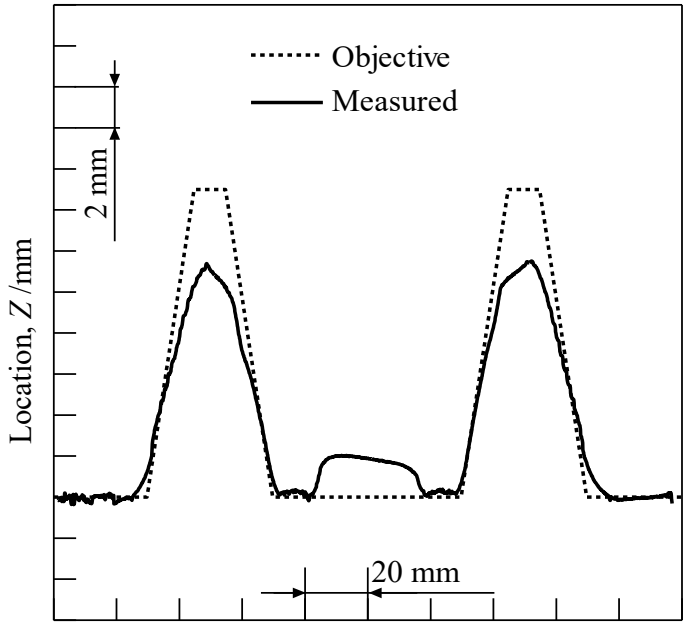

(b) convex-concave

Fig. 5.14 Concave-convex mixed shapes formed by PT-FSIF under ATP. (ω_f = 1000 rpm, v_f = 1000 mm/min, p_z = 0.5 mm)

5.4 Conclusions

It is confirmed that alternating tool paths can improve forming limit in height in PTFSIF. The first step was to form a truncated cone from A1050-O sheets having size of 200 mm × 200 mm × 2 mm. The results of forming limits in height using alternating tool paths and one-way tool paths were compared. Formable working conditions were also investigated. The thickness of the formed sheet in penetrating tool friction stir incremental forming with alternating tool paths was measured. The following conclusions were drawn:

In forming with alternating tool paths, two types of fracture morphologies, fractures caused by groove-like defects and large upheavals in the center, occurred randomly under a few forming conditions. The experimental repeatability of the same fracture morphology is high.

(1) The forming limit in height using alternating tool paths demonstrates a drastic improvement over using one-way tool paths, achieving an approximately 200% increase in forming limit in height. This is due to material being distributed more evenly both inside and outside of the forming region.

(2) Compared with conventional friction stir incremental forming, the formable working conditions were narrow. This was observed because two shoulders were used for generating frictional heat and plastic flow of materials caused by the probe generate the heat in penetrating tool friction stir incremental forming.

(3) Concave–convex mixed shapes were formed successfully by penetrating tool friction stir incremental forming with an alternating tool path.

References

[1] W. Jiang, T. Miura, M. Otsu, M. Okada, R. Matsumoto, H. Yoshimura and T. Muranaka, Development of penetrating tool friction stir incremental forming, *Mater. Trans.* **60** (2019), 2416-2425.

[2] Japan welding society, *Friction stir welding* (Sanpo Pub. Tokyo. 2006) 15. (In Japanese).

[3] M. Otsu, H. Matsuo, M. Matsuda and K. Takashima, Friction stir incremental forming of aluminum alloy sheets, *Steel Res. Int.*, 81 (2010), 942-945.

[4] M. Otsu, T. Ichikawa, M. Matsuda and K. Takashima, Improvement of formability of magnesium alloy sheets by friction stir incremental forming, *Steel Res. Int.* Special Eds., (2011), 537-541.

CHAPTER 6

CONCLUDING REMARKS

6.1 Summary

6.1.1 Development of Penetrating Tool Friction Stir Incremental Forming

A novel incremental forming method which can form the sheets into concave, convex and concave-convex shapes without using any dies or specific machine was proposed. A separable penetrating tool was designed and manufactured for forming. The designed separable penetrating tool has the merits of an adjustable gap and a replaceable probe. A machining center was used as the forming machine and the aluminum alloy of JIS A1050-O was used as the workpiece. Friction stir welding with stir-in plate was conducted as preliminary experiment for finding the suitable working conditions. By the proposed penetrating tool friction stir incremental forming, concave and convex shapes of 7 mm height/depth and a concave-convex mixed shape has 7 mm of depth and 7 mm of height was also formed successfully. The sheets were fractured in penetrating tool friction stir incremental forming due to formation of the groove-like defects, and the groove-like defects penetrates the sheet as it grows with the forming proceeded. Clockwise and counterclockwise directions of tool path were used to investigate the material flow during the forming. It was found that material flowed from the advancing side to the retreating side. The groove-like defect was caused by this material flow.

6.1.2 Relationship between Groove-like Defect Formation and Several Experimental Parameters

For improving the forming limit in height of penetrating tool friction stir incremental forming, relationship between groove-like defect formation and several experimental parameters was investigated. Since groove-like defect occurred during the

forming, the number of formed circles before groove-like defect occurred was used as an evaluated item. Experimental parameters were varied and N was recorded. A large number of formed circles before groove-like defect occurred represents that the forming conditions were hard to cause the groove-like defects. A small number of formed circles before groove-like defect occurred represents that the forming conditions were easy to cause the groove-like defects. The varied experimental parameters including the pitch in radial direction, wall angle and radius of the forming objective cone. When the wall angle is 90°, the penetrating tool friction stir incremental forming changes to friction stir welding with stir-in plate. It was found that even the wall angle was 90°, groove-like defect occurred. The number of formed circles before groove-like defect occurred increases with the increasing of radius of the forming objective shape. The number of formed circles before groove-like defect occurred decreases with the increasing of pitch in radical direction.

6.1.3 Relationship between Tool Temperature, Revolutionary Pitch and Defect Formation

For improving the forming limit in height of penetrating tool friction stir incremental forming, relationship between tool temperature, revolutionary pitch and defect formation was investigated. Tool rotation and feed rates were varied to vary the revolutionary pitch, and penetrating tool friction stir incremental forming was conducted. A sheath thermocouple was embedded in the top tool for measuring the tool temperature, and a USB type data logger was installed in a self-made holder which can rotates with the spindle together. In the forming results, the sheet fractured in all of the forming due to the formation of the defects. The defects occurred in the forming were classified into three kinds of defect, which was called defect I, II and III, depending on the fracture morphology. In defect I and III, the sheet fractured directly and in defect II, the sheet was fractured due to the formation of groove-like defect. Difference between defect I and III was the appearance of edge of fractured area. In defect I, an irregular edge was obtained and in defect III, the edge of fracture area is smooth and regular. It was thought that defect I and III were caused by the unsuitable forming temperature, which is too high or too low. It was considered that the tool temperature of defect formation has the

tendency of decreasing with the increasing of revolutionary pitch. The defect formation cannot be determined only by the tool temperature or revolutionary pitch.

6.1.4 Improving Forming Limit in Height with Alternating Tool Path Direction

Alternating and one-way tool paths were applied to penetrating tool friction stir incremental forming to compare the forming limit in height without sheet fracture. A truncated cone was formed. After the cone was formed, the forming limit in height when employing penetrating tool friction stir incremental forming with alternating tool paths were compared with those formed with one-way tool path. The forming limit in height with alternating tool paths was approximately 30 mm and the limit in height for one-way tool paths was less than 10 mm. Volume change per unit length in radial direction for both formed sheets with alternating and one-way tool paths were calculated such that improvement of forming limit in height could be examined. The volume change per unit length observed with alternating tool paths was smaller than for that with one-way tool paths, which means that a more uniform material distribution was achieved when penetrating tool friction stir incremental forming was employed with alternating tool paths.

6.2 Further Prospects

6.2.1 Reason of Occurring Groove-like Defect and Large Upheaval in the Center

The experimental results in penetrating tool friction stir incremental forming with alternating tool paths showed a poor reliability, which means two kinds of experimental results, referring the groove-like defects and the large upheaval in center, randomly occurred. In this study, reason of this has not been understand. A manufacturing method of poor reliability is hard be applied in the industrial manufacture. It is important to find the reason of occurring two experimental results. In friction stir welding, it had known

that the initial temperature of the backing plate effects the welding results. As the initial temperature of the die, which works as the backing plate in penetrating tool friction stir incremental forming, was not controlled in penetrating tool friction stir incremental forming, poor reliability may be caused by it.

6.2.2 Forming Without Defects

By using alternating tool path strategy, forming limit in height got a great improvement. But, the sheet fractured finally due to the groove-like defects, which means that alternating tool path strategy postpones the groove-like defects formation only. But it did not eliminate the groove-like defects formation. Forming without defects is a basic requirement in the industrial manufacturing. So, it should propose a method of forming without defects.

6.2.3 Key Holes

A key hole was inevitably left on the sheets in penetrating tool friction stir incremental forming in this thesis. For some products, this key hole may be a defect. Thus, it is better to eliminate this hole. In general friction stir welding, the key hole can be eliminated through two methods. Method one is cutting the parts of the key hole, which means stopping the tool at a useless part of the sheet. Method two is using a specific tool which allows the probe retracting to the shoulder. In bobbin tool friction stir welding, as the bottom shoulder was connected by the probe, only method one can be used. The penetrating tool has the similar shape with bobbin tool, therefore, in penetrating tool friction stir incremental forming only method one can be used in eliminate the key hole. For moving the tool to a useless part, a 6 axis CNC machining center or an industrial robot is need. A 6 axis CNC machining center or an industrial robot allows the penetrating tool travels in the sheets not only in the sheet plane, but also along the formed 3D surfaces, during which the axis of the penetrating tool always perpendicular to the formed 3D surfaces. Considering the formed sheets of varied thickness, gap between top and bottom tools may be another problem in the way of eliminating key hole.